SNP analysis and binding site prediction

Marc A. Marti-Renom

http://sgu.bioinfo.cipf.es

Structural Genomics Unit
Bioinformatics Department
Prince Felipe Resarch Center (CIPF), Valencia, Spain

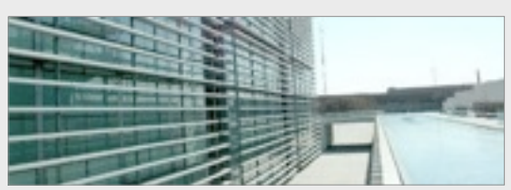

Program

SNP analysis from sequence

SNP analysis from structure

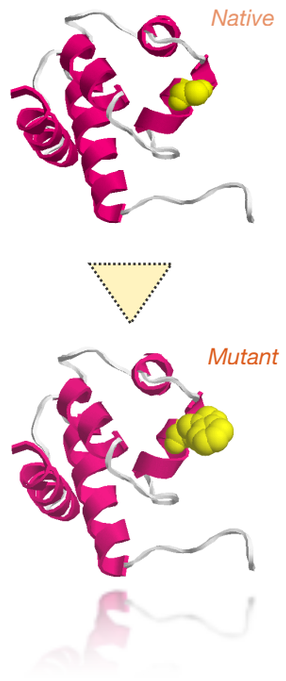

Binding site prediction

AutoDock

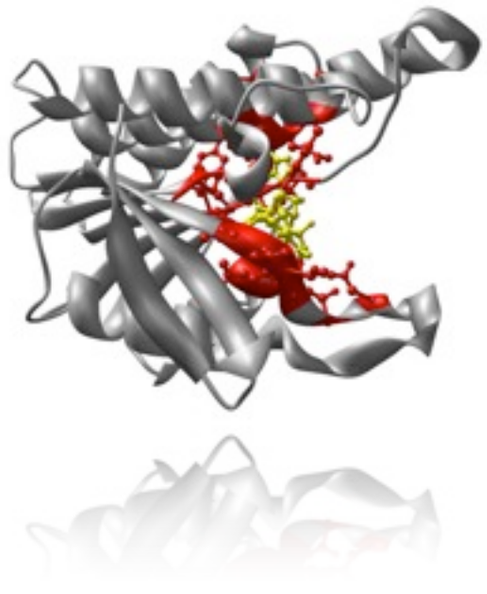

Disease?

Objective

TO UNDERSTAND THAT SNPs HAVE EFFECTS THAT CAN BE PREDICTED AND TO LEARN HOW-TO USE AutoDock FOR DOCKING SMALL MOLECULES IN THE SURFACE OF A PROTEIN

Nomenclature

SNP: Single Nucleotide Polymorphism. A single change in the DNA sequence, which may or may not result in a change in the protein sequence.

Ligand: Structure (usually a small molecule) that binds to the binding site.

Receptor: Structure (usually a protein) that contains the active binding site.

Binding site: Set of aminoacids (residues) that physically interact with the lingad (usually within 6 Ångstroms).

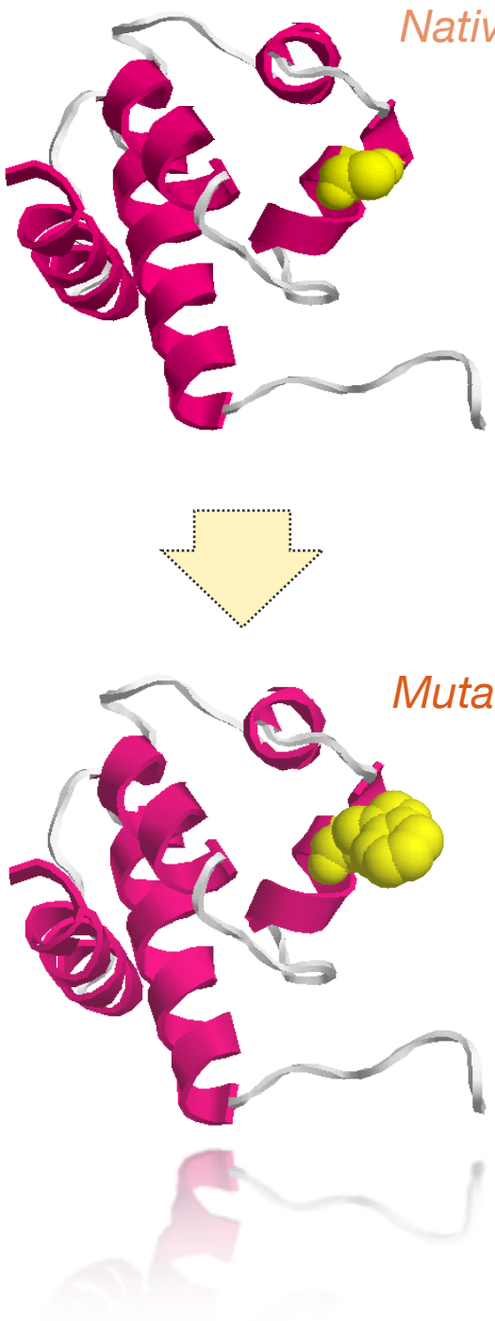

Disease?

Gene Sequence << +Protein Sequence << +Protein Structure

Single Nucleotide Polymorphism

Single Nucleotide Polymorphism or SNP
is a DNA sequence variation occurring when a single nucleotide - A, T, C, or G - in the genome differs between members of the species.
Usually one will want to refer to SNPs when the population frequency is ≥ 1%

SNPs occur at any position and can be classified on the base of their locations.

Coding SNPs can be subdivided into two groups:

Synonymous: when single base substitutions do not cause a change in the resultant amino acid

Non-synonymous: when single base substitutions cause a change in the resultant amino acid.

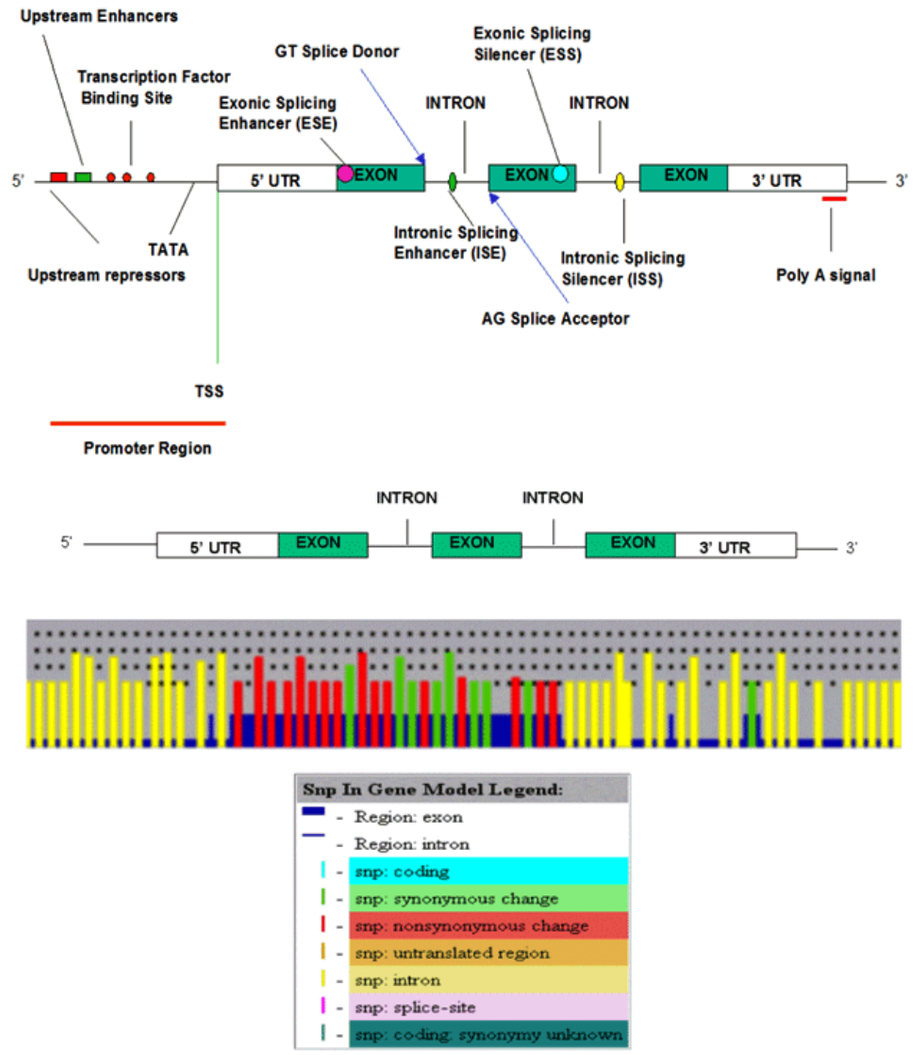

http://www.ncbi.nlm.nih.gov

SNPs and disease

Single nucleotide polymorphism are the most common type of genetic variations in human accounting for about 90% of sequence differences (Collins et al., 1998).

Studying SNPs distribution in different human populations can lead to important considerations about the history of our species (Barbujani and Goldstein, 2004; Edmonds et al., 2004).

SNPs can also be responsible of genetic diseases (Ng and Henikoff, 2002; Bell, 2004).

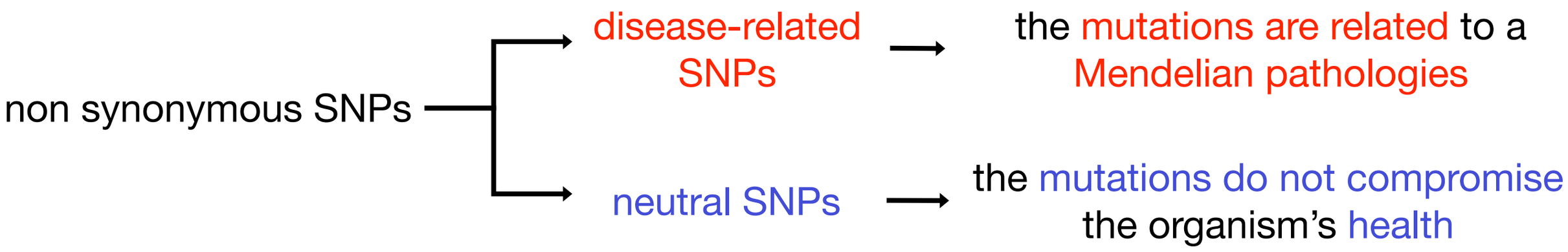

SNP databases

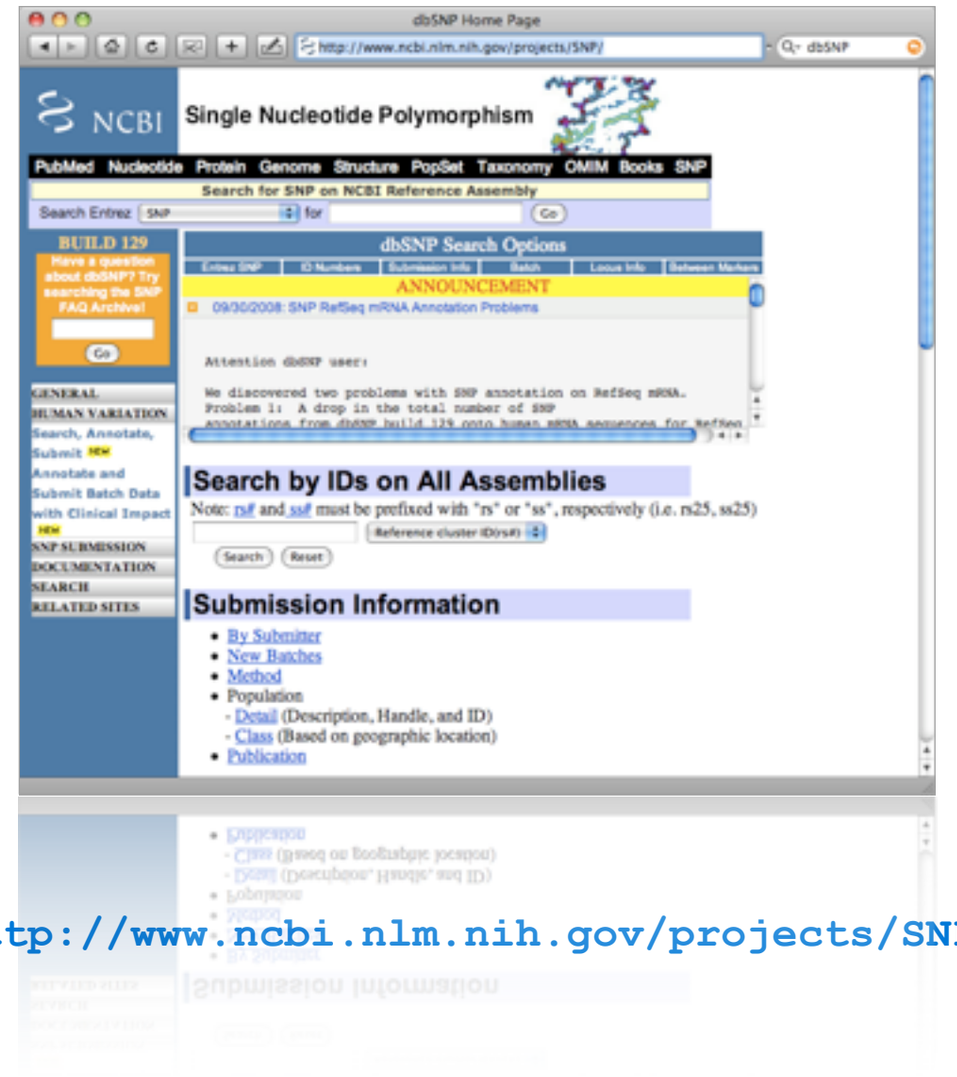

http://www.ncbi.nlm.nih.gov/projects/SNP/

http://www.uniprot.org/

Evolution and disease.

Capriotti et al. Use of estimated evolutionary strength at the codon level improves the prediction of disease-related protein mutations in humans. Hum Mutat (2008) vol. 29 (1) pp. 198-204

HUMAN MUTATION 29(1), 198–204, 2008

METHODS

Use of Estimated Evolutionary Strength at the Codon Level Improves the Prediction of Disease-Related Protein Mutations in Humans

Emidio Capriotti,[1] Leonardo Arbiza,[2] Rita Casadio,[4] Joaquín Dopazo,[3] Hernán Dopazo,[2]* and Marc A. Marti-Renom[1]*

[1]*Structural Genomics Unit, Centro de Investigación Príncipe Felipe (CIPF), Valencia, Spain;* [2]*Pharmacogenomics and Comparative Genomics Unit, Centro de Investigación Príncipe Felipe (CIPF), Valencia, Spain;* [3]*Functional Genomics Unit, Bioinformatics Department, Centro de Investigación Príncipe Felipe (CIPF), Valencia, Spain;* [4]*Laboratory of Biocomputing, CIRB/Department of Biology, University of Bologna, Bologna, Italy*

Communicated by David N. Cooper

Predicting the functional impact of protein variation is one of the most challenging problems in bioinformatics. A rapidly growing number of genome-scale studies provide large amounts of experimental data, allowing the application of rigorous statistical approaches for predicting whether a given single point mutation has an impact on human health. Up until now, existing methods have limited their source data to either protein or gene information. Novel in this work, we take advantage of both and focus on protein evolutionary information by using estimated selective pressures at the codon level. Here we introduce a new method (SeqProfCod) to predict the likelihood that a given protein variant is associated with human disease or not. Our method relies on a support vector machine (SVM) classifier trained using three sources of information: protein sequence, multiple protein sequence alignments, and the estimation of selective pressure at the codon level. SeqProfCod has been benchmarked with a large dataset of 8,987 single point mutations from 1,434 human proteins from SWISS-PROT. It achieves 82% overall accuracy and a correlation coefficient of 0.59, indicating that the estimation of the selective pressure helps in predicting the functional impact of single-point mutations. Moreover, this study demonstrates the synergic effect of combining two sources of information for predicting the functional effects of protein variants: protein sequence/profile-based information and the evolutionary estimation of the selective pressures at the codon level. The results of large-scale application of SeqProfCod over all annotated point mutations in SWISS-PROT (available for download at http://sgu.bioinfo.cipf.es/services/Omidios/; last accessed: 24 August 2007), could be used to support clinical studies. Hum Mutat 29(1), 198–204, 2008. **© 2007 Wiley-Liss, Inc.**

KEY WORDS: SNP; nsSNP; disease; sequence profile; evolutionary strength; bioinformatics

INTRODUCTION

Studies characterizing the relationship between protein variants and human disease have grown rapidly over the past years, in part due to genomic-scale sequencing efforts [Krawczak et al., 2000; Sherry et al., 2001; Stenson et al., 2003]. For example, it is now known that single nucleotide polymorphisms (SNPs) constitute about the 90% of human protein sequence variability [Collins et al., 1998]. Synonymous and nonsynonymous SNPs (nsSNPs) may occur every ~350 bp in coding regions [Cargill et al., 1999] and about 50% of nsSNPs may be associated to pathologies of genetic origin. Therefore, predicting which nsSNPs are responsible for human disease is one of the major challenges in bioinformatics.

Recently, different methods have been developed for predicting the effect of single point mutations in humans [Arbiza et al., 2006; Bao and Cui, 2005; Bao et al., 2005; Capriotti et al., 2006; Chan et al., 2007; Karchin et al., 2005a; Ng and Henikoff, 2003; Ramensky et al., 2002; Santibanez Koref et al., 2003; Thomas et al., 2003b; Yue and Moult, 2006]. In spite of the effort, however,

Received 30 May 2007; accepted revised manuscript 17 July 2007.

*Correspondence to: Marc A. Marti-Renom and Hernán Dopazo, Bioinformatics Department, Centro de Investigación Príncipe Felipe (CIPF). Av. Autopista del Saler, 16, 46013 Valencia, Spain. E-mail for Marc A. Marti-Renom: mmarti@cipf.es; E-mail for Hernán Dopazo hdopazo@cipf.es

Grant sponsor: Ministerio dell' Universitá e della Ricerca, Italy; Grant: Fondo per gli Investimenti della Ricerca di Base 2003 LIBI-International Laboratory of Bioinformatics; Grant sponsor: Marie Curie International Reintegration Grant; Grant number: FP6-039722; Grant sponsor: Generalitat Valenciana; Grant numbers: GV/2007/065 and GV06/080; Grant sponsor: Ministerio de Educación y Ciencia, Spain; Grant number: BFU2006-15413-C02-02/BMC; Grant sponsor: European Union, (EU) Network of Excellence BIOSAPIENS: Grant number: LSHG-CT-2003-503265.

DOI 10.1002/humu.20628

Published online 12 October 2007 in Wiley InterScience (www.interscience.wiley.com).

ALMA MATER STUDIORUM
UNIVERSITÀ DI BOLOGNA

PRINCIPE FELIPE
CENTRO DE INVESTIGACION

Sequence and evolutive - based predictors

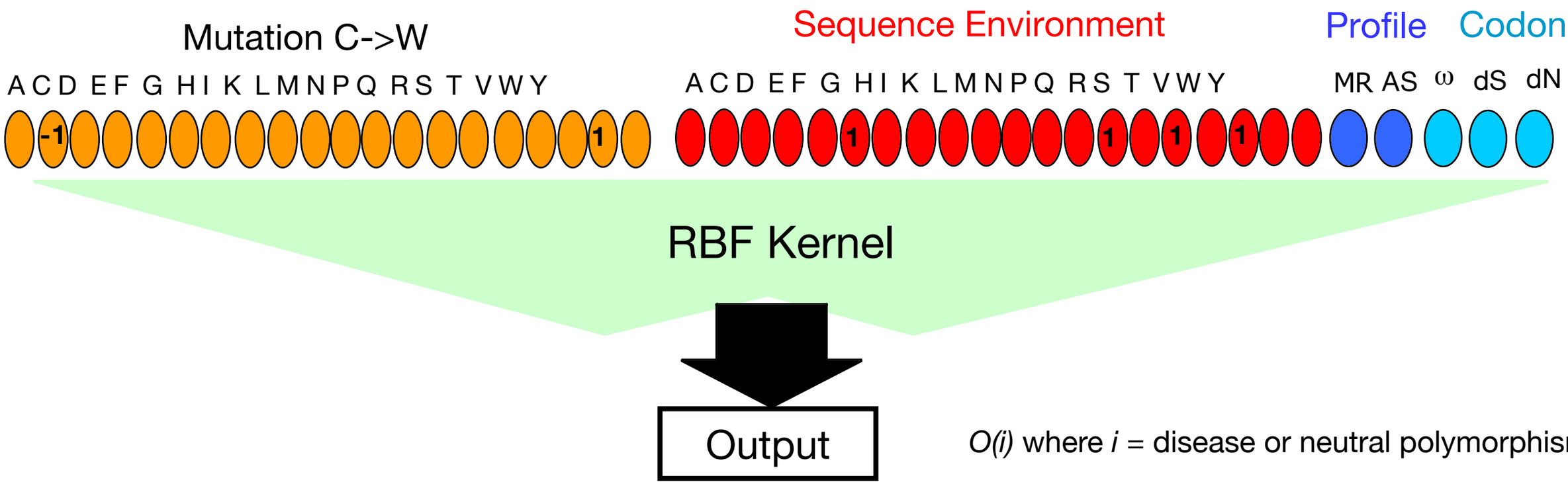

O(i) where *i* = disease or neutral polymorphism

SEQ: Mutation+ Sequence Environment
SEQPROF: Mutation+ Sequence Environment + Profile
SEQCOD Mutation+ Sequence Environment + Codon
OMIDIOS: Mutation+ Sequence Environment + Profile + Codon

Profile: MR and AS sequence profile information
Codon: omega, dS,dN: selective pressure at codon level, synonymous and non-synonymous rate at branch level.

Omidios method

Omidios has higher accuracy than the previous two methods increasing the accuracy up to 82% and the correlation coefficient to 0.59.

	Q2	P[D]	Q[D]	P[N]	Q[N]	C
Omidios	82	88	84	68	76	0.59

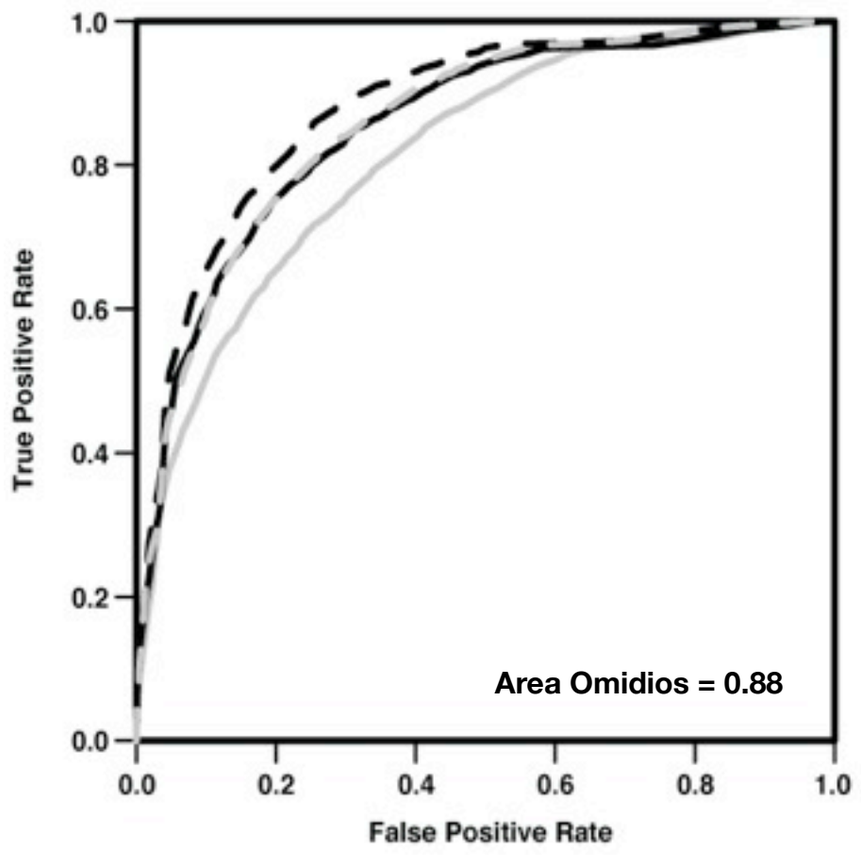

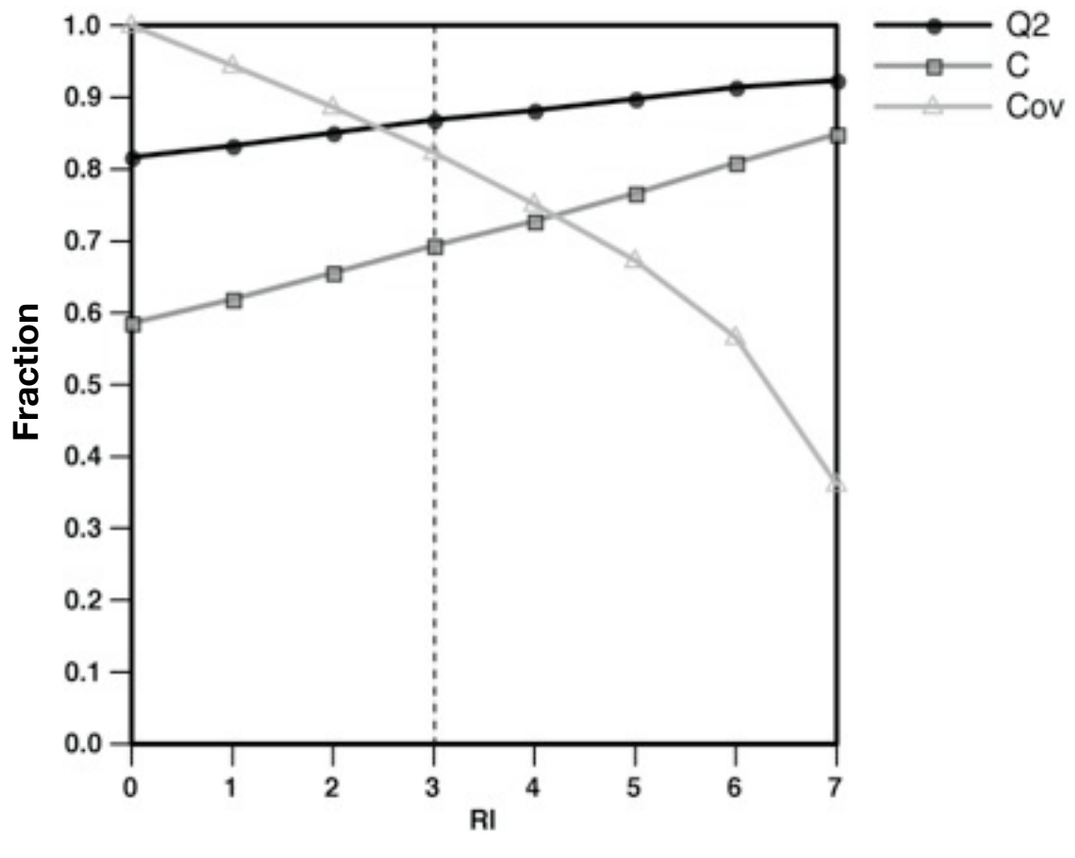

Q2: Overall Accuracy **C:** Correlation Coefficient **DB:** Fraction of database that are predicted with a reliability ≥ the given threshold

Comparison

Omidios results in higher accuracy and correlation than the other available methods covering the 100% of the dataset (see column %PM).
Omidios results in higher accuracy with respect to SIFT and although the quality of Omidios is comparable to PANTHER, when our prediction are selected by RI index the accuracy of our method is higher than PANTHER.

	Q2	P[D]	Q[D]	P[N]	Q[N]	C	PM
Omidios	82	89	84	68	76	59	100
SIFT	71	84	72	51	69	38	97
PANTHER	74	87	75	53	72	43	83

HM-Dic05: 8987 mutations

	Q2	P[D]	Q[D]	P[N]	Q[N]	C	PM
Omidios	74	65	79	83	72	48	100
SIFT	71	63	70	78	72	42	96
PANTHER	77	73	71	79	81	52	77

HM-Dic06: 2008 mutations

Omidios server

http://sgu.bioinfo.cipf.es/services/Omidios

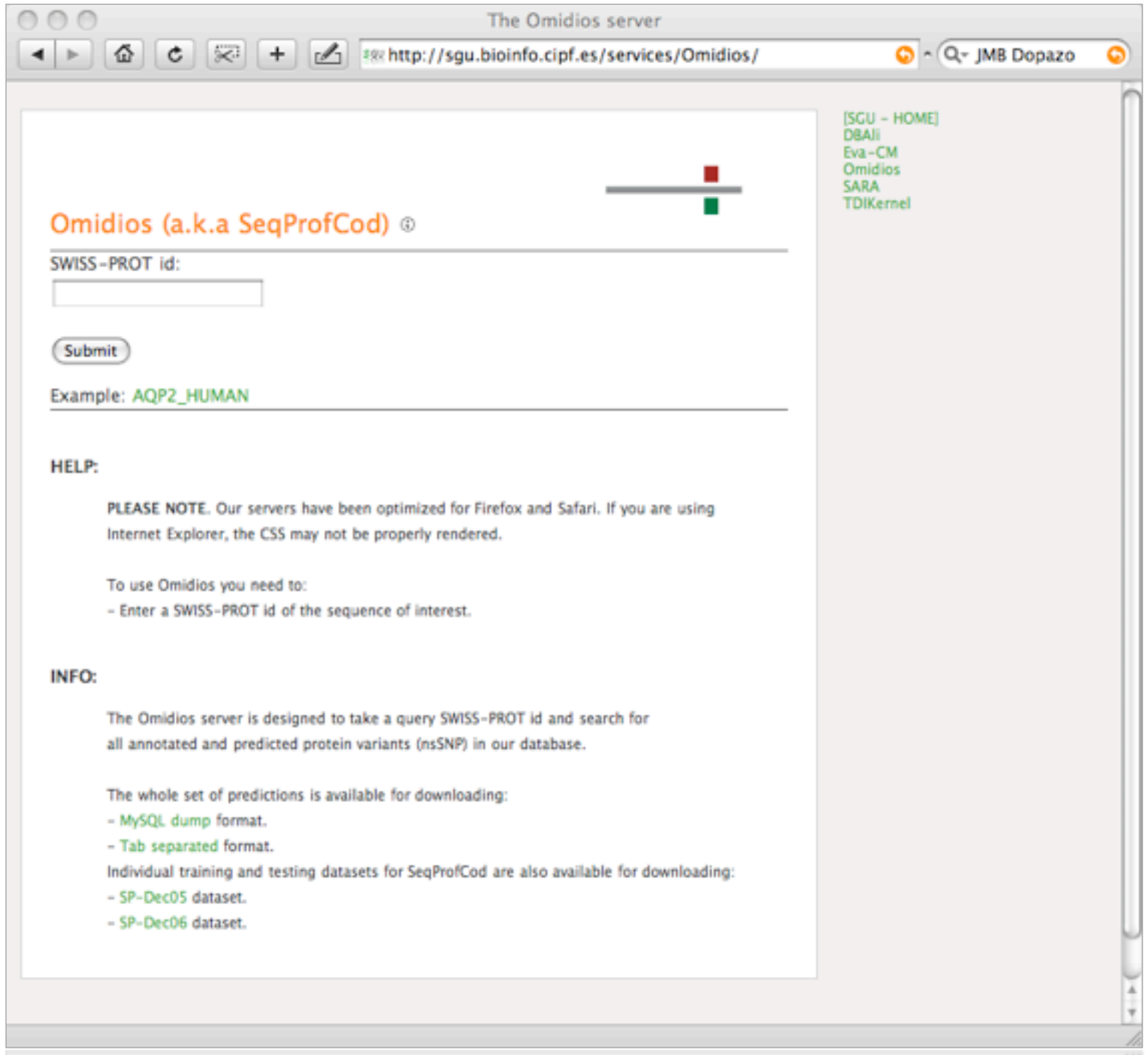

Structural analysis of missense mutations in human BRCA1 BRCT domains

Mirkovic et al. Structure-based assessment of missense mutations in human BRCA1: implications for breast and ovarian cancer predisposition. Cancer Res (2004) vol. 64 (11) pp. 3790-7

[CANCER RESEARCH 64, 3790–3797, June 1, 2004]

Structure-Based Assessment of Missense Mutations in Human BRCA1: Implications for Breast and Ovarian Cancer Predisposition

Nebojsa Mirkovic,[1] Marc A. Marti-Renom,[2] Barbara L. Weber,[3] Andrej Sali,[2] and Alvaro N. A. Monteiro[4,5]

[1]Laboratory of Molecular Biophysics, Pels Family Center for Biochemistry and Structural Biology, Rockefeller University, New York, New York; [2]Departments of Biopharmaceutical Sciences and Pharmaceutical Chemistry, and California Institute for Quantitative Biomedical Research, University of California at San Francisco, San Francisco, California; [3]Abramson Family Cancer Research Institute, University of Pennsylvania, Philadelphia, Pennsylvania; [4]Strang Cancer Prevention Center, New York, New York; and [5]Department of Cell and Developmental Biology, Weill Medical College of Cornell University, New York, New York

ABSTRACT

The *BRCA1* gene from individuals at risk of breast and ovarian cancers can be screened for the presence of mutations. However, the cancer association of most alleles carrying missense mutations is unknown, thus creating significant problems for genetic counseling. To increase our ability to identify cancer-associated mutations in *BRCA1*, we set out to use the principles of protein three-dimensional structure as well as the correlation between the cancer-associated mutations and those that abolish transcriptional activation. Thirty-one of 37 missense mutations of known impact on the transcriptional activation function of BRCA1 are readily rationalized in structural terms. Loss-of-function mutations involve nonconservative changes in the core of the BRCA1 C-terminus (BRCT) fold or are localized in a groove that presumably forms a binding site involved in the transcriptional activation by BRCA1; mutations that do not abolish transcriptional activation are either conservative changes in the core or are on the surface outside of the putative binding site. Next, structure-based rules for predicting functional consequences of a given missense mutation were applied to 57 germ-line BRCA1 variants of unknown cancer association. Such a structure-based approach may be helpful in an integrated effort to identify mutations that predispose individuals to cancer.

INTRODUCTION

Many germ-line mutations in the human *BRCA1* gene are associated with inherited breast and ovarian cancers (1, 2). This information has allowed clinicians and genetic counselors to identify individuals at high risk for developing cancer. However, the disease association of over 350 missense mutations remains unclear, primarily because their relatively low frequency and ethnic specificity limit the usefulness of the population-based statistical approaches to identifying cancer-causing mutations. To address this problem, we use here the three-dimensional structure of the human BRCA1 BRCT domains to assess the transcriptional activation functions of BRCA1 mutants. Our study is made possible by the recently determined sequences (3–6) and three-dimensional structures of the BRCA1 homologs (7, 8). In addition, we benefited from prior studies that attempted to rationalize and predict functional effects of mutations in various proteins (9–12), including those of BRCA1 (13, 14).

BRCA1 is a nuclear protein that activates transcription and facilitates DNA damage repair (15, 16). The tandem BRCT domains at the COOH-terminus of BRCA1 are involved in several of its functions, including modulation of the activity of several transcription factors (15), binding to the RNA polymerase II holoenzyme (17), and activating transcription of a reporter gene when fused to a heterologous DNA-binding domain (18, 19). Importantly, cancer-associated mutations in the BRCT domains, but not benign polymorphisms, inactivate transcriptional activation and binding to RNA polymerase II (18–21). These observations suggest that abolishing the transcriptional activation function of BRCA1 leads to tumor development and provides a genetic framework for characterization of BRCA1 BRCT variants.

MATERIALS AND METHODS

The multiple sequence alignment (MSA) of orthologous BRCA1 BRCT domains from seven species, including *Homo sapiens* (GenBank accession number U14680), *Pan troglodytes* (AF207822), *Mus musculus* (U68174), *Rattus norvegicus* (AF036760), *Gallus gallus* (AF355273), *Canis familiaris* (U50709), and *Xenopus laevis* (AF416868), was obtained by using program ClustalW (22) and contains only one gapped position (Supplementary Fig. 1). According to PSI-BLAST (23), the latter six sequences are the only sequences in the nonredundant protein sequence database at National Center for Biotechnology Information that have between 30% and 90% sequence identity to the human BRCA1 BRCT domains (residues 1649–1859).

The multiple structure-based alignment of the native structures of the BRCT-like domains was obtained by the SALIGN command in MODELLER (Supplementary Fig. 2). It included the experimentally determined structures of the two human BRCA1 BRCT domains (Protein Data Bank code 1JNX; Refs. 8, 24), rat BRCA1 BRCT domains (1L0B; Ref. 7), human p53-binding protein (1KZY; Ref. 7), human DNA-ligase IIIα (1IMO; Ref. 25), and human XRCC1 protein (1CDZ; Ref. 13). Structure variability was defined by the root-mean-square deviation among the superposed Cα positions, as calculated by the COMPARE command of MODELLER. The purpose of these calculations was to gain insight into the variability of surface-exposed residues (*left panel* in Fig. 2). In conjunction with observed mutation clustering, these data may point to putative functional site(s) on the surface of BRCT repeats.

Comparative protein structure modeling by satisfaction of spatial restraints, implemented in the program MODELLER-6 (26), was used to produce a three-dimensional model for each of the 94 mutants. The crystallographic structure of the human wild-type BRCA1 BRCT domains was used as the template for modeling (8). The four residues missing in the crystallographic structure (1694 and 1817–1819) were modeled *de novo* (27). All of the models are available in the BRCA1 model set deposited in our ModBase database of comparative protein structure models (28).[6]

For the native structure of the human BRCT tandem repeat and each of the 94 mutant models, a number of sequence and structure features were calculated. These features were used in the classification tree in Fig. 3 (values for all 94 mutations are given in Supplementary Tables 1 and 2).

Buriedness. Accessible surface area of an amino acid residue was calculated by the program DSSP (29) and normalized by the maximum accessible surface area for the corresponding amino acid residue type. A residue was considered exposed if its accessible surface area was larger than 40Å^2 and if its relative accessible surface area was larger than 9% and buried otherwise. A mutation of a more exposed residue is less likely to change the structure and therefore its function.

Received 9/24/03; revised 1/30/04; accepted 3/15/04.

Grant support: This work was supported by Lee Kaplan Foundation, the Fashion Footwear Association of New York/QVC; United States Army award DAMD17-99-1-9389 and NIH CA92309 (A. N. A. M.); the Mathers Foundation, Sandler Family Supporting Foundation, Sun, IBM and Intel (A. S.); and NIH GM 54762 GM61390 (A. S.); and the Breast Cancer Research Foundation (B. L. W.). M. A. M-R. is a Rockefeller University Presidential Postdoctoral Fellow; A. S. is an Irma T. Hirschl Trust Career Scientist; and B. L. W. is an Abramson Investigator.

The costs of publication of this article were defrayed in part by the payment of page charges. This article must therefore be hereby marked *advertisement* in accordance with 18 U.S.C. Section 1734 solely to indicate this fact.

Note: The authors declare that they have no competing financial interests. Supplemental data for this article are available at Cancer Research Online (http: cancerres@aacrjournals.org).

Requests for reprints: Alvaro N. A. Monteiro, H. Lee Moffitt Cancer Center and Research Institute, MRC 3 West, 12902 Magnolia Drive, Tampa, FL 33612. Phone: (813) 745-6321; Fax: (813) 903-6847; E-mail: monteian@moffitt.usf.edu.

[6] http://salilab.org/modbase/.

Human BRCA1 and its two BRCT domains

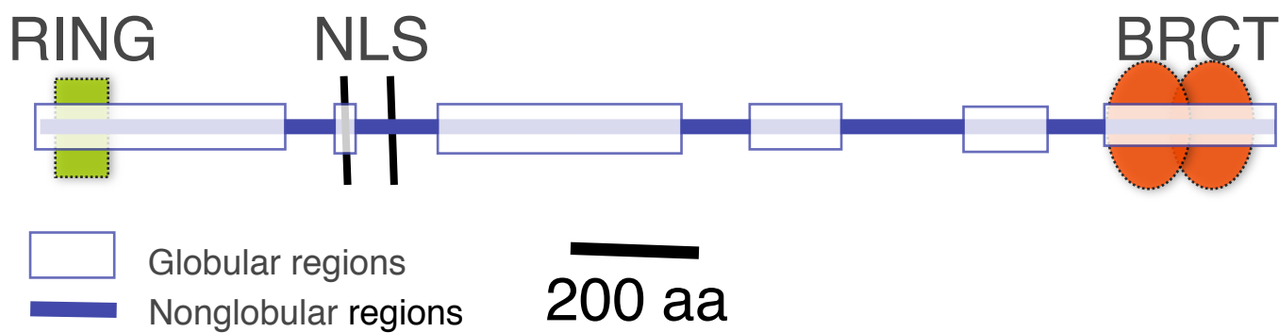

BRCA1 BRCT repeats, 1jnx

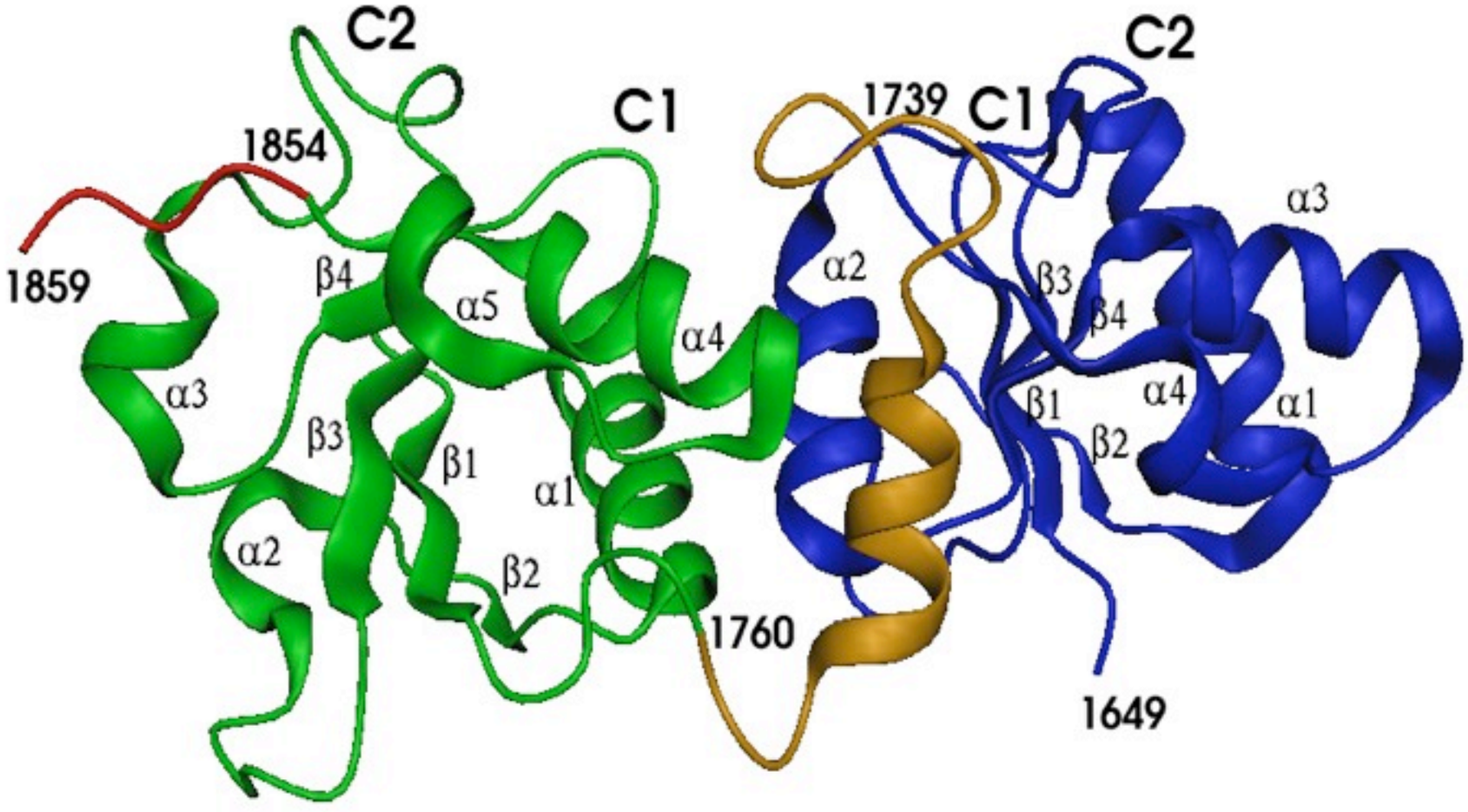

Williams, Green, Glover. Nat.Struct.Biol. 8, 838, 2001

CONFIDENTIAL

MYRIAD

BRACAnalysis™

Comprehensive BRCA1-BRCA2 Gene Sequence Analysis Result

Niecee Singer, MS
Strang Cancer Prevention Center
428 E 72nd St
New York, NY 10021

Physician: Fred Gilbert, MD

SPECIMEN	
Specimen Type:	Blood
Draw Date:	n/a
Accession Date:	Oct 27, 2000
Report Date:	Nov 17, 2000

PATIENT	
Name:	
Date of Birth:	Feb 02, 1953
Patient ID:	
Gender:	Female
Accession #:	00019998
Requisition #:	56594

Test Result

Gene Analyzed	Specific Genetic Variant
BRCA2	H2116R
BRCA1	None Detected

Interpretation

GENETIC VARIANT OF UNCERTAIN SIGNIFICANCE

The BRCA2 variant H2116R results in the substitution of arginine for histidine at amino acid position 2116 of the BRCA2 protein. Variants of this type may or may not affect BRCA2 protein function. Therefore, the contribution of this variant to the relative risk of breast or ovarian cancer cannot be established solely from this analysis. The observation by Myriad Genetic Laboratories of this particular variant in an individual with a deleterious truncating mutation in BRCA2, however, reduces the likelihood that H2116R is itself deleterious.

Authorized Signature:

Brian E. Ward, Ph.D.
Laboratory Director

Thomas S. Frank, M.D.
Medical Director

These test results should only be used in conjunction with the patient's clinical history and any previous analysis of appropriate family members. It is strongly recommended that those results be communicated to the patient in a setting that includes appropriate counseling. The accompanying Technical Specifications summary describes the analysis, method, performance characteristics, nomenclature, and interpretive criteria of this test. This test may be considered investigational by some states. This test was developed and its performance characteristics determined by Myriad Genetic Laboratories. It has not been reviewed by the U.S. Food and Drug Administration. The FDA has determined that such clearance or approval is not necessary.

Missense mutations in BRCT domains by function

	cancer associated	not cancer associated	?
no transcription activation	C1697R R1699W A1708E S1715R P1749R M1775R		M1652K L1657P E1660G H1686Q R1699Q K1702E Y1703HF 1704S L1705PS 1715NS1 722FF17 34LG173 8EG1743 RA1752P F1761I F1761S M1775E M1775K L1780P I1807S V1833E A1843T
transcription activation		M1652I A1669S	V1665M D1692N G1706A D1733G M1775V P1806A
?			M1652T V1653M L1664P T1685A T1685I M1689R D1692Y F1695L V1696L R1699L G1706E W1718C W1718S T1720A W1730S F1734S E1735K V1736A G1738R D1739E D1739G D1739Y V1741G H1746N R1751P R1751Q R1758G L1764P I1766S P1771L T1773S P1776S D1778N D1778G D1778H M1783T C1787S G1788D G1788V G1803A V1804D V1808A V1809A V1809F V1810G Q1811R P1812S N1819S A1823T V1833M W1837R W1837G S1841N A1843P T1852S P1856T P1859R

"Decision" tree for predicting functional impact of genetic variants

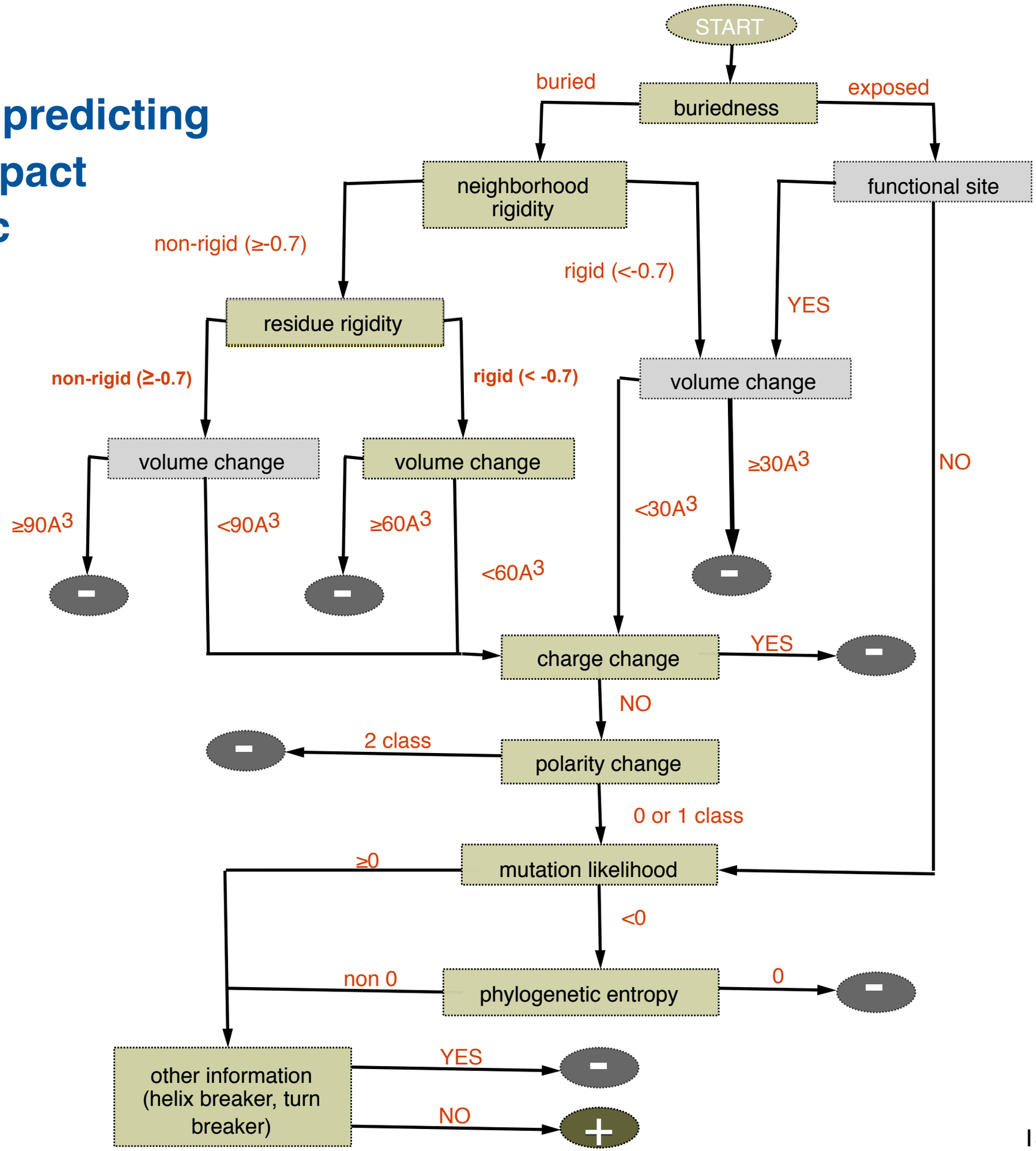

Putative binding site on BRCA1

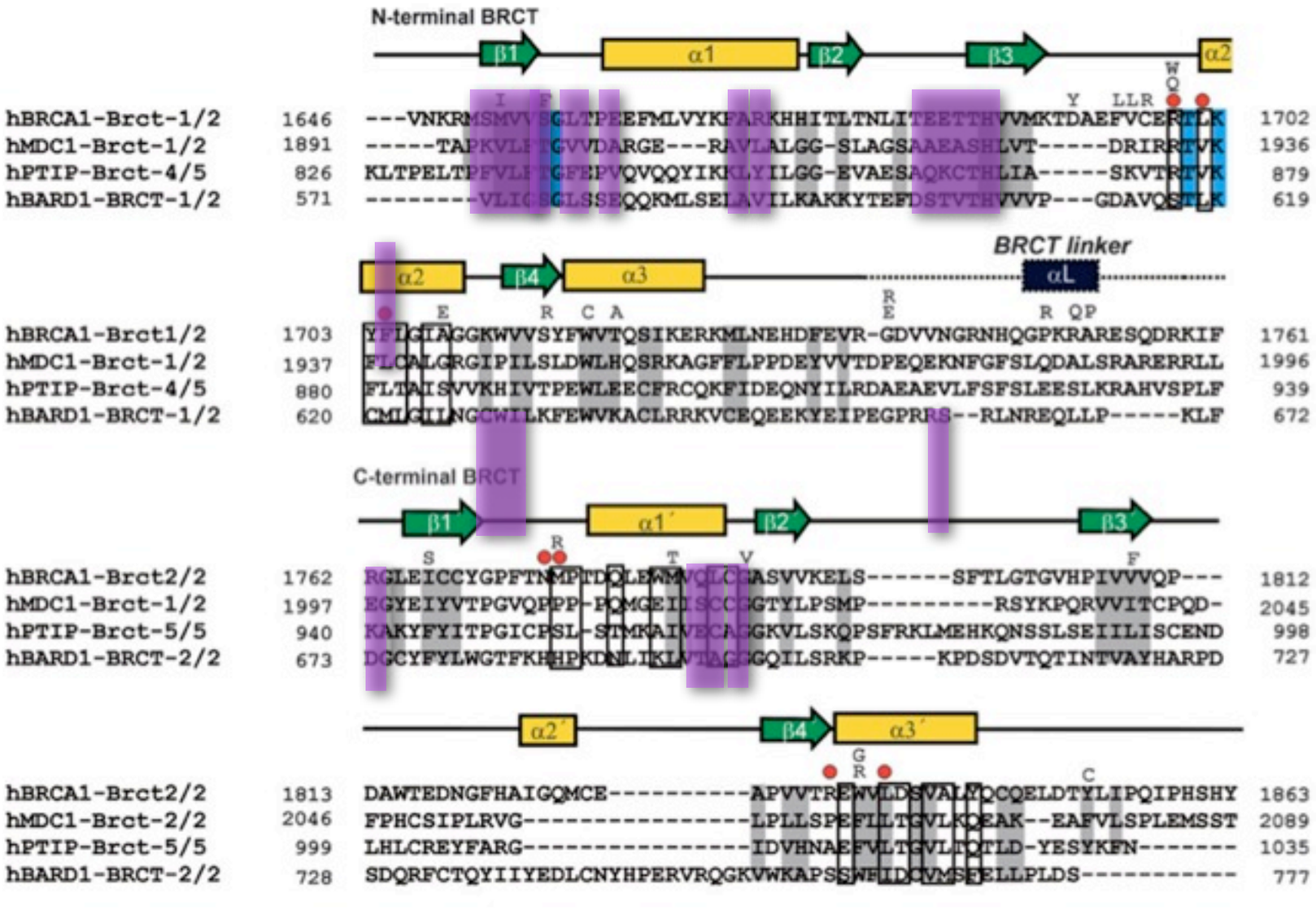

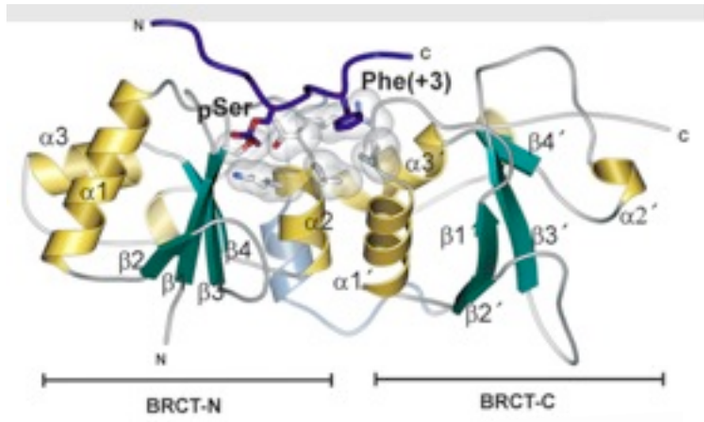

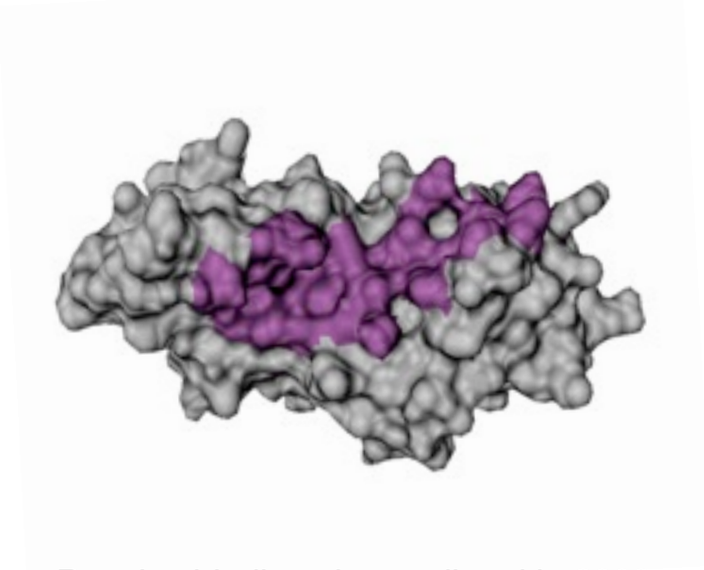

Putative binding site predicted in 2003
and accepted for publication on March 2004.

Williams *et al.* 2004 Nature Structure Biology. **June 2004 11**:519

Mirkovic *et al.* 2004 Cancer Research. **June 2004 64**:3790

Supervised learning approach

Karchin et al. Functional Impact of Missense Variants in BRCA1 Predicted by Supervised Learning.
PLoS Comput Biol (2007) vol. 3 (2) pp. e26

OPEN ACCESS Freely available online

PLoS COMPUTATIONAL BIOLOGY

Functional Impact of Missense Variants in BRCA1 Predicted by Supervised Learning

Rachel Karchin[1,2*], Alvaro N. A. Monteiro[3], Sean V. Tavtigian[4], Marcelo A. Carvalho[3], Andrej Sali[5,6*]

1 Department of Biomedical Engineering, Johns Hopkins University, Baltimore, Maryland, United States of America, **2** Institute of Computational Medicine, Johns Hopkins University, Baltimore, Maryland, United States of America, **3** Risk Assessment, Detection, and Intervention Program, H. Lee Moffitt Cancer Center and Research Institute, Tampa, Florida, United States of America, **4** International Agency for Research on Cancer, Lyon, France, **5** Department of Pharmaceutical Chemistry, University of California San Francisco, San Francisco, California, United States of America, **6** California Institute for Quantitative Biomedical Research, University of California San Francisco, San Francisco, California, United States of America

Many individuals tested for inherited cancer susceptibility at the *BRCA1* gene locus are discovered to have variants of unknown clinical significance (UCVs). Most UCVs cause a single amino acid residue (missense) change in the BRCA1 protein. They can be biochemically assayed, but such evaluations are time-consuming and labor-intensive. Computational methods that classify and suggest explanations for UCV impact on protein function can complement functional tests. Here we describe a supervised learning approach to classification of *BRCA1* UCVs. Using a novel combination of 16 predictive features, the algorithms were applied to retrospectively classify the impact of 36 BRCA1 C-terminal *(BRCT)* domain UCVs biochemically assayed to measure transactivation function and to blindly classify 54 documented UCVs. Majority vote of three supervised learning algorithms is in agreement with the assay for more than 94% of the UCVs. Two UCVs found deleterious by both the assay and the classifiers reveal a previously uncharacterized putative binding site. Clinicians may soon be able to use computational classifiers such as those described here to better inform patients. These classifiers can be adapted to other cancer susceptibility genes and systematically applied to prioritize the growing number of potential causative loci and variants found by large-scale disease association studies.

Citation: Karchin R, Monteiro ANA, Tavtigian SV, Carvalho MA, Sali A (2007) Functional impact of missense variants in BRCA1 predicted by supervised learning. PLoS Comput Biol 3(2): e26. doi:10.1371/journal.pcbi.0030026

Introduction

The *BRCA1* gene encodes a large multifunction protein involved in cell-cycle and centrosome control, transcriptional regulation, and in the DNA damage response [1–3]. Inherited mutations in this gene have been associated with an increased lifetime risk of breast and ovarian cancer (6–8 times that of the general population) [4]. There are several thousand known deleterious *BRCA1* mutations that result in frameshifts and/or premature stop codons, producing a truncated protein product [5]. In contrast, the functional impact of most missense variants that result in a single amino acid residue change in BRCA1 protein is not known. The Breast Cancer Information Core database (http://research.nhgri.nih.gov/bic/), a central repository of *BRCA1* and *BRCA2* mutations identified in genetic tests, currently contains 487 unique missense *BRCA1* variants (April 2006), of which only 17 have sufficient genetic/epidemiological evidence to be classified as deleterious (Clinically Important) and 33 as neutral or of little clinical importance (Not Clinically Important). As genetic testing for inherited disease predispositions becomes more commonplace, predicting the clinical significance of missense variants and other UCVs will be increasingly important for risk assessment.

Because most UCVs in *BRCA1* and *BRCA2* occur at very low population frequencies (<0.0001) [6], direct epidemiological measures, such as familial cosegregation with disease, are often not sufficiently powerful to identify the variants associated with cancer predisposition. A promising approach is to supplement epidemiological and clinical analysis of UCVs with indirect approaches such as biochemical studies of protein function and bioinformatics analysis [6–8]. In the future, physicians and genetic counselors may be able to rely on all these sources of information about UCVs when counseling their patients.

Previous bioinformatics analysis of *BRCA1* UCVs has depended primarily on measures of evolutionary conservation in multiple sequence alignments of human *BRCA1* and related proteins from other organisms [9–11]. Two groups have attempted to include information about BRCA1 protein structure. Williams et al. predicted the impact of 25 missense variants in BRCA1's C-terminal BRCT domains by considering both conservation and location of variant amino acid residues in an X-ray crystal structure [12]. Variants were predicted deleterious if their properties were similar to

Editor: Greg Tucker-Kellogg, Lilly Systems Biology, Singapore

Received September 5, 2006; **Accepted** December 27, 2006; **Published** February 16, 2007

A previous version of this article appeared as an Early Online Release on December 28, 2006 (doi:10.1371/journal.pcbi.0030026.eor).

Abbreviations: Align-GVGD, Align Grantham Variation Grantham Deviation; AUC, area under the ROC curve; BIC, breast information core database; BRCT, BRCA1 C-terminal domains; BRCT-C, BRCT C-terminal domain; BRCT-N, BRCT N-terminal domain; GD, Grantham Deviation; GV, Grantham Variation; ROC, receiver operating characteristic; Rule-based decision tree, empirically derived rules encoded in a decision tree; SIFT, Sorting Intolerant from Tolerant; UCV, variant of unknown clinical significance

* To whom correspondence should be addressed. E-mail: karchin@karchinlab.org (RK); sali@salilab.org (AS)

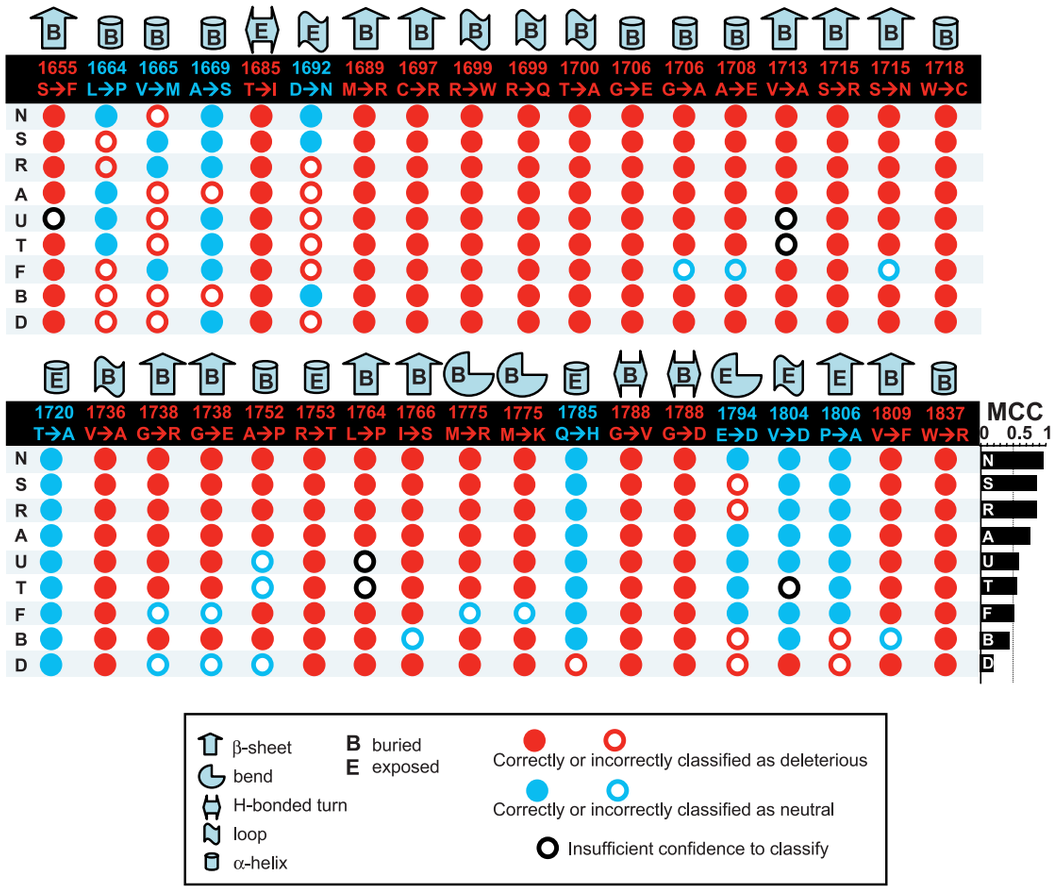

Predictors are combined in support vector machine supervised learning

$X_1..X_k$= TRAINING

relative entropy
Grantham distance
solvent accessibility
methyl(ene) groups
volume change

■
■
■

+	−
0.12	3.1
21	120
7	30
45	8
-3.2	1.5

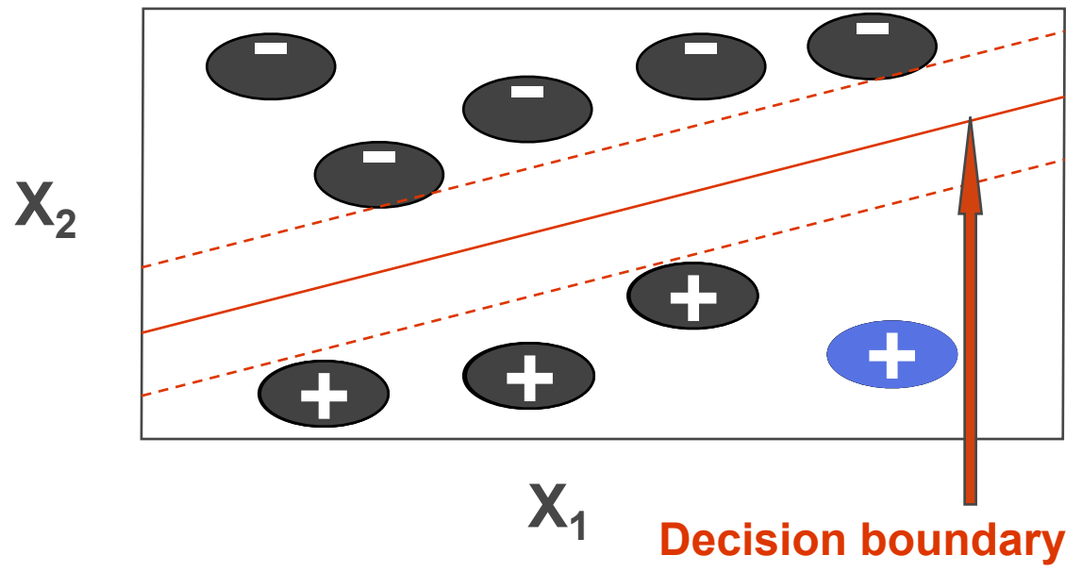

0.7
26
0
17
1.5

?

TESTING? PREDICTING...

Features

Feature Category	Feature Description
Structural	Solvent Accessiblity of wild-type amino acid residue (Å^2)
	Solvent Accessibility of wild-type residue normalized by maximum exposed Solvent Accessibility of that residue type in a GLY-X-GLY tripeptide, using values given by Rose et al. [80]
	Solvent Accessibility of variant residue
	Normalized Solvent Accessibility of variant residue
	Number of methyl(ene) groups within 6 Å of the variant sidechain [81]
	Number of unsatisfied spatial restraints in the MODELLER objective function after in silico mutation and simulated annealing refinement of the variant[a]
	Φ and Ψ backbone dihedral angles at the mutated position
	Whether the mutation results in buried charge
Physiochemical differences between wild-type and variant amino acid residues	Change in formal charge
	Change in volume (Å^3) [82]
	Change in polarity [83]
	Grantham difference [37]
Evolutionary conservation of amino acid residues in protein orthologs	Relative entropy estimated by amino acids in the variant's alignment column [84]
	Positional hidden Markov model conservation score based on the probabilities of the wild-type, variant, and most probable amino acid residue in the variant's alignment column[b] [24]

[a]Violated restraints suggest that the mutated sidechain introduced steric clashes or unusual geometries into the protein model. Examples of violated restraints include extreme values of the Lennard-Jones 6–12 potential [85], bond angle potential, bond length potential, sidechain dihedral angle restraints, and nonbonded restraints. Two thresholds are used to identify violated restraints yielding two features.

[b]The probabilities are estimated by a hidden Markov model built with SAM-T2K and the w0.5 script [23].

$PHC = \log(|p(\text{Wild-type}) - p(\text{Variant})|) + \log(p(\text{Wild-type})) + \log(P(\text{Most Probable})) - \log(p(\text{Variant}))$

The features were computed for 618 TP53 missense variants, 36 BRCA1 BRCT missense variants biochemically characterized in our companion paper [14], and 54 BRCA1 BRCT UCVs found in BIC.

doi:10.1371/journal.pcbi.0030026.t002

Results

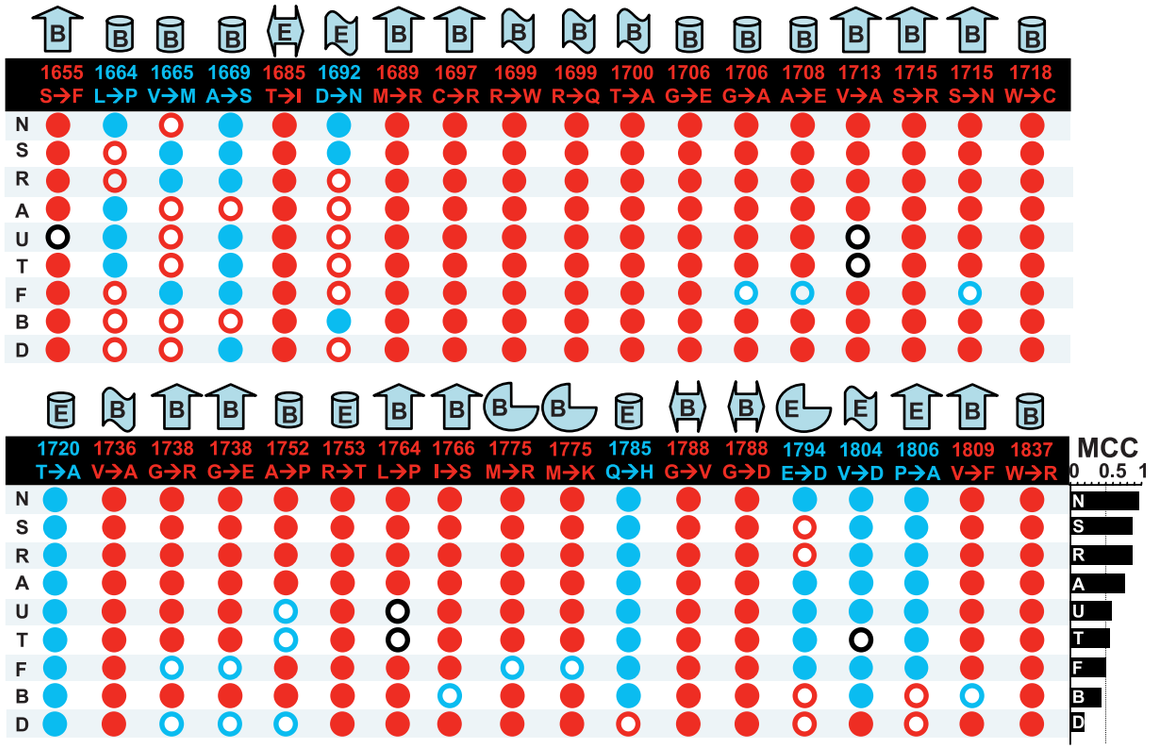
1655 S→F 1664 L→P 1665 V→M 1669 A→S 1685 T→I 1692 D→N 1689 M→R 1697 C→R 1699 R→W 1699 R→Q 1700 T→A 1706 G→E 1706 G→A 1708 A→E 1713 V→A 1715 S→R 1715 S→N 1718 W→C
N S R A U T F B D
1720 T→A 1736 V→A 1738 G→R 1738 G→E 1752 A→P 1753 R→T 1764 L→P 1766 I→S 1775 M→R 1775 M→K 1785 Q→H 1788 G→V 1788 G→D 1794 E→D 1804 V→D 1806 P→A 1809 V→F 1837 W→R
MCC 0 0.5 1
N S R A U T F B D
β-sheet
bend
H-bonded turn
loop
α-helix
B buried
E exposed
Correctly or incorrectly classified as deleterious
Correctly or incorrectly classified as neutral
Insufficient confidence to classify

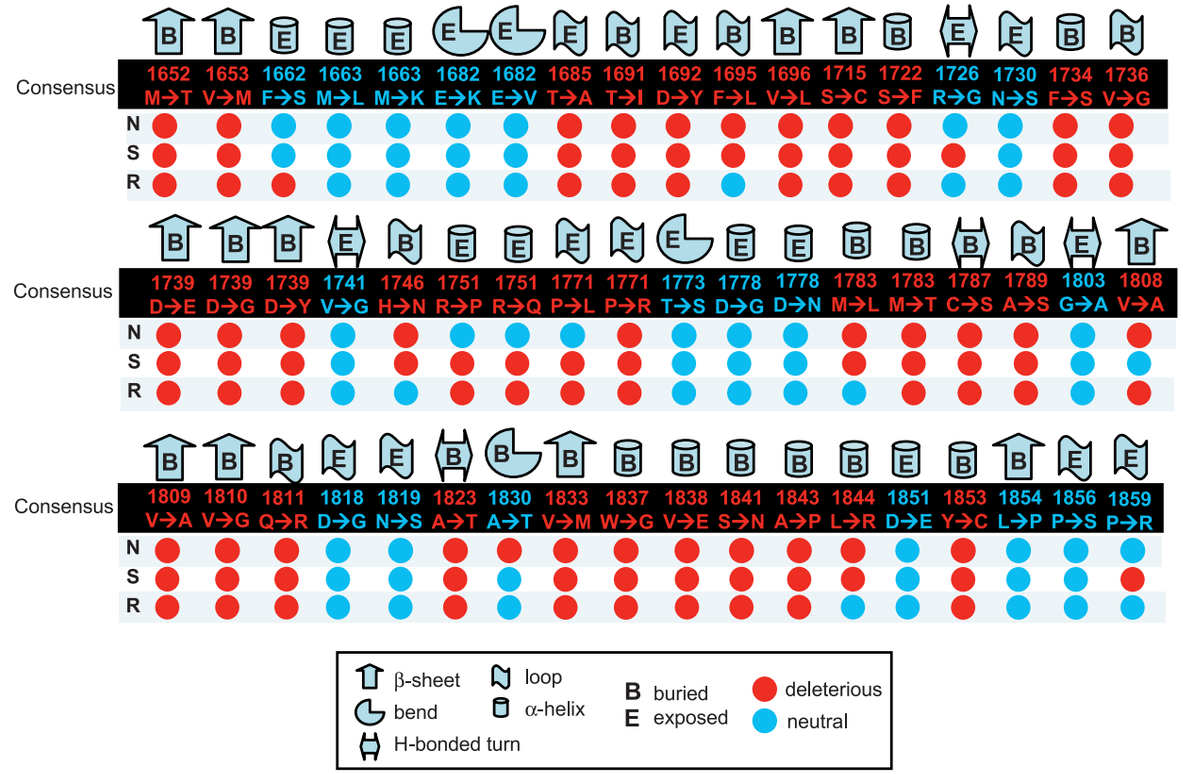
Consensus
1652 M→T 1653 V→M 1662 F→S 1663 M→L 1663 M→K 1682 E→K 1682 E→V 1685 T→A 1691 T→I 1692 D→Y 1695 F→L 1696 V→L 1715 S→C 1722 S→F 1726 R→G 1730 N→S 1734 F→S 1736 V→G
N S R
Consensus
1739 D→E 1739 D→G 1739 D→Y 1741 V→G 1746 H→N 1751 R→P 1751 R→Q 1771 P→L 1771 P→R 1773 T→S 1778 D→G 1778 D→N 1783 M→L 1783 M→T 1787 C→S 1789 A→S 1803 G→A 1808 V→A
N S R
Consensus
1809 V→A 1810 V→G 1811 Q→R 1818 D→G 1819 N→S 1823 A→T 1830 A→T 1833 V→M 1837 W→G 1838 V→E 1841 S→N 1843 A→P 1844 L→R 1851 D→E 1853 Y→C 1854 L→P 1856 P→S 1859 P→R
N S R
β-sheet
bend
H-bonded turn
loop
α-helix
B buried
E exposed
deleterious
neutral

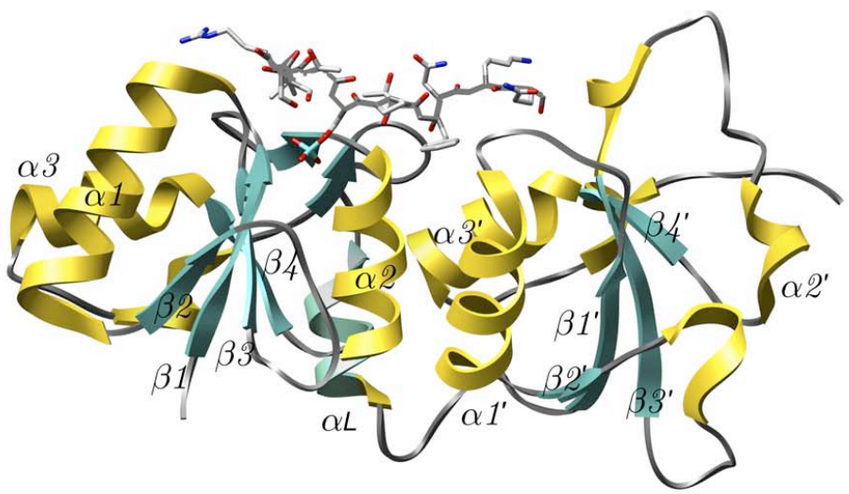
α3
α1
β4
α2
α3'
β4'
α2'
β2
β1'
β3
β1
β2'
β3'
αL
α1'

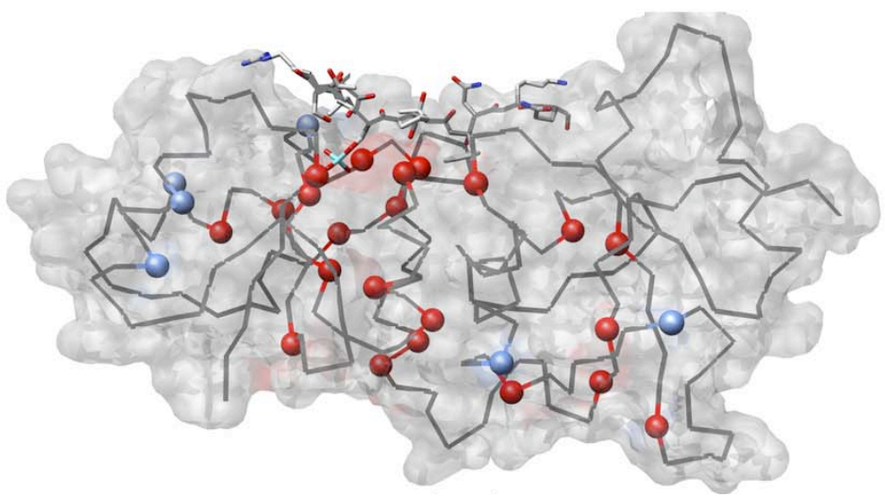

LS-SNP Large Scale SNP analysis

http://salilab.org/LS-SNP/

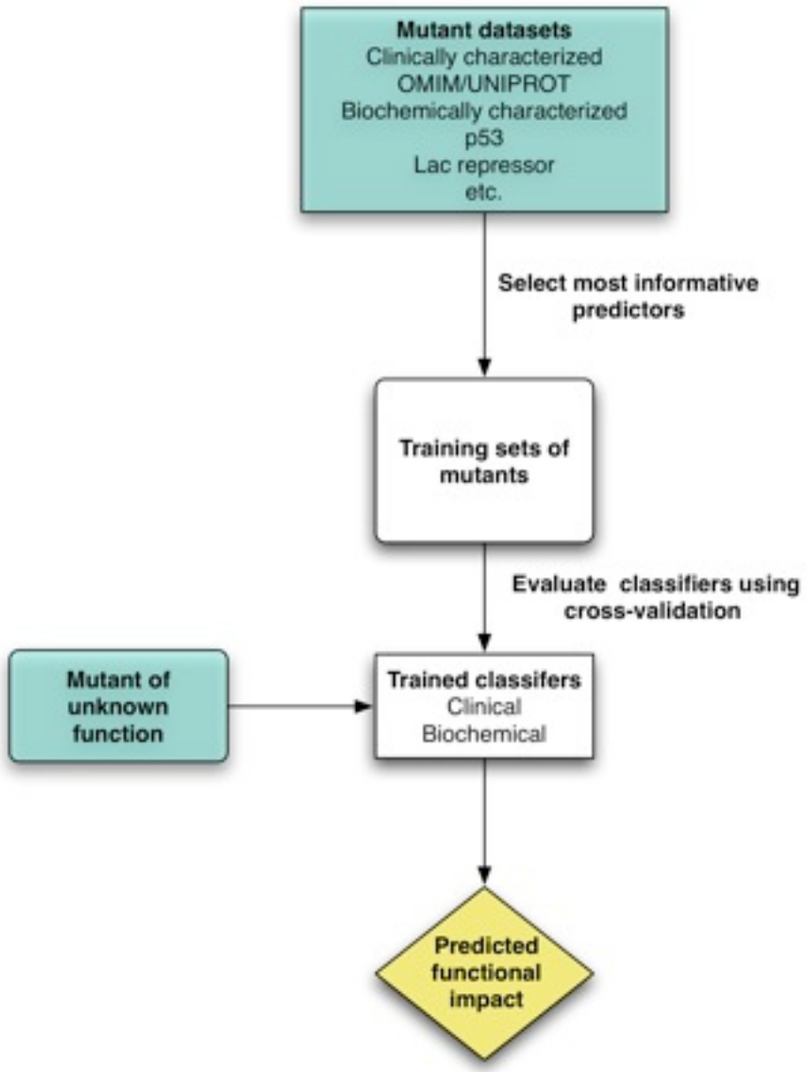

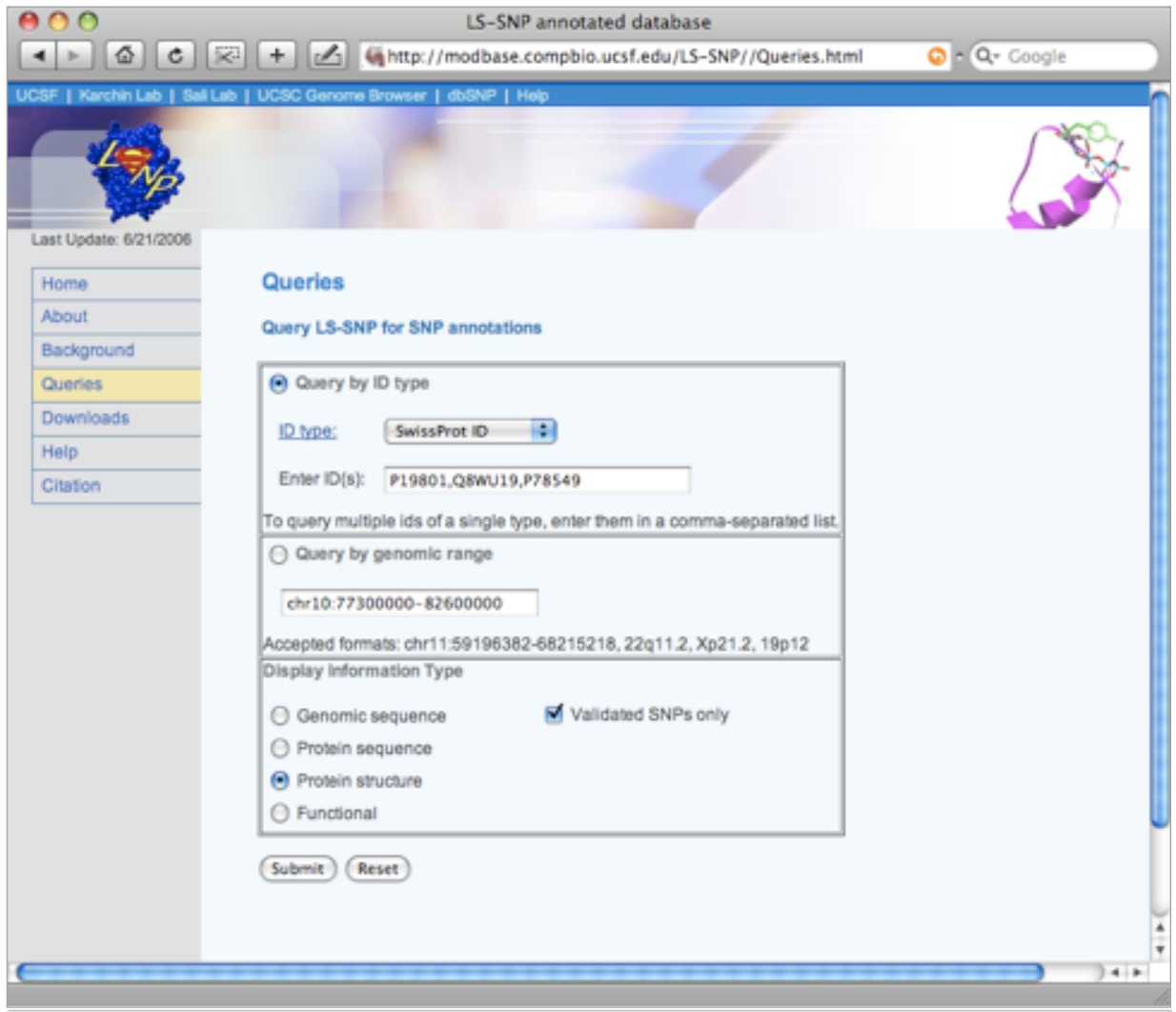

Protein function from structure

ab-initio *localization of binding sites*

Rossi. Localization of binding sites in protein structures by optimization of a composite scoring function. Protein Science (2006) vol. 15 (10) pp. 2366-2380

Localization of binding sites in protein structures by optimization of a composite scoring function

ANDREA ROSSI, MARC A. MARTI-RENOM, AND ANDREJ SALI
Departments of Biopharmaceutical Sciences and Pharmaceutical Chemistry, California Institute for Quantitative Biomedical Research, University of California, San Francisco, California 94143-2552, USA

(RECEIVED March 28, 2006; FINAL REVISION July 10, 2006; ACCEPTED July 11, 2006)

Abstract

The rise in the number of functionally uncharacterized protein structures is increasing the demand for structure-based methods for functional annotation. Here, we describe a method for predicting the location of a binding site of a given type on a target protein structure. The method begins by constructing a scoring function, followed by a Monte Carlo optimization, to find a good scoring patch on the protein surface. The scoring function is a weighted linear combination of the z-scores of various properties of protein structure and sequence, including amino acid residue conservation, compactness, protrusion, convexity, rigidity, hydrophobicity, and charge density; the weights are calculated from a set of previously identified instances of the binding-site type on known protein structures. The scoring function can easily incorporate different types of information useful in localization, thus increasing the applicability and accuracy of the approach. To test the method, 1008 known protein structures were split into 20 different groups according to the type of the bound ligand. For nonsugar ligands, such as various nucleotides, binding sites were correctly identified in 55%–73% of the cases. The method is completely automated (http://salilab.org/patcher) and can be applied on a large scale in a structural genomics setting.

Keywords: protein function annotation; small ligand binding-site localization

Many protein targets of structural biologists are no longer chosen because of their function, but rather by their location in the protein sequence-structure space (Burley et al. 1999; Brenner 2000, 2001; Sali 2001; Vitkup et al. 2001; Chance et al. 2002; Goldsmith-Fischman and Honig 2003). Therefore, the number of functionally uncharacterized protein structures is growing. Of the 36,606 entries in the Protein Data Bank (PDB) (Kouranov et al. 2006) as of February 23, 2006, 1407 structures were deposited by structural genomics consortia, 985 (70%) of which had an unknown function according to the HEADER record of their PDB files. In contrast, only 174 (0.5%) of the 35,199 protein structures solved outside of structural genomics had no functional annotations in their PDB files.

To classify the functions of thousands of uncharacterized protein structures that will become available over the next few years and millions of comparative models based on the known structures, automated structure-based functional annotation is required (Wallace et al. 1996, 1997; Kleywegt 1999; Thornton et al. 2000; Babbitt 2003; Laskowski et al. 2003). In particular, we need to be able to identify the locations and types of binding sites on a given structure, because the binding sites define the molecular function of a protein.

The most principled computational approach to predicting the molecular function is to dock a large library of potential ligands against the surface of the protein. In

Reprint requests to: Andrea Rossi or Andrej Sali, Departments of Biopharmaceutical Sciences and Pharmaceutical Chemistry, California Institute for Quantitative Biomedical Research, University of California, San Francisco Byers Hall, Office 503B, 1700 4th Street, San Francisco, CA 94143-2552, USA; e-mail: andrea@salilab.org or sali@salilab.org; fax: (415) 514-4231.

Article published online ahead of print. Article and publication date are at http://www.proteinscience.org/cgi/doi/10.1110/ps.062247506.

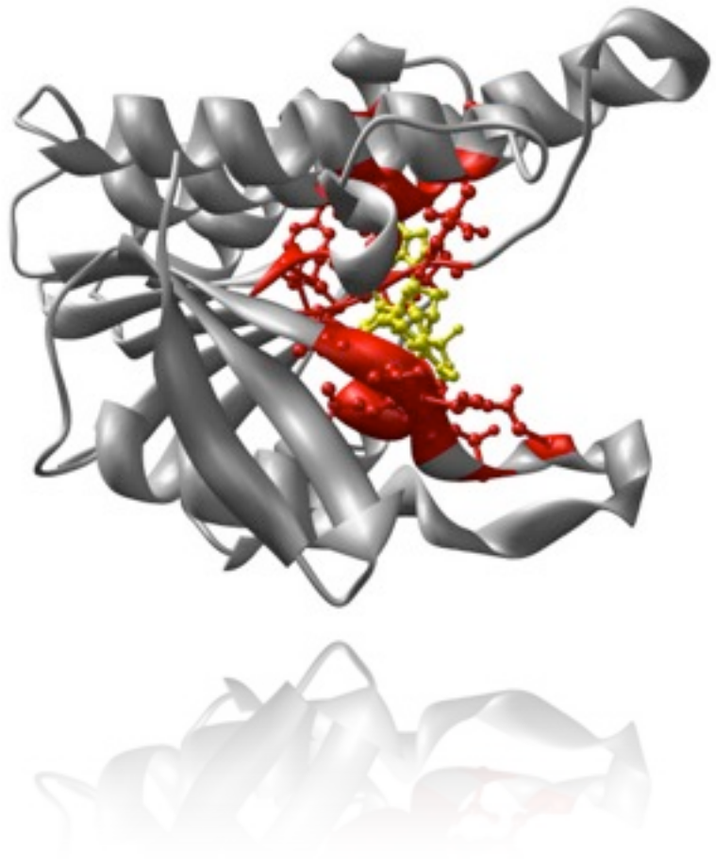

For 20% protein structures function is *unknown*

	Structural Genomics*	Traditional methods
Annotated**	654	28,342
Not Annotated	506 (43.6%)	6,815 (19,4%)
Total deposited	1,160	35,157

** annotated as STRUCTURAL GENOMICS in the header of the PDB file*
***annotated with either CATH, SCOP, Pfam or GO terms in the MSD database*
36,317 protein structures, as of August 8th, 2006

Representation

Sequence conservation

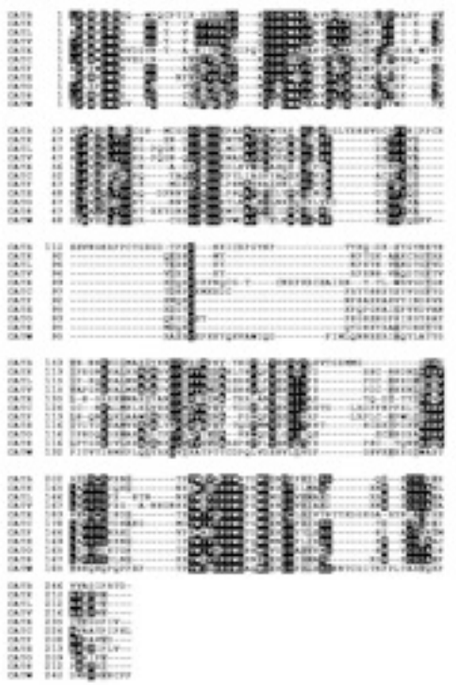

Surface geometry

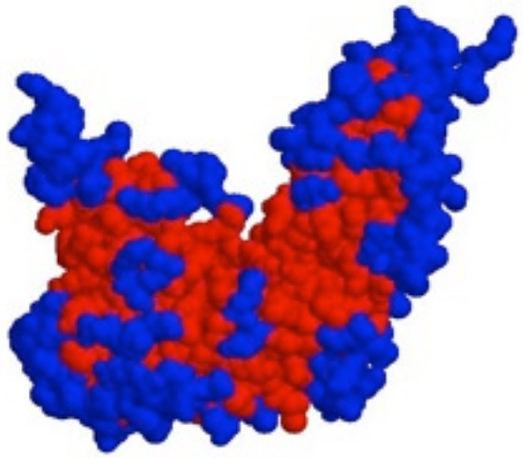

Structure conservation

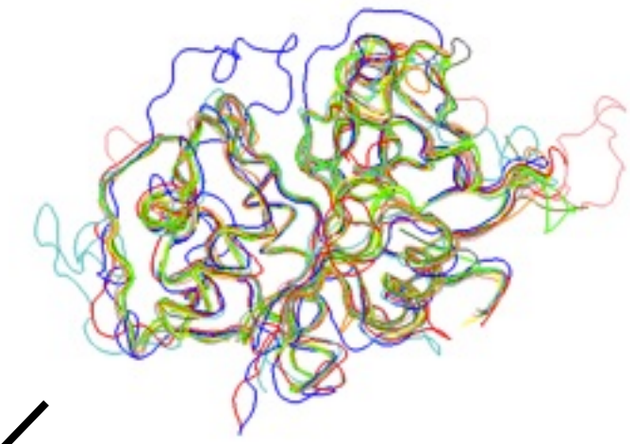

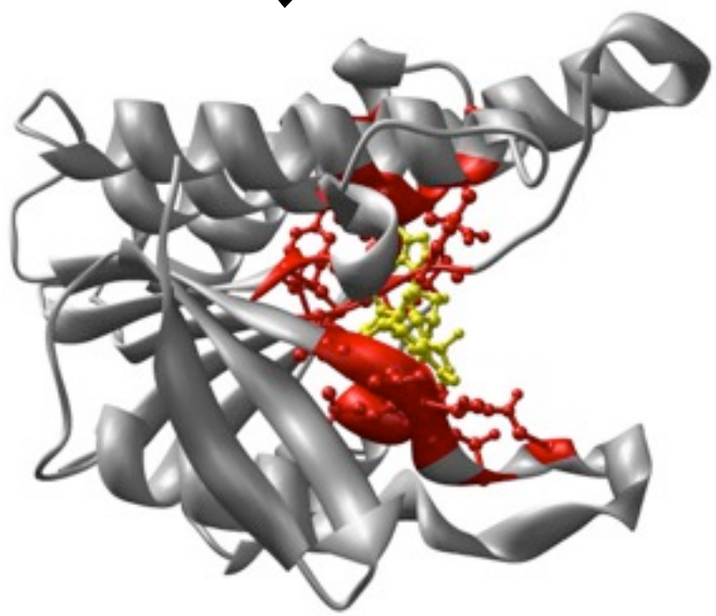

Electrostatics

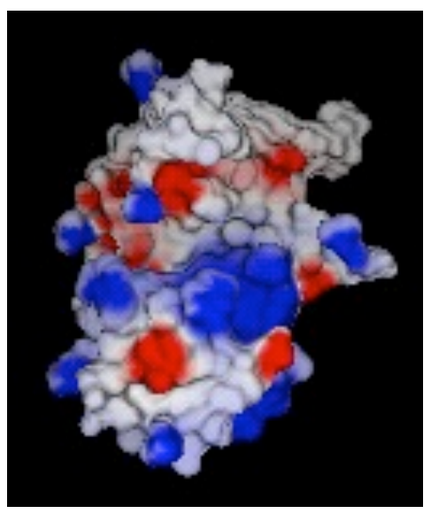

Solvent accessibility

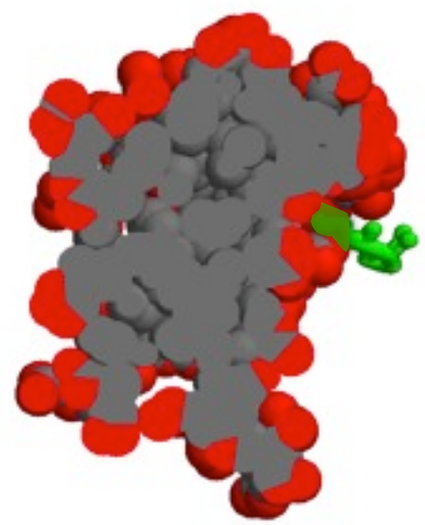

Scoring

NAD

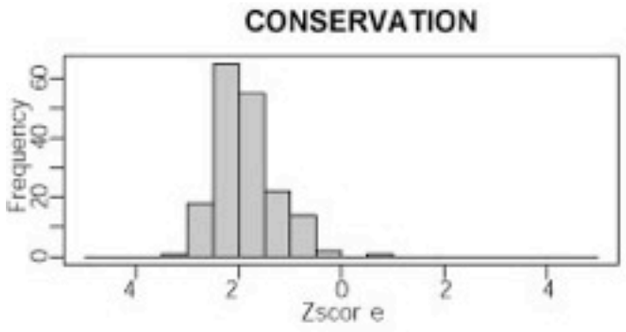

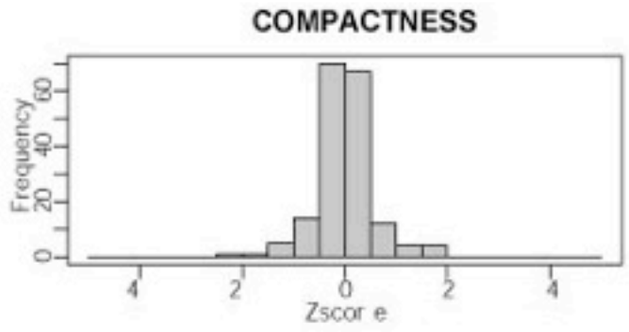

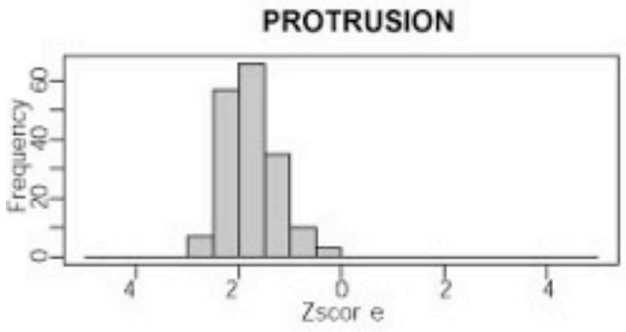

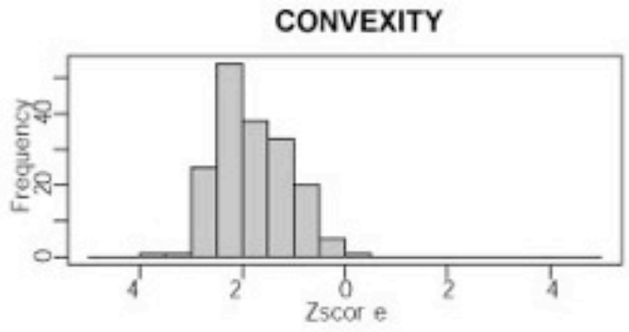

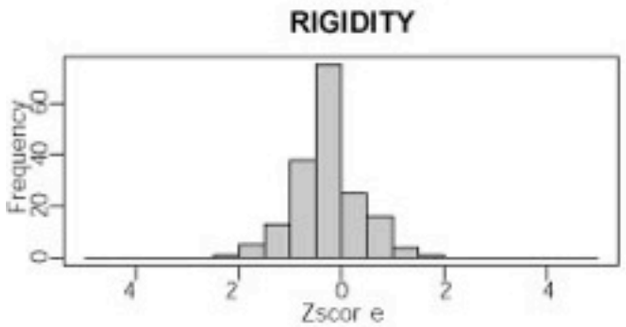

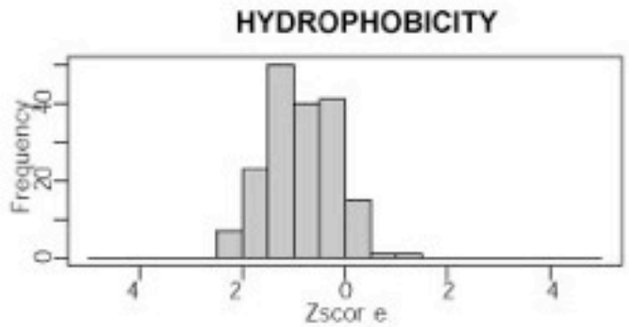

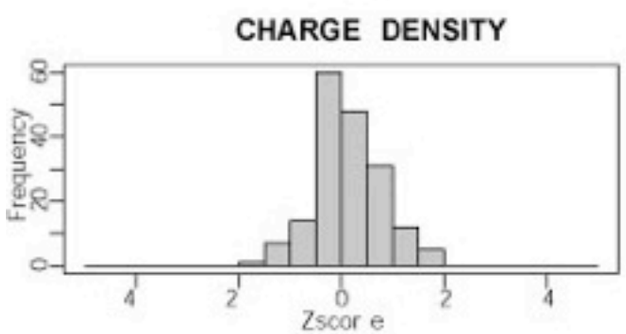

$$\rightarrow \quad w_k = \frac{1}{M} \sum_{\alpha=1}^{M} \tilde{f}_k^{(\alpha)}$$

M = number of proteins in training set

Ligand fingerprints

	Compactness	Conservation	Charge density	B-factor	Protrusion coefficient	Convexity score	Hydrophobicity
ADP	-1.266	-2.009	0.447	-0.414	-1.521	-1.388	-0.118
AMP	-1.62	-1.962	0.341	-0.381	-1.909	-1.944	-0.518
ANP	-1.007	-2.227	0.176	-0.392	-1.706	-1.595	-0.14
ATP	-1.122	-2.156	0.228	-0.274	-1.845	-1.768	0.038
BOG	-2.067	-0.012	0.552	-0.465	-0.356	-0.49	-0.781
CIT	-2.948	-1.58	0.563	-0.527	-0.922	-0.838	-0.113
FAD	0.505	-2.108	0.366	-0.702	-1.735	-1.725	-0.75
FMN	-1.132	-1.98	0.382	-0.387	-1.803	-1.886	-0.695
FUC	-3.43	0.016	-0.295	-0.123	0.002	0.132	0.459
GAL	-3.186	-0.538	-0.234	-0.068	-0.906	-0.987	0.298
GDP	-1.061	-1.471	0.409	-0.81	-1.472	-1.423	0.182
GLC	-2.813	-1.247	-0.207	-0.399	-1.247	-1.337	-0.089
HEC	-0.172	-0.912	0.286	-0.325	-1.153	-1.27	-1.282
HEM	-0.651	-1.571	0.683	-0.51	-1.797	-1.937	-1.47
MAN	-3.72	0.131	0.105	-0.52	-0.605	-0.509	0.405
MES	-3.049	-0.24	-0.338	-0.479	-0.714	-0.926	0.296
NAD	-0.005	-1.852	0.156	-0.232	-1.775	-1.804	-0.858
NAG	-3.419	-0.46	-0.126	-0.154	-0.341	-0.523	-0.078
NAP	-0.009	-1.898	0.612	-0.321	-1.587	-1.656	-0.336
NDP	0.217	-1.741	0.535	-0.312	-1.463	-1.562	-0.498

Ligand fingerprints

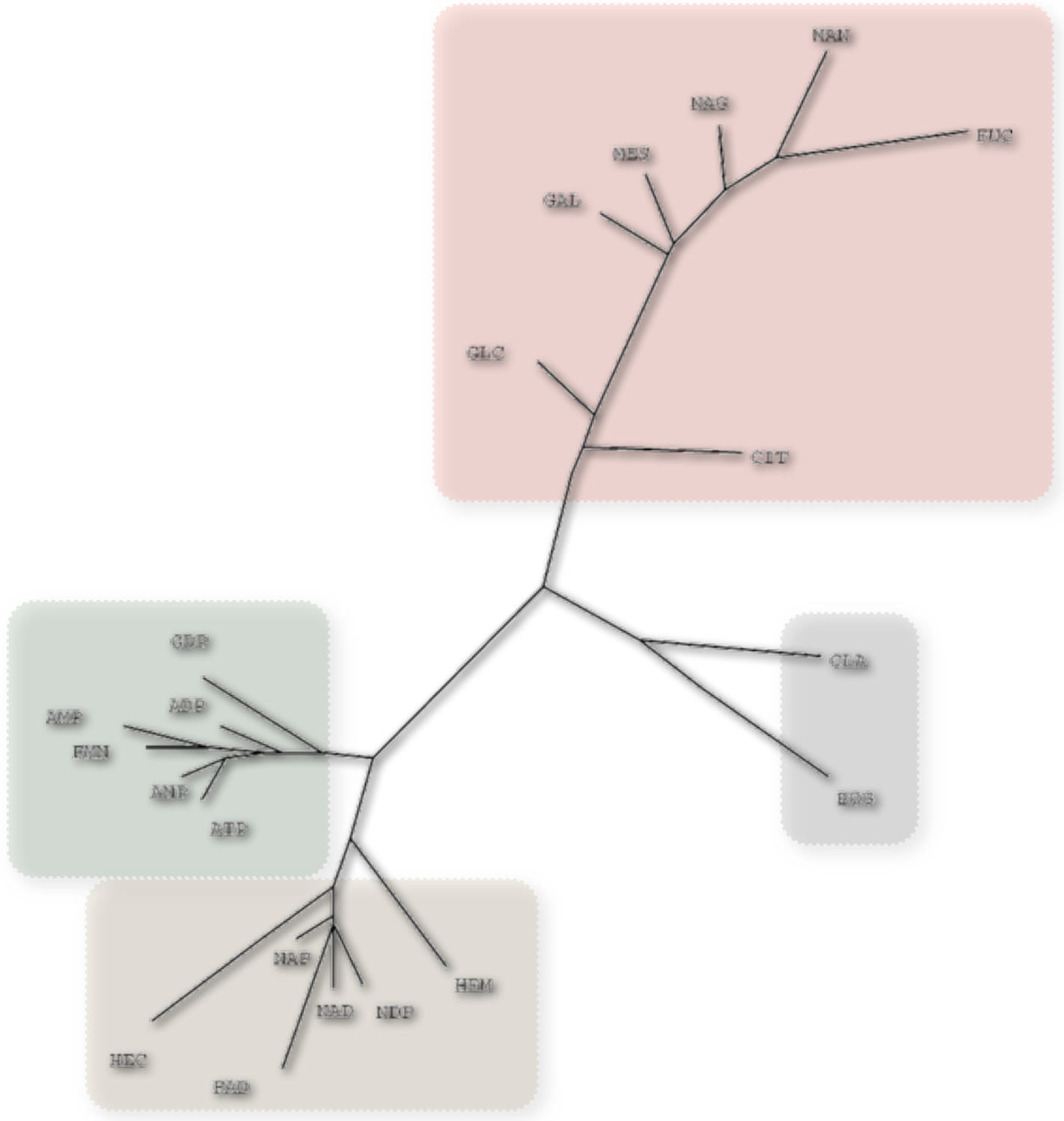

Prediction accuracy

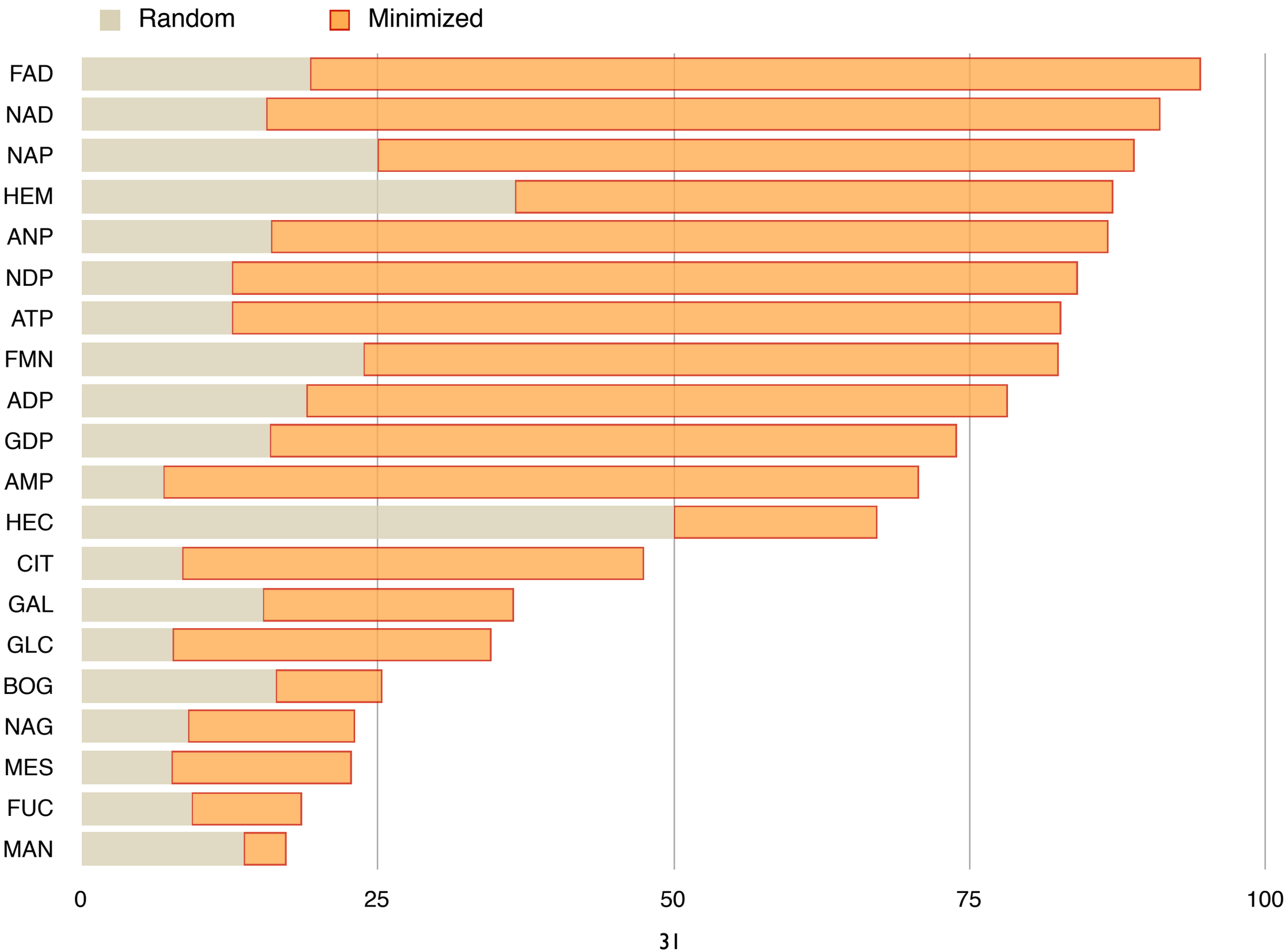

Protein function from structure

Comparative annotation. AnnoLite and AnnoLyze.

Marti-Renom et al. The AnnoLite and AnnoLyze programs for comparative annotation of protein structures. BMC Bioinformatics (2007) vol. 8 (Suppl 4) pp. S4

BMC Bioinformatics

BioMed Central

Proceedings

Open Access

The AnnoLite and AnnoLyze programs for comparative annotation of protein structures

Marc A Marti-Renom*[1], Andrea Rossi[2], Fátima Al-Shahrour[3], Fred P Davis[2], Ursula Pieper[2], Joaquín Dopazo[3] and Andrej Sali[2]

Address: [1]Structural Genomics Unit, Bioinformatics Department, Centro de Investigación Príncipe Felipe (CIPF), Valencia, Spain, [2]Departments of Biopharmaceutical Sciences and Pharmaceutical Chemistry, and California Institute for Quantitative Biomedical Research, University of California at San Francisco, San Francisco, CA 94143, USA and [3]Functional Genomics Unit, Bioinformatics Department, Centro de Investigación Príncipe Felipe (CIPF), Valencia, Spain

Email: Marc A Marti-Renom* - mmarti@cipf.es; Andrea Rossi - andrea@salilab.org; Fátima Al-Shahrour - falshahrour@cipf.es; Fred P Davis - fred@salilab.org; Ursula Pieper - Ursula@salilab.org; Joaquín Dopazo - jdopazo@cipf.es; Andrej Sali - sali@salilab.org

* Corresponding author

from The Second Automated Function Prediction Meeting
La Jolla, CA, USA. 30 August – 1 September 2006

Published: 22 May 2007

BMC Bioinformatics 2007, **8**(Suppl 4):S4 doi:10.1186/1471-2105-8-S4-S4

This article is available from: http://www.biomedcentral.com/1471-2105/8/S4/S4

Abstract

Background: Advances in structural biology, including structural genomics, have resulted in a rapid increase in the number of experimentally determined protein structures. However, about half of the structures deposited by the structural genomics consortia have little or no information about their biological function. Therefore, there is a need for tools for automatically and comprehensively annotating the function of protein structures. We aim to provide such tools by applying comparative protein structure annotation that relies on detectable relationships between protein structures to transfer functional annotations. Here we introduce two programs, AnnoLite and AnnoLyze, which use the structural alignments deposited in the DBAli database.

Description: AnnoLite predicts the SCOP, CATH, EC, InterPro, PfamA, and GO terms with an average sensitivity of ~90% and average precision of ~80%. AnnoLyze predicts ligand binding site and domain interaction patches with an average sensitivity of ~70% and average precision of ~30%, correctly localizing binding sites for small molecules in ~95% of its predictions.

Conclusion: The AnnoLite and AnnoLyze programs for comparative annotation of protein structures can reliably and automatically annotate new protein structures. The programs are fully accessible via the Internet as part of the DBAli suite of tools at http://salilab.org/DBAli/.

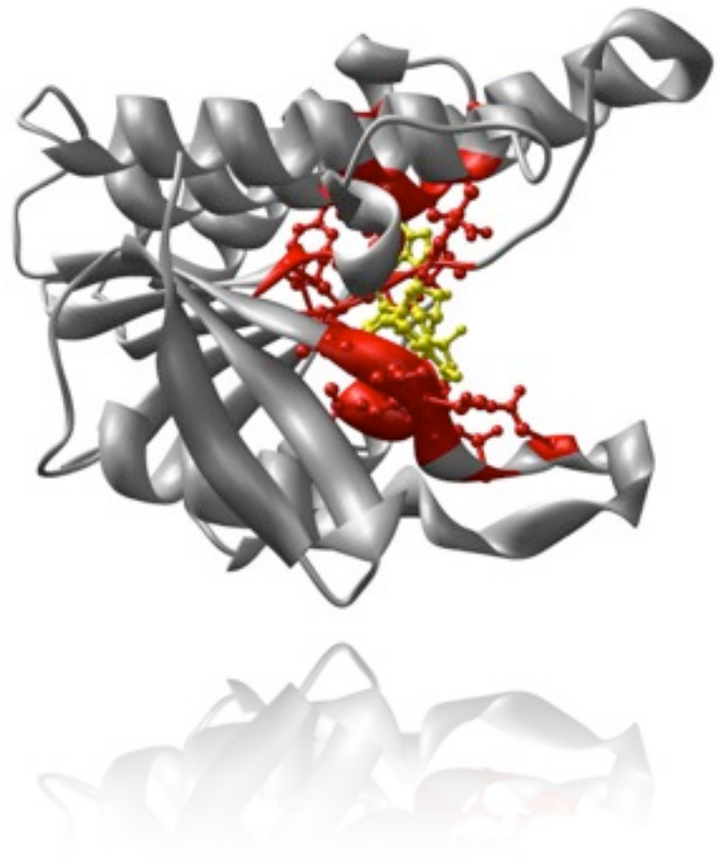

Background

Genomic efforts are providing us with complete genetic blueprints for hundreds of organisms, including humans. We are now faced with assigning, understanding, and modifying the functions of proteins encoded by these genomes. This task is generally facilitated by protein 3D

DBAli$_{v2.0}$ database

http://www.dbali.org

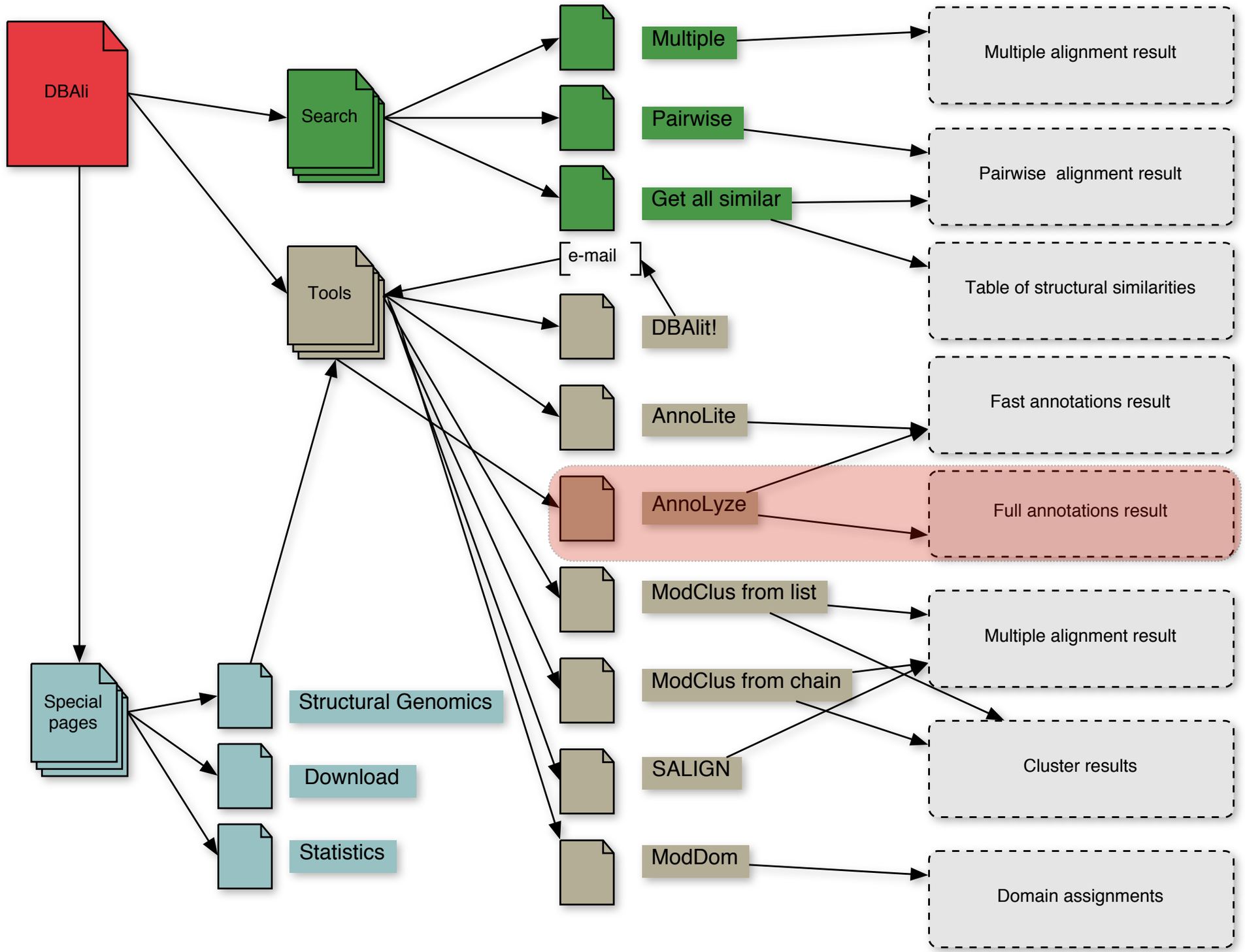

AnnoLyze

Inherited ligands: 4

Ligand	Av. binding site seq. id.	Av. residue conservation	Residues in predicted binding site (size proportional to the local conservation)
MO2	59.03	0.185	48 49 52 62 63 66 67 113 116
CRY	20.00	0.111	23 29 31 37 44 48 49 83 85 94 96 103 121
BOG	20.00	0.111	19 20 21 48 49 51 96 98 136
ACY	15.87	0.163	23 29 31 37 44 45 81 83 85 94 96 98 103 121 135

Inherited partners: 1

Partner	Av. binding site seq. id.	Av. residue conservation	Residues in predicted binding site (size proportional to the local conservation)
d.113.1.1	23.68	0.948	19 20 50 51 52 53 54 55 56 57 58 77 78 79 80 81 82 83 84 85 93 95 97 99 134 135 138 142 145

Benchmark

	Number of chains
Initial set*	78,167
LigBase**	30,126
Non-redundant set***	4,948 (8,846 ligands)

*all PDB chains larger than 30 aminoacids in length (8th of August, 2006)
**annotated with at least one ligand in the LigBase database
***not two chains can be structurally aligned within 3A, superimposing more than 75% of their Cα atoms, result in a sequence alignment with more than 30% identity, and have a length difference inferior to 50aa

	Number of chains
Initial set*	78,167
πBase**	30,425
Non-redundant set***	4,613 (11,641 partnerships)

*all PDB chains larger than 30 aminoacids in length (8th of August, 2006)
**annotated with at least one partner in the πBase database
***not two chains can be structurally aligned within 3A, superimposing more than 75% of their Cα atoms, result in a sequence alignment with more than 30% identity, and have a length difference inferior to 50aa

Method

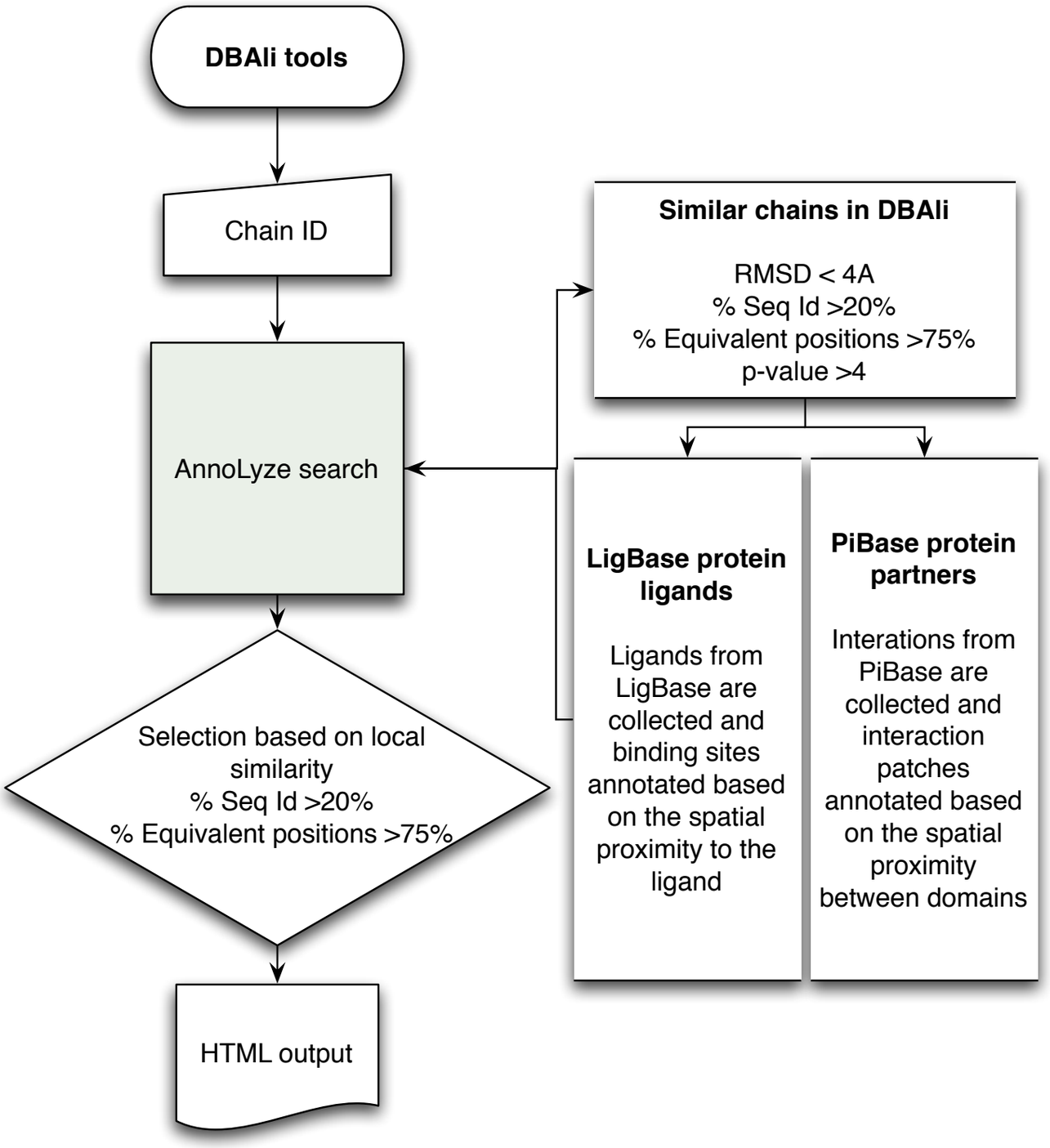

Inherited ligands: 4

Ligand	Av. binding site seq. id.	Av. residue conservation	Residues in predicted binding site (size proportional to the local conservation)
MO2	59.03	0.185	48 49 52 62 63 66 67 113 116
CRY	20.00	0.111	23 29 31 37 44 48 49 83 85 94 96 103 121
8OG	20.00	0.111	19 20 21 48 49 51 96 98 136
ACY	15.87	0.163	23 29 31 37 44 45 81 83 85 94 96 98 103 121 135

Inherited partners:1

Partner	Av. binding site seq. id.	Av. residue conservation	Residues in predicted binding site (size proportional to the local conservation)
d.113.1.1	23.68	0.948	19 20 50 51 52 53 54 55 56 57 58 77 78 79 80 81 82 83 84 85 93 95 97 99 134 135 138 142 145

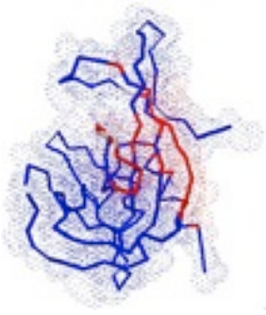

Scoring function

Ligands

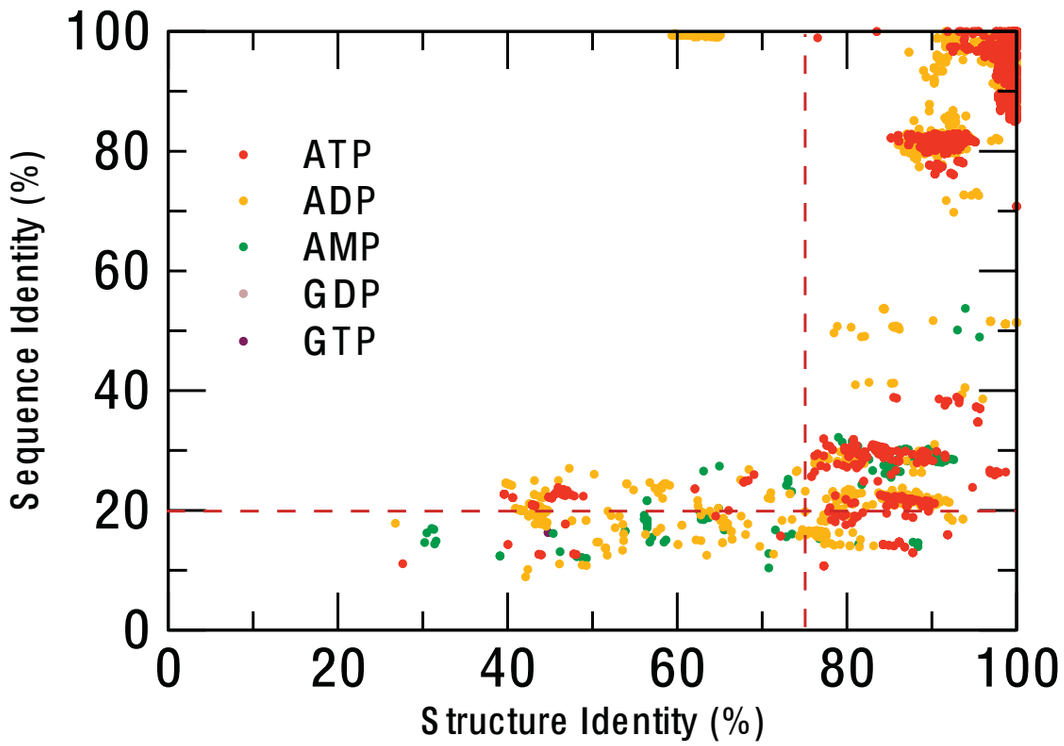

Partners

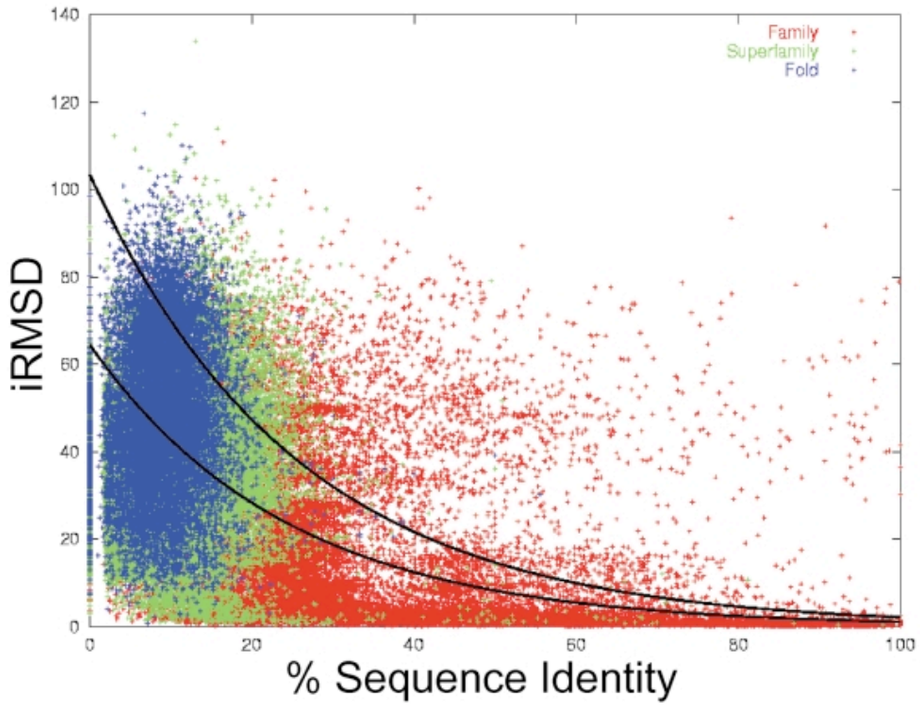

Aloy *et al.* (2003) J.Mol.Biol. 332(5):989-98.

Sensitivity .vs. Precision

	Optimal cut-off	Sensitivity (%) Recall or TPR	Precision (%)
Ligands	30%	71.9	13.7
Partners	40%	72.9	55.7

$$\text{Sensitivity} = \frac{TP}{TP + FN} \qquad \text{Precision} = \frac{TP}{TP + FP}$$

Example (2azwA)

Structural Genomics Unknown Function

Molecule: MutT/nudix family protein

PDB ID: 2azw:A

Header:
STRUCTURAL GENOMICS, UNKNOWN FUNCTION

Compound:
MOL_ID: 1; MOLECULE: MUTT/NUDIX FAMILY PROTEIN; CHAIN: A; ENGINEERED: YES

Source:
MOL_ID: 1; ORGANISM_SCIENTIFIC: ENTEROCOCCUS FAECALIS V583; ORGANISM_COMMON: BACTERIA; EXPRESSION_SYSTEM: ESCHERICHIA COLI; EXPRESSION_SYSTEM_COMMON: BACTERIA; EXPRESSION_SYSTEM_STRAIN: BL21(DE3); EXPRESSION_SYSTEM_VECTOR_TYPE: PLASMID; EXPRESSION_SYSTEM_PLASMID: PET15B

Resolution: 1.90Å

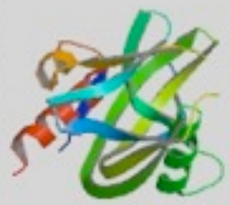

Links: none

SCOP: none

CATH: none

Ligands: none

Interacting partners: none

Sequence:
Md5: 09b13d23ceae0fdfcaddec636e2ddfa6KTPTAAAS
Length: 146

```
KTPTPGKREE TLTYQTRYAA YIIVSKPENN TMVLVQAPNG AYFLPGGEIE
GTETKEEAIH REVLEELGIS VEIGCYLGEA DEYFYSNHRQ TAYYNPGYFY
VANTWRQLSE PLRTNTLHWV APEEAVRLLK RGSHRWAVEK WLAAAS
```

Similar structures: 20
Similar sequences: 890
Most similar structure in DBAli:

Code	SeqId(%)	EqPos	RMSD	P-Value	See
1vc9:A	22.76	123	3.57	17.28	ali

Most similar sequence in DBAli:

Code	SeqId(%)	EqPos	RMSD	P-Value	See
1vcd:B	24.59	122	3.47	17.00	ali

P-value distribution:

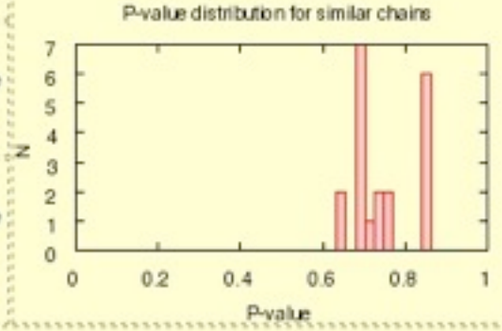

Keyword distribution:

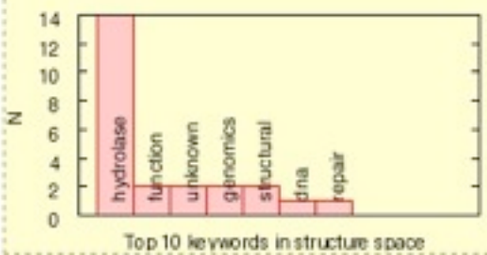

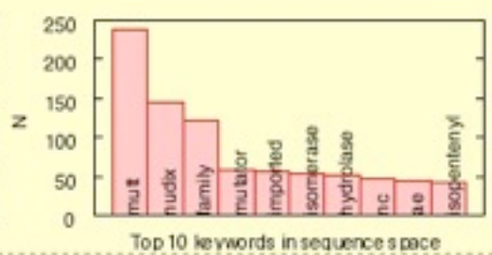

SCOP and CATH distribution for similar structures:

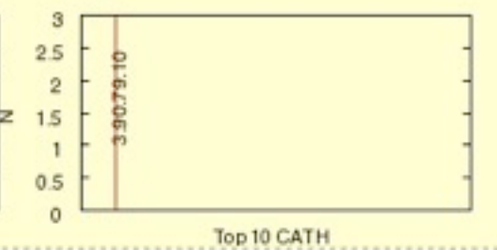

Inherited ligands: 4

Ligand	Av. binding site seq. id.	Av. residue conservation	Residues in predicted binding site (size proportional to the local conservation)
MO2	59.03	0.185	48 49 52 62 63 66 67 113 116
CRY	20.00	0.111	23 29 31 37 44 48 49 83 85 94 96 103 121
8OG	20.00	0.111	19 20 21 48 49 51 96 98 136
ACY	15.87	0.163	23 29 31 37 44 45 81 83 85 94 96 98 103 121 135

Inherited partners: 1

Partner	Av. binding site seq. id.	Av. residue conservation	Residues in predicted binding site (size proportional to the local conservation)
d.113.1.1	23.68	0.948	19 20 50 51 52 53 54 55 56 57 58 77 78 79 80 81 82 83 84 85 93 95 97 99 134 135 138 142 145

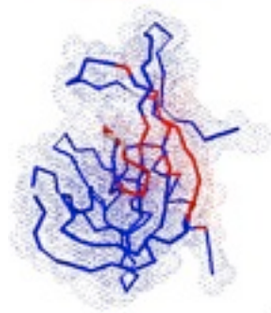

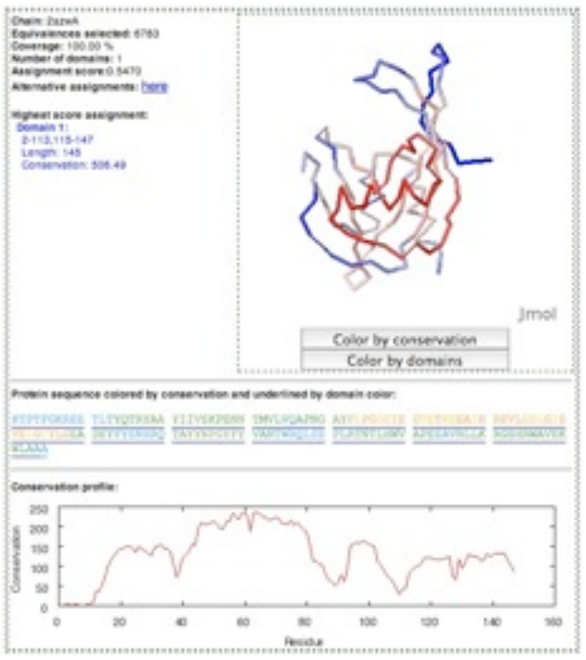

	Conf.	P-value	Link	Description
CATH:	●	1.1e-20	3.90.79.10	Nucleoside Triphosphate Pyrophosphohydrolase
SCOP:	●	4.2e-29	d.113.1.1	MutT-like
PFAM:	●	2.0e-74	PF00293	NUDIX domain
InterPro:	●	1.9e-65	IPR000086	NUDIX hydrolase
	●	2.7e-20	IPR003561	Mutator MutT
	●	2.9e-14	IPR002667	Isopentenyl-diphosphate delta-isomerase
EC Number:	●	1.7e-4	3.6.1.17	Bis(5'-nucleosyl)-tetraphosphatase (asymmetrical).
GO Molecular Function:	●	4.5e-19	0008413	8-oxo-7,8-dihydroguanine triphosphatase activity ;
	●	3.8e-13	0004452	isopentenyl-diphosphate delta-isomerase activity ;
	●	1.9e-6	0016787	hydrolase activity ;
	●	5.4e-3	0004081	bis(5'-nucleosyl)-tetraphosphatase (asymmetrical) activity ;
	●	1.9e-2	0000287	magnesium ion binding ;
GO Biological Process:	●	7.7e-11	0008299	isoprenoid biosynthesis ;
	●	1.5e-5	0006974	response to DNA damage stimulus ;
	●	1.7e-5	0006260	DNA replication ;
	●	2.4e-5	0006281	DNA repair ;

AnnoLyze

http://www.dbali.org

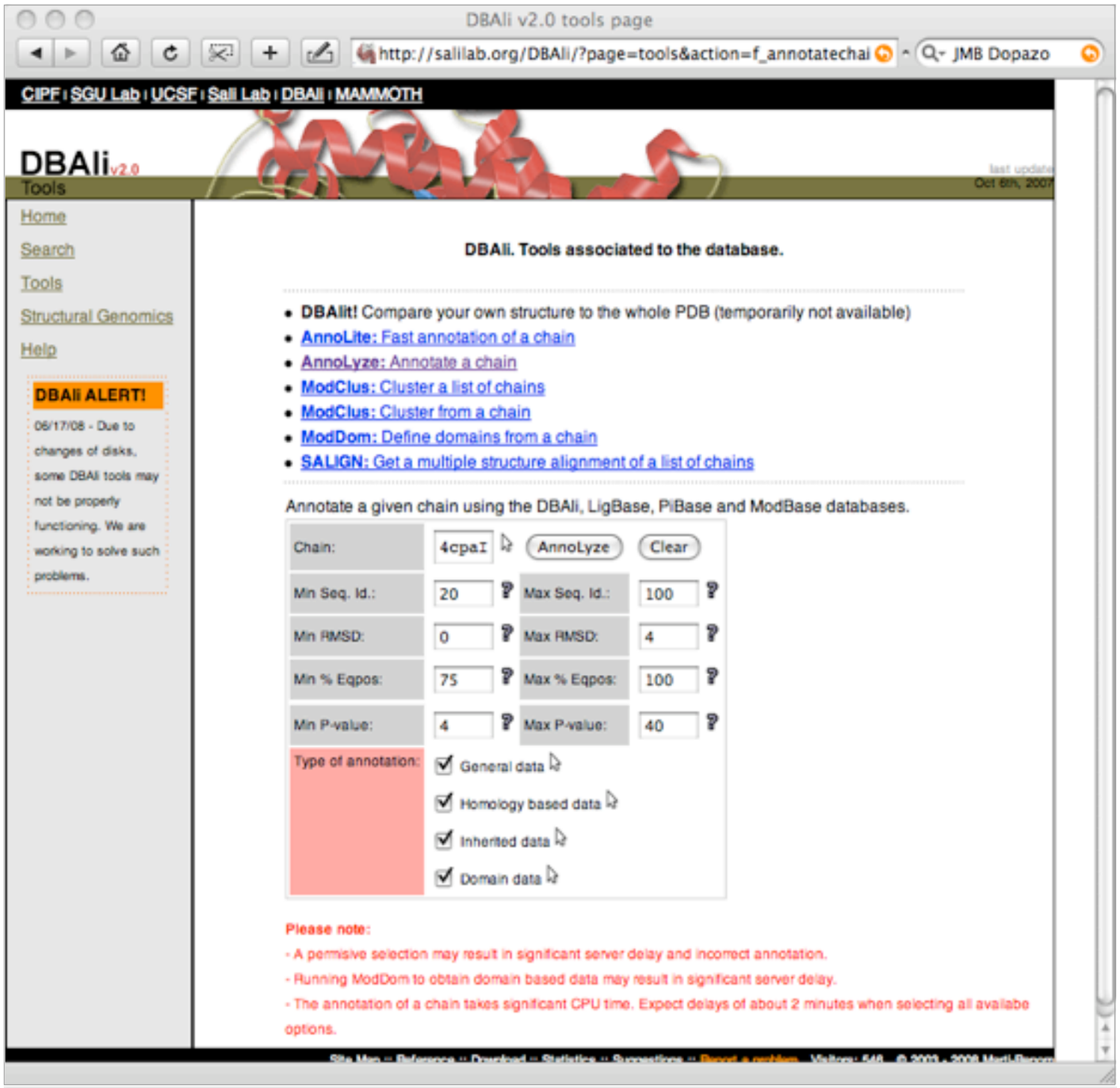

Docking of small molecules. Vina.

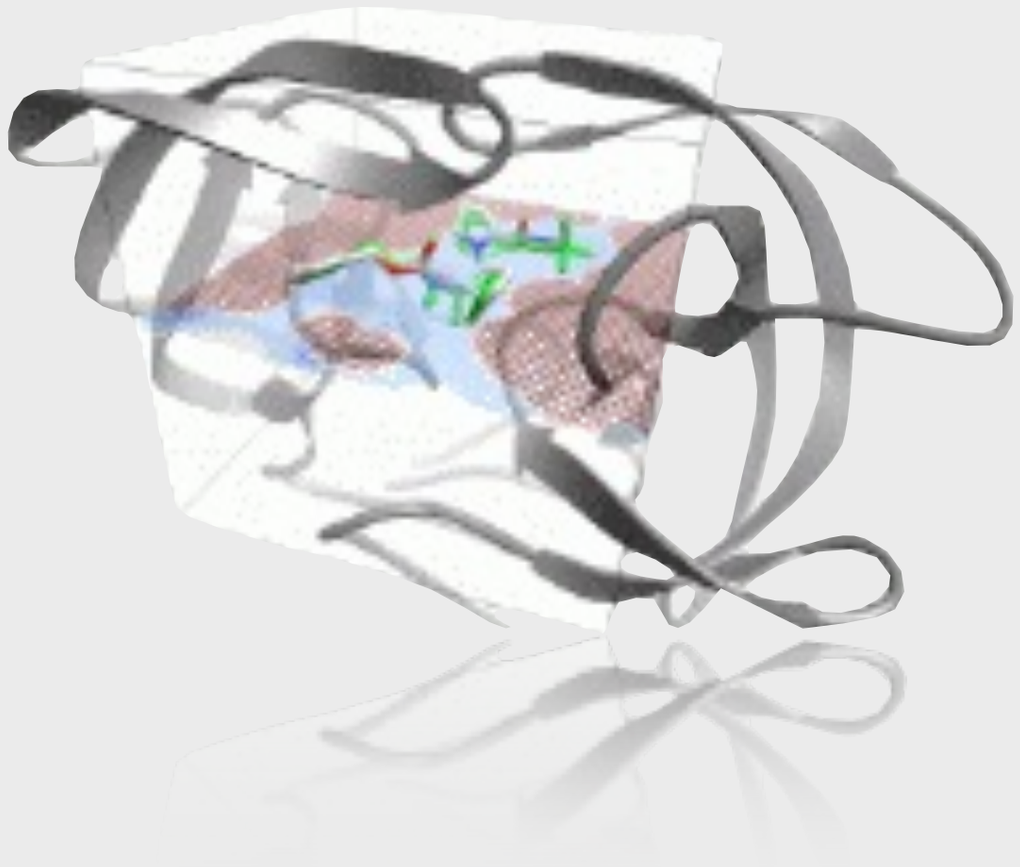

Marc A. Marti-Renom

http://bioinfo.cipf.es/sgu/

Structural Genomics Unit

Bioinformatics Department

Prince Felipe Resarch Center (CIPF), Valencia, Spain

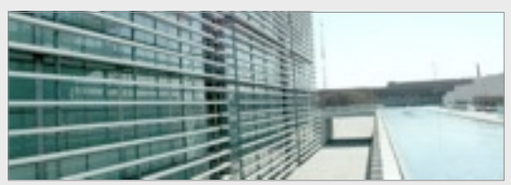

PRINCIPE FELIPE

CENTRO DE INVESTIGACION

DISCLAIMER!

Credit should go to Dr. Oleg Trott, Dr. Ruth Huey and Dr. Garret M. Morris

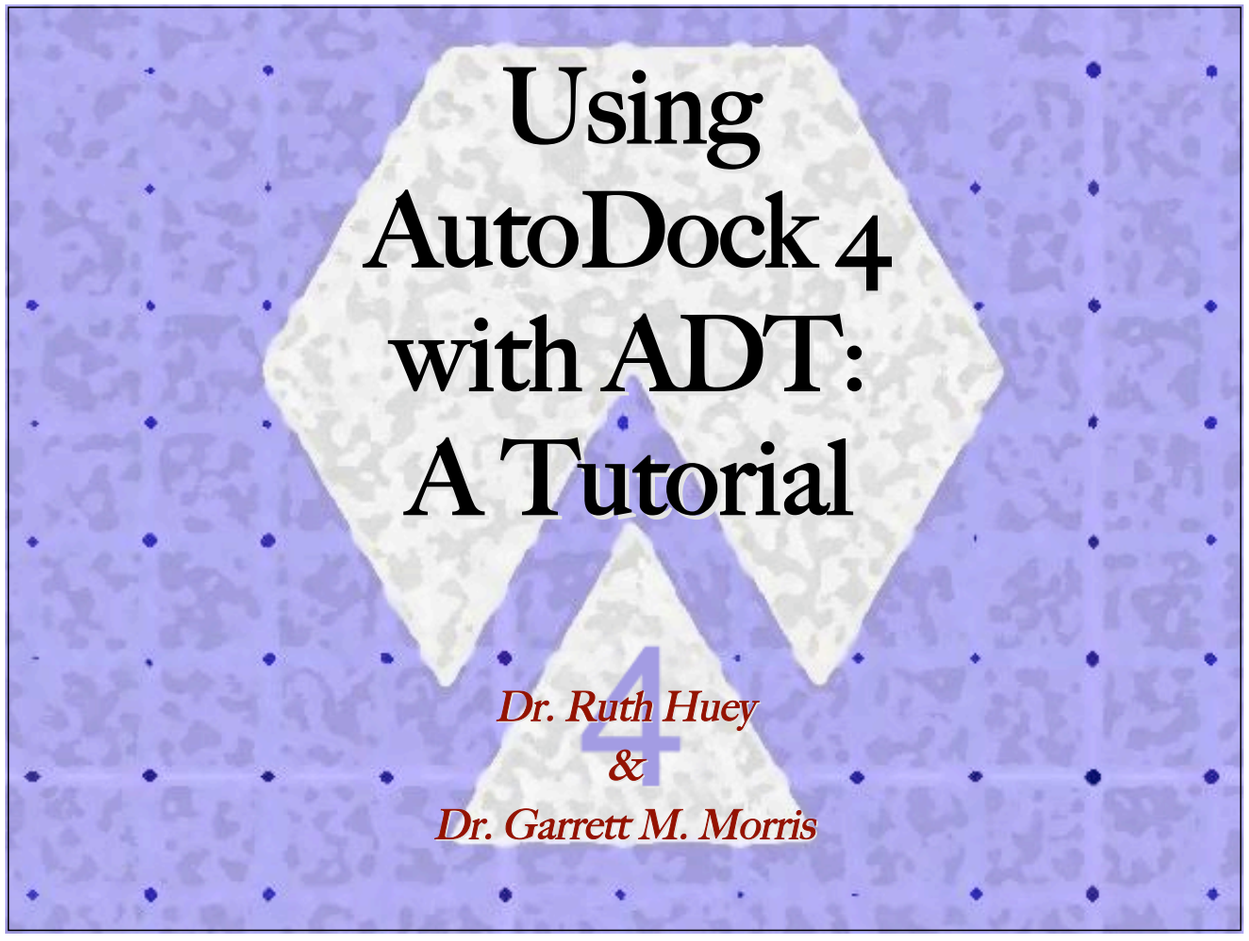

Software News and Update
AutoDock Vina: Improving the Speed and Accuracy of Docking with a New Scoring Function, Efficient Optimization, and Multithreading

OLEG TROTT, ARTHUR J. OLSON
Department of Molecular Biology, The Scripps Research Institute, La Jolla, California

Received 3 March 2009; Accepted 21 April 2009
DOI 10.1002/jcc.21334
Published online in Wiley InterScience (www.interscience.wiley.com).

Abstract: AutoDock Vina, a new program for molecular docking and virtual screening, is presented. AutoDock Vina achieves an approximately two orders of magnitude speed-up compared with the molecular docking software previously developed in our lab (AutoDock 4), while also significantly improving the accuracy of the binding mode predictions, judging by our tests on the training set used in AutoDock 4 development. Further speed-up is achieved from parallelism, by using multithreading on multicore machines. AutoDock Vina automatically calculates the grid maps and clusters the results in a way transparent to the user.

© 2009 Wiley Periodicals, Inc. J Comput Chem 00: 000–000, 2009

Key words: AutoDock; molecular docking; virtual screening; computer-aided drug design; multithreading; scoring function

Introduction

Molecular docking is a computational procedure that attempts to predict noncovalent binding of macromolecules or, more frequently, of a macromolecule (receptor) and a small molecule (ligand) efficiently, starting with their unbound structures, structures obtained from MD simulations, or homology modeling, etc. The goal is to predict the bound conformations and the binding affinity.

The prediction of binding of small molecules to proteins is of particular practical importance because it is used to screen virtual libraries of drug-like molecules to obtain leads for further drug development. Docking can also be used to try to predict the bound conformation of known binders, when the experimental holo structures are unavailable.[1]

One is interested in maximizing the accuracy of these predictions while minimizing the computer time they take, because the computational resources spent on docking are considerable. For example, hundreds of thousands of computers are used for running docking in `FightAIDS@Home` and similar projects.[2]

Theory

In the spectrum of computational approaches to modeling receptor-ligand binding,

a. molecular dynamics with explicit solvent,
b. molecular dynamics and molecular mechanics with implicit solvent, and
c. molecular docking

can be seen as making an increasing trade-off of the representational detail for computational speed.[3]

Among the assumptions made by these approaches is the commitment to a particular protonation state of and charge distribution in the molecules that do not change between, for example, their bound and unbound states. Additionally, docking generally assumes much or all of the receptor rigid, the covalent lengths, and angles constant, while considering a chosen set of covalent bonds freely rotatable (referred to as active rotatable bonds here).

Importantly, although molecular dynamics directly deals with energies (referred to as force fields in chemistry), docking is ultimately interested in reproducing chemical potentials, which determine the bound conformation preference and the free energy of binding. It is a qualitatively different concept governed not only by the minima in the energy profile but also by the shape of the profile and the temperature.[4,5]

Docking programs generally use a scoring function, which can be seen as an attempt to approximate the standard chemical potentials of the system. When the superficially physics-based terms like the 6–12 van der Waals interactions and Coulomb energies are used in the scoring function, they need to be significantly empirically weighted, in part, to account for this difference between energies and free energies.[4,5]

Correspondence to: A.J. Olson; e-mail: olson@scripps.edu
Contract/grant sponsor: NIH; contract/grant number: 2R01GM069832

http://autodock.scripps.edu

http://vina.scripps.edu

O. Trott, A. J. Olson, Journal of Computational Chemistry (2009)

Summary

- INTRO
- DOCKING
- SEARCH METHODS
- EXAMPLE

- Vina 1.1.1 with ADT

What is docking?

Predicting the best ways two molecules interact.

- Obtain the 3D structures of the two molecules
- Locate the best binding site (**Remember AnnoLyze? :-)**)
- Determine the best binding mode.

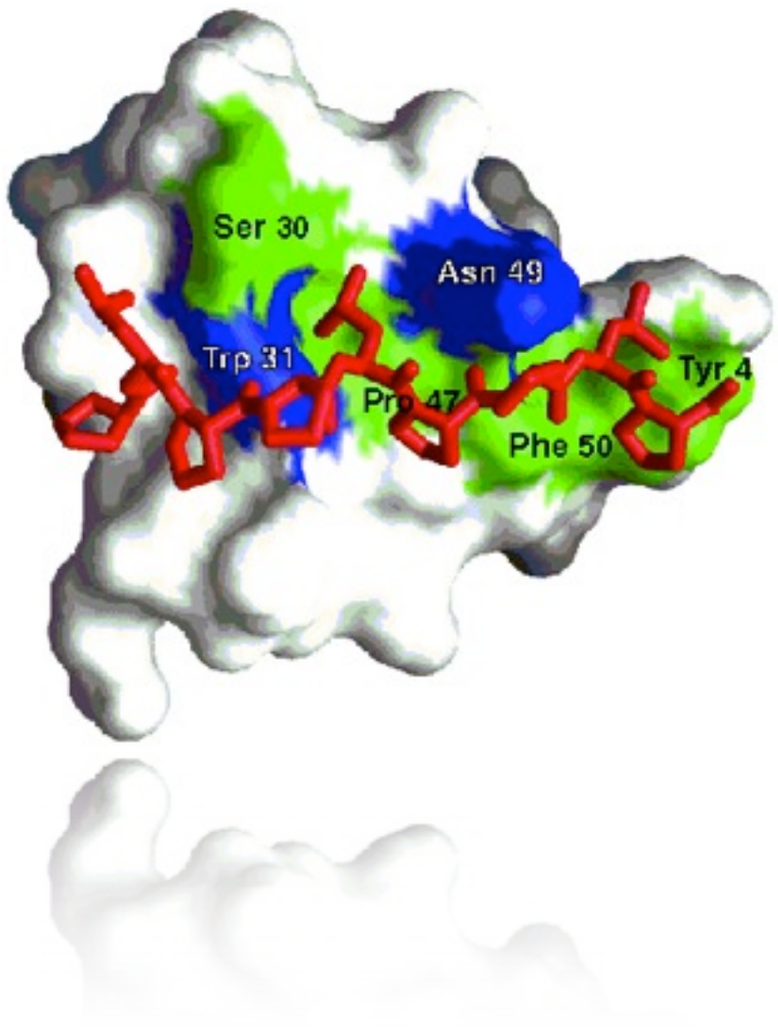

What is docking?

Predicting the **best** ways two molecules interact.

- We need to quantify or rank solutions
- We need a good scoring function for such ranking

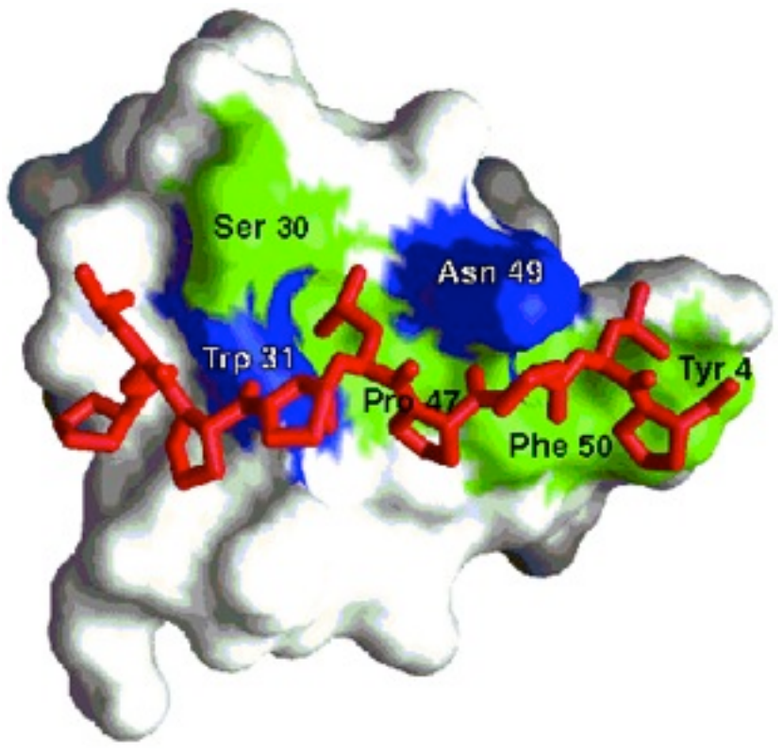

Scoring!

What is docking?

Predicting the best **ways** two molecules interact.

- X-ray and NMR structures are just ONE of the possible solutions
- There is a need for a search solution

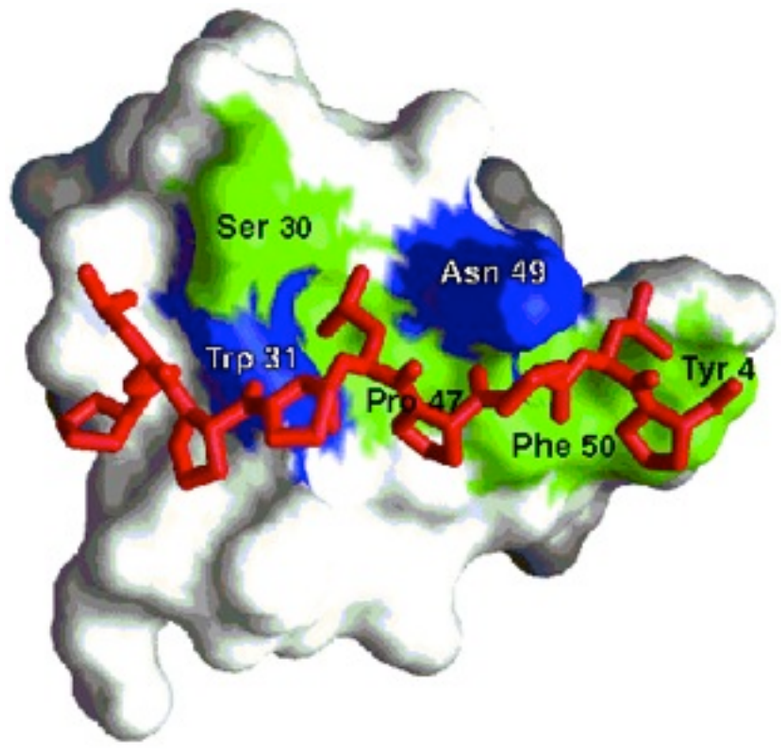

Sampling!

BIOINFORMATICS

REPRESENTATION
SCORING
SAMPLING

REPRESENTATION

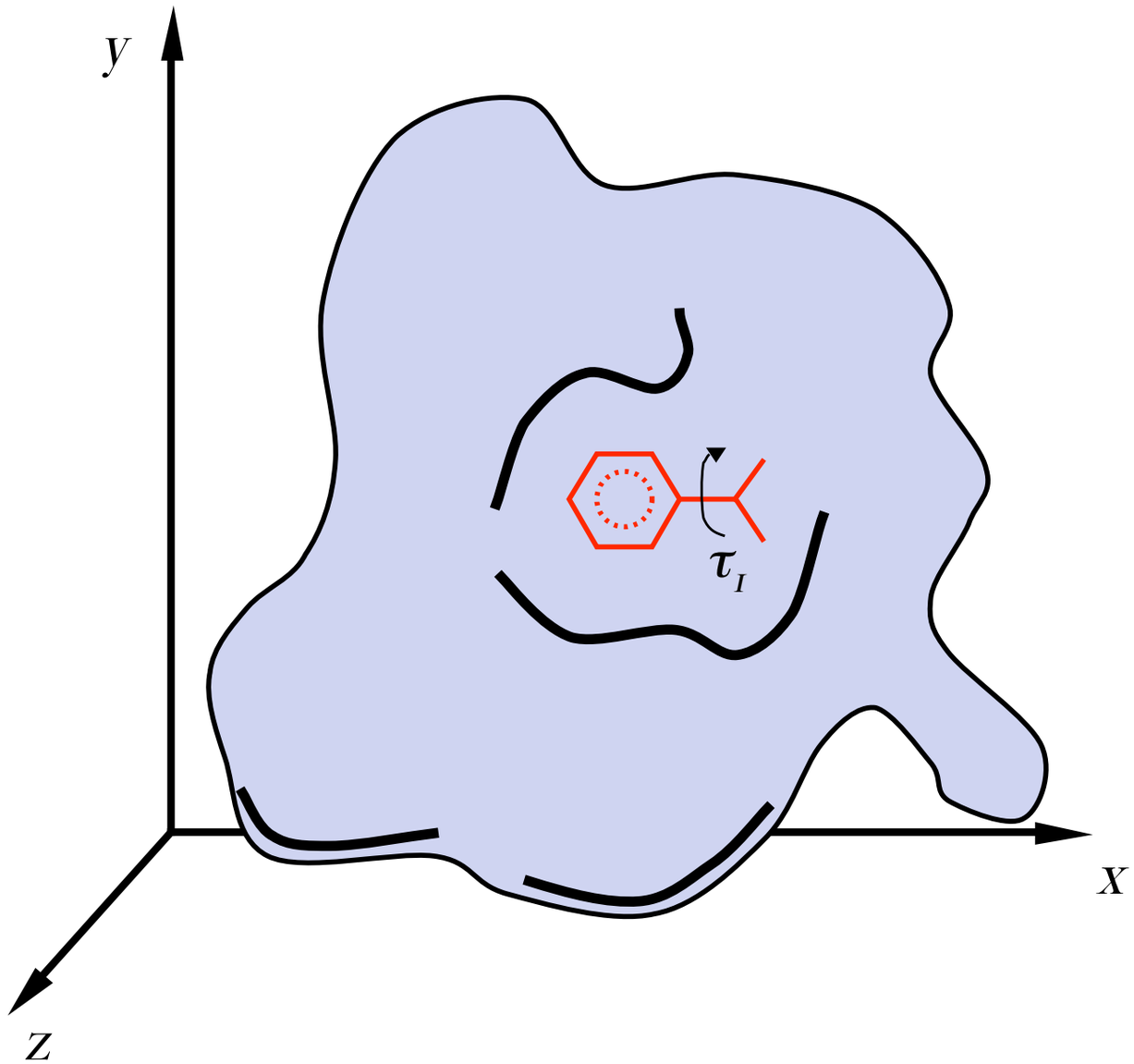

SCORING

AutoDock Vina

$$\Delta G_{binding} = \Delta G_{vdW} + \Delta G_{elec} + \Delta G_{hbond} + \Delta G_{desolv} + \Delta G_{tors}$$

- ΔG_{vdW}

  12-6 Lennard-Jones potential

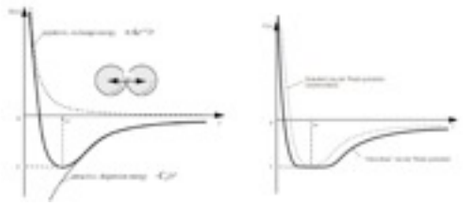

- ΔG_{elec}

  Coulombic with Solmajer-dielectric

$$\varepsilon(r) = A + \frac{B}{1 + ke^{-\lambda B r}}$$

- ΔG_{hbond}

  12-10 Potential with Goodford Directionality

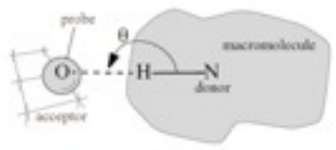

- ΔG_{desolv}

  Stouten Pairwise Atomic Solvation Parameters

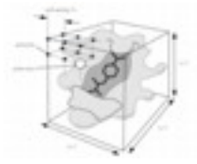

- ΔG_{tors}

  Number of rotatable bonds

PROBLEM!

Very CPU time consuming...

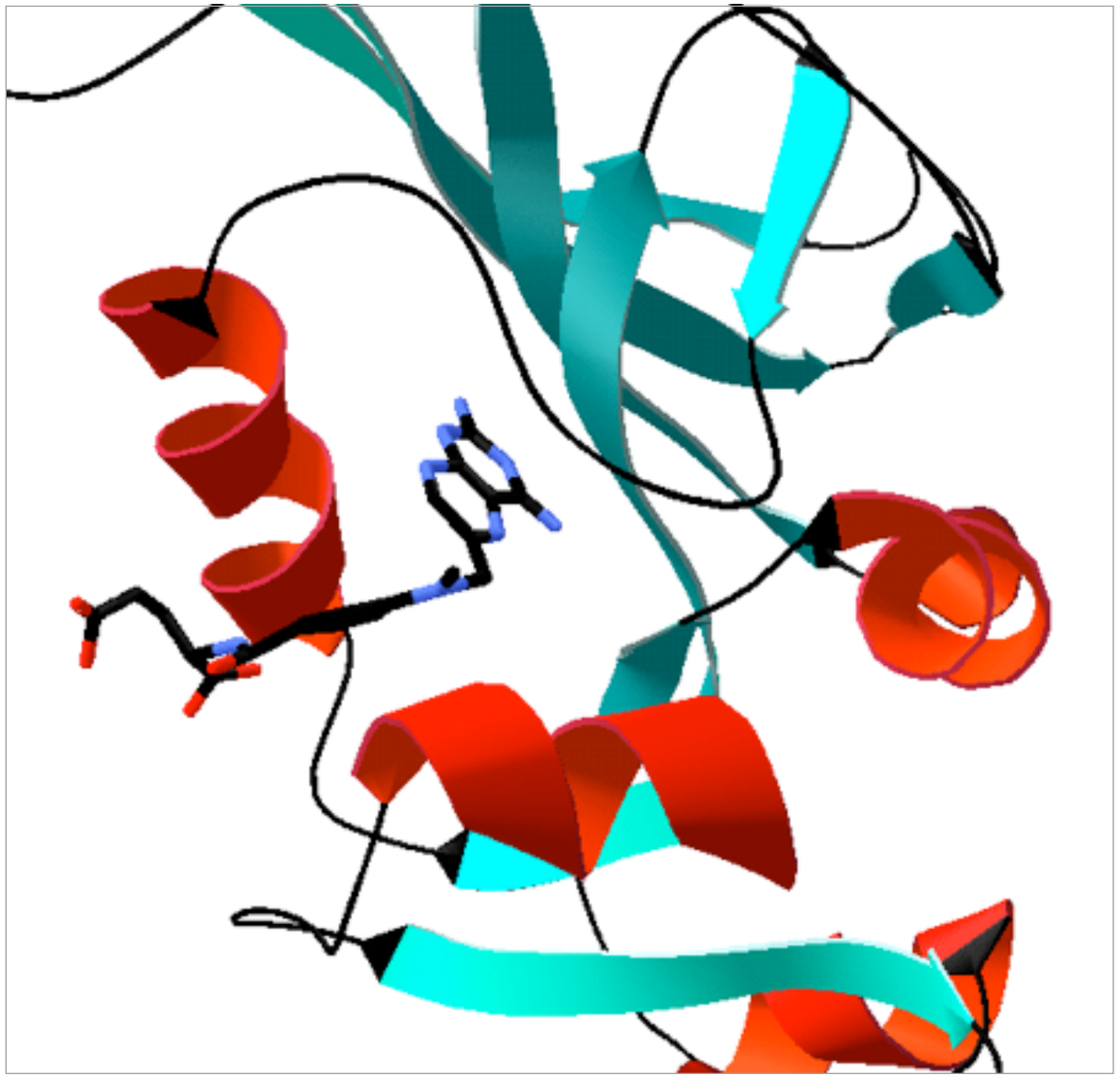

Dihidrofolate reductase with a metotrexate (4dfr.pdb)

$$N=T^{360/i}$$

N: number of conformations

T: number of rotable bonds

I: incremental degrees

Metotrexato

10 rotable bonds

30° increments (discrete)

10^{12} plausible conformations!

SOLUTION

Use of grid maps!

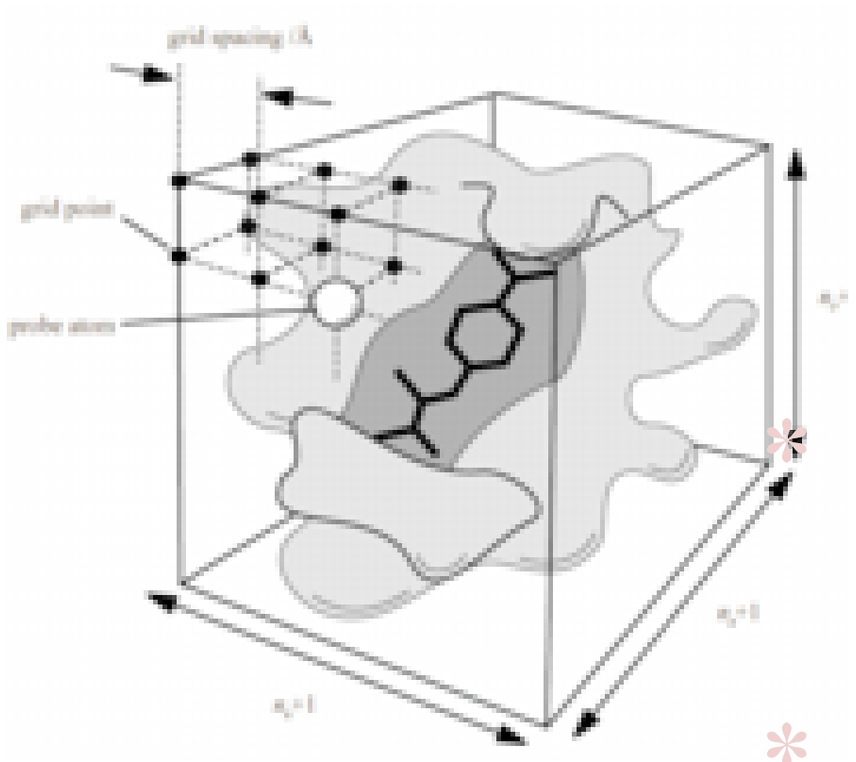

- Saves lots of time (compared to classical MM/MD)
- Need to map each atom to a grid point
- Limits the search space!

AutoGrid Vina

Use of grid maps!

- Center of grid *
  - center of ligand
  - center of receptor
  - a selected atom or coordinate
- Box dimension *
- Grid resolution (spacing)
  - default 0.375 Angstroms
- Number of grid points (dimension)
  - use ONLY even numbers
- MAKE SURE ALL LIGAND IS INSIDE GRID AND CAN MOVE!

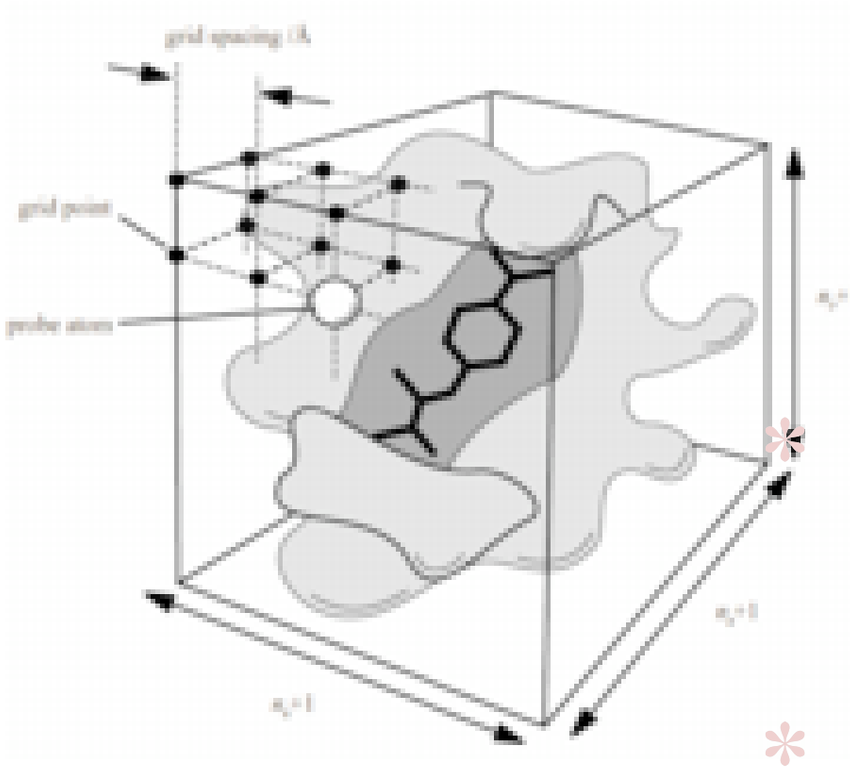

With VINA much simplified (*)

Search algorithms

Simulated Annealing

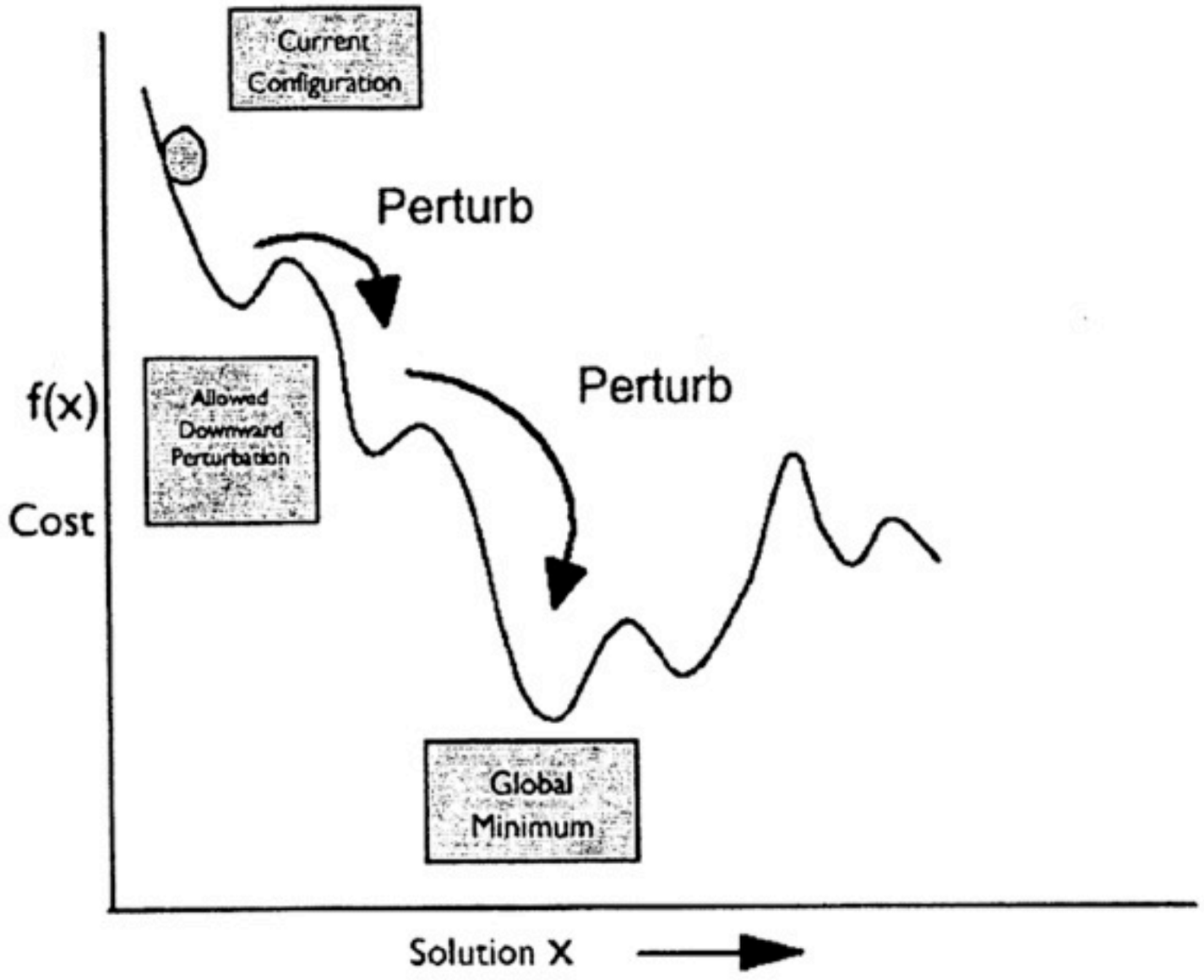

Search algorithms

Genetic Algorithm

Use of a Genetic Algorithm as a sampling method

- Each conformation is described as a set of rotational angles.
- 64 possible angles are allowed to each of the bond in the ligand.
- Each plausible dihedral angle is codified in a set of binary bits (2^6=64)
- Each conformation is codified by a so called chromosome with 4 × 6 bits (0 or 1)

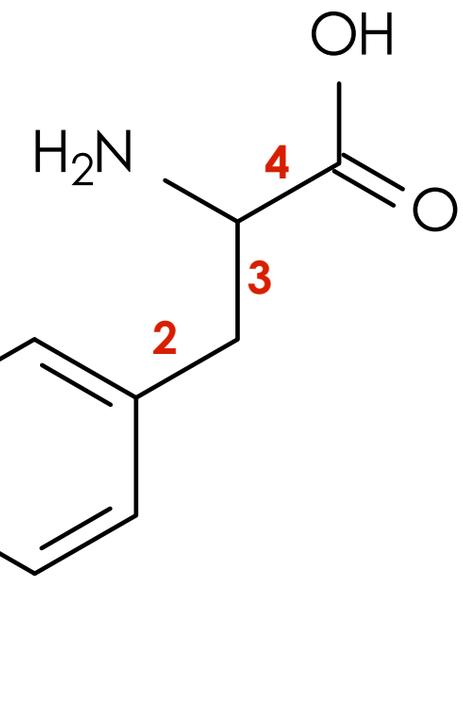

111010.010110.001011.010010

Φ_1 Φ_2 …

$$\Phi_1 = 1\times2^5 + 1\times2^4 + 1\times2^3 + 0\times2^2 + 1\times2^1 + 0\times2^0 = 58°$$

Search algorithms

Genetic Algorithm

Population (*ie*, set of chromosomes or configurations)

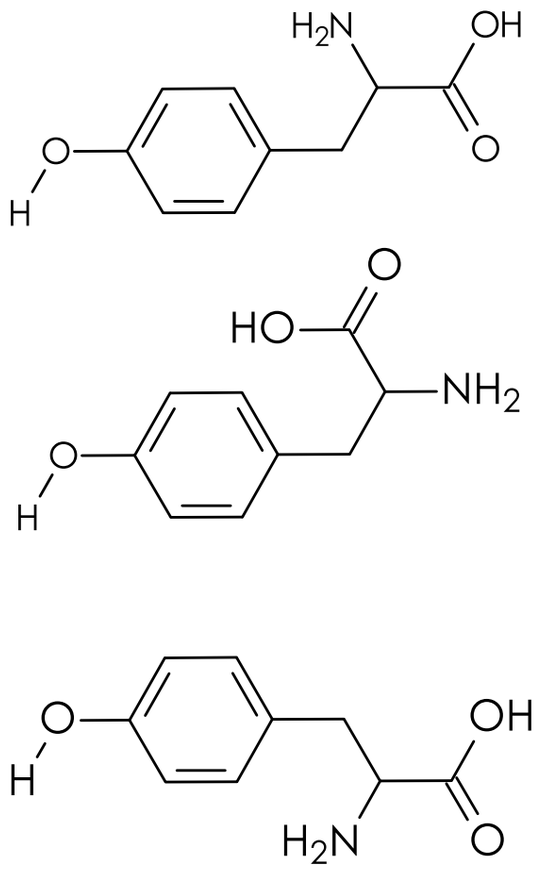

011010.010110.011010.010111 ← Chromosome

111010.010110.001011.010010

001010.010101.000101.010001

101001.101110.101010.001000

001010.101000.011101.001011

Gene

Search algorithms

Genetic Algorithm

Genetic operators...

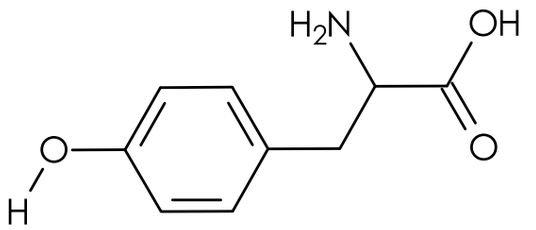

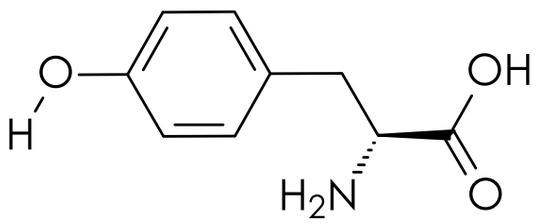

011010.010110.011010.010111

Single mutation

011010.011110.011110.010111

Search algorithms

Genetic Algorithm

Genetic operators...

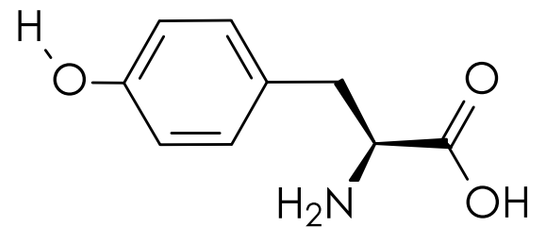

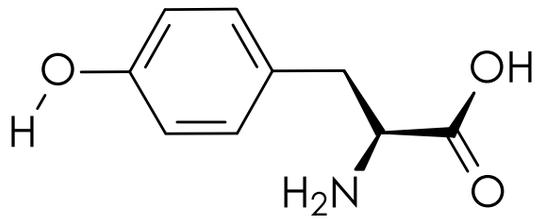

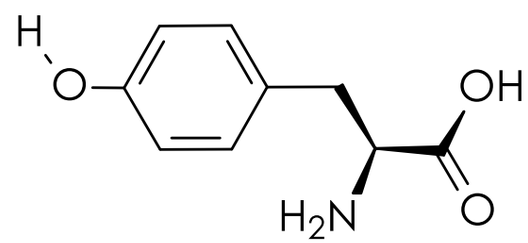

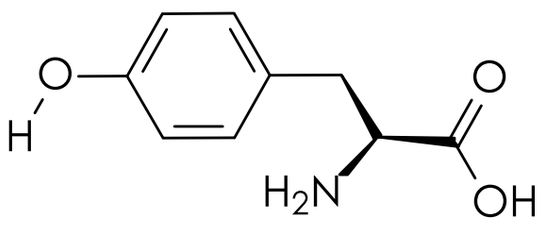

001010.010101.000101.010001

011010.010110.011010.010111

Recombination

001010.010101.011010.010111

011010.010110. 000101.010001

Search algorithms

Genetic Algorithm

Genetic operators...

011010.010110.011010.010111
111010.010110.001011.010010
001010.010101.000101.010001
101001.101110.101010.001000
001010.101000.011101.001011

Migration

111110.010010.011110.010101
101010.110110.011011.011010
001010.010101.000101.010001
101101.101010.101011.001100
011010.100000.011001.101011

AutoDock Example

Discovery of a novel binding trench in HIV Integrase

Schames, J.R., R.H. Henchman, J.S. Siegel, C.A. Sotriffer, H. Ni, and J.A. McCammon, Discovery of a novel binding trench in HIV integrase. J Med Chem, 2004. 47(8): 1879-81

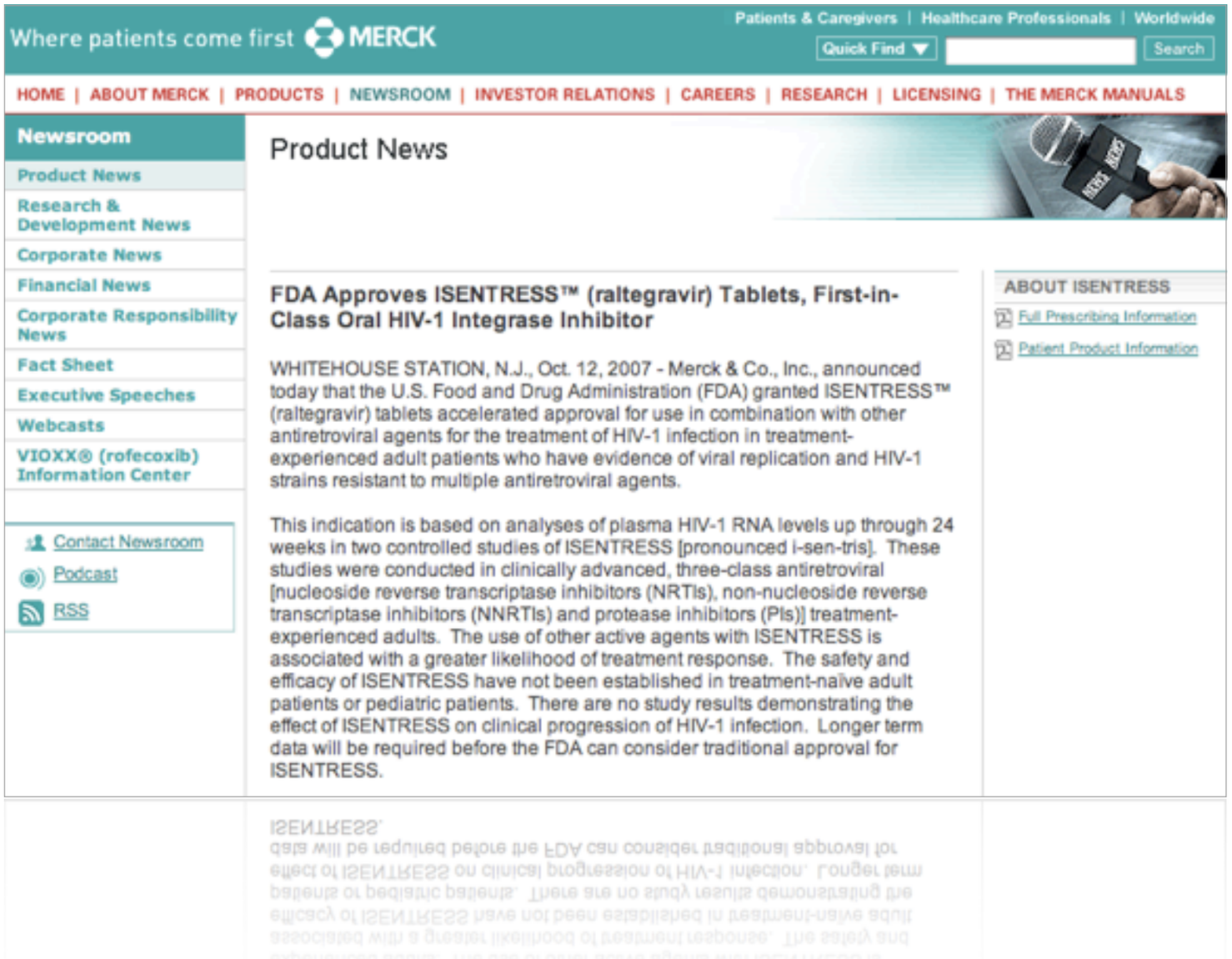

ISENTRESS example

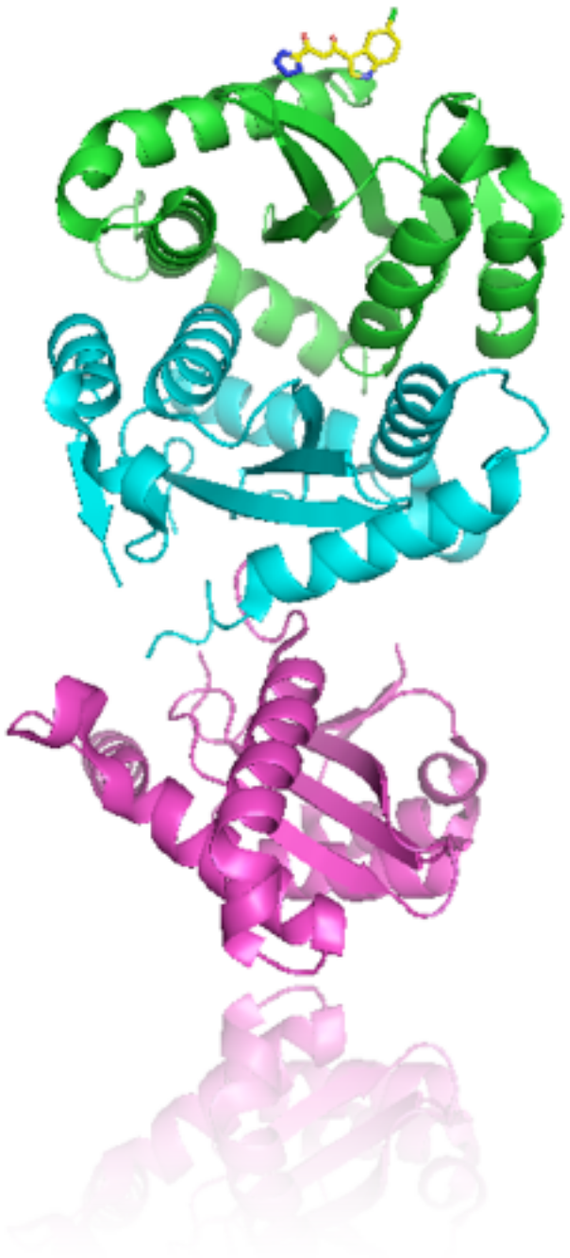

- One structure known with 5CITEP
  - Not clear (low resolution)
  - Binding near to DNA interacting site
  - Loop near the binding
- Docking + Molecular Dynamics
  - AMBER snapshots
  - AutoDock flexible torsion thetetrazolering and indole ring.

Schames, J.R., R.H. Henchman, J.S. Siegel, C.A. Sotriffer, H. Ni, and J.A. McCammon, Discovery of a novel binding trench in HIV integrase. J Med Chem, 2004. 47(8): 1879-81

ISENTRESS example

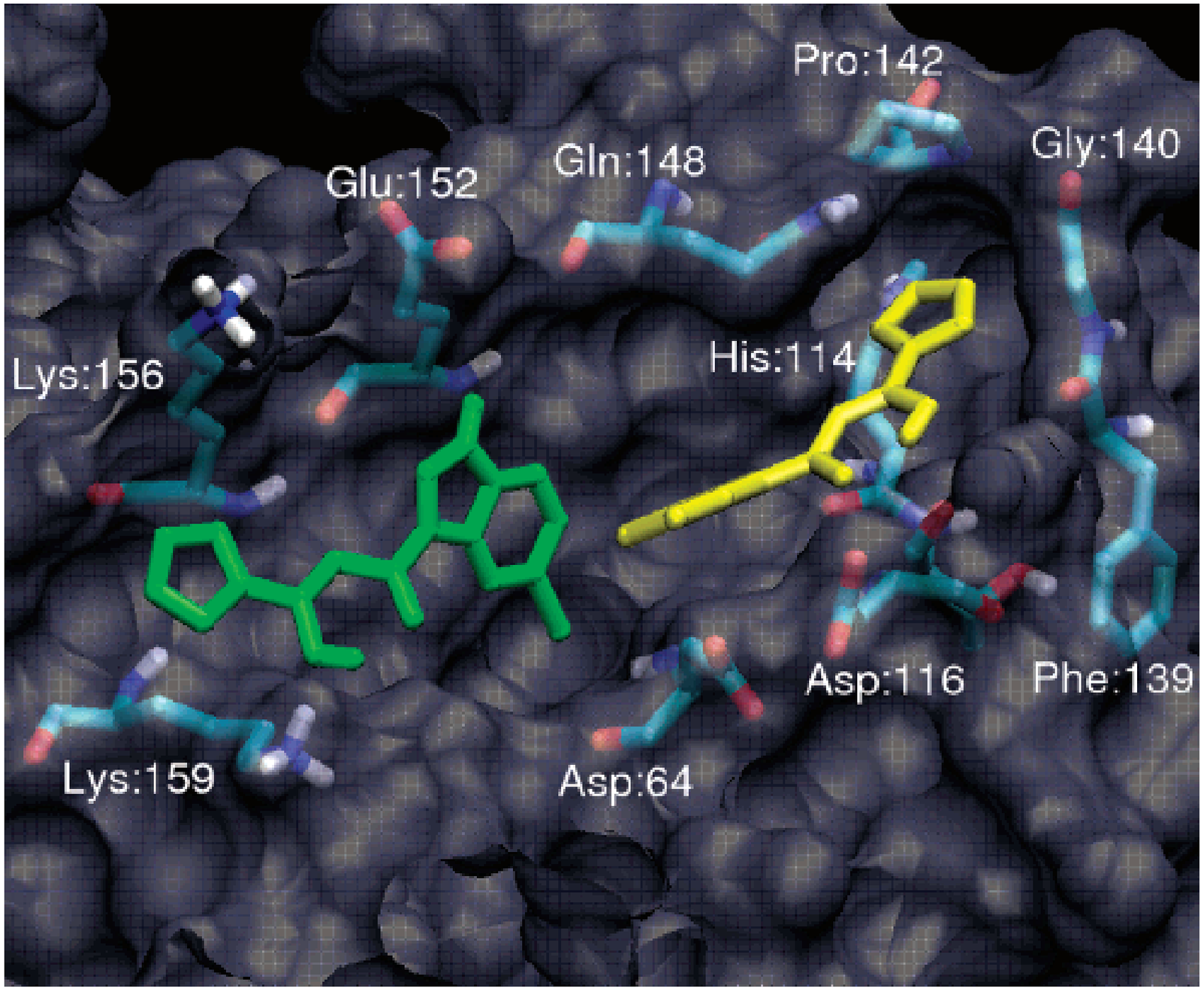

Schames, J.R., R.H. Henchman, J.S. Siegel, C.A. Sotriffer, H. Ni, and J.A. McCammon, Discovery of a novel binding trench in HIV integrase. J Med Chem, 2004. 47(8): 1879-81

ISENTRESS example

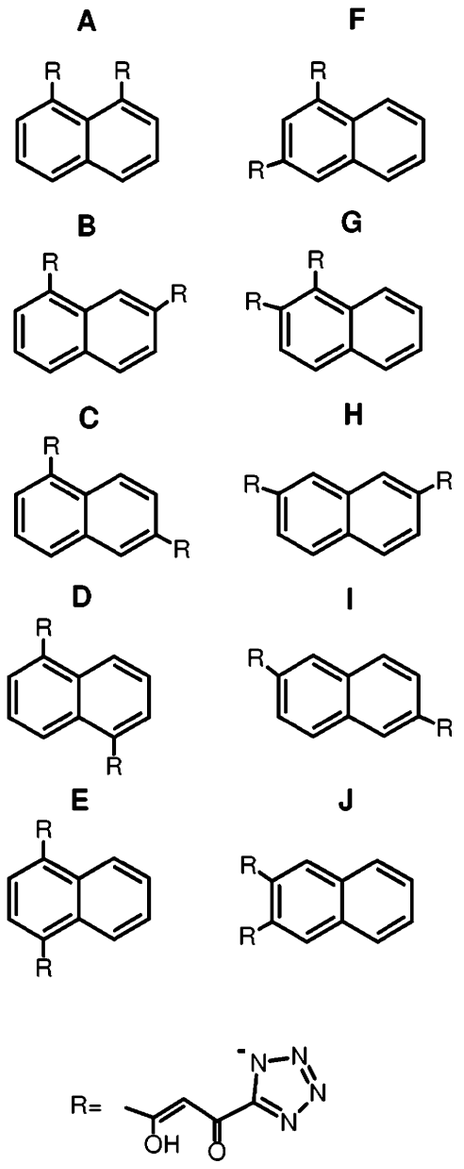

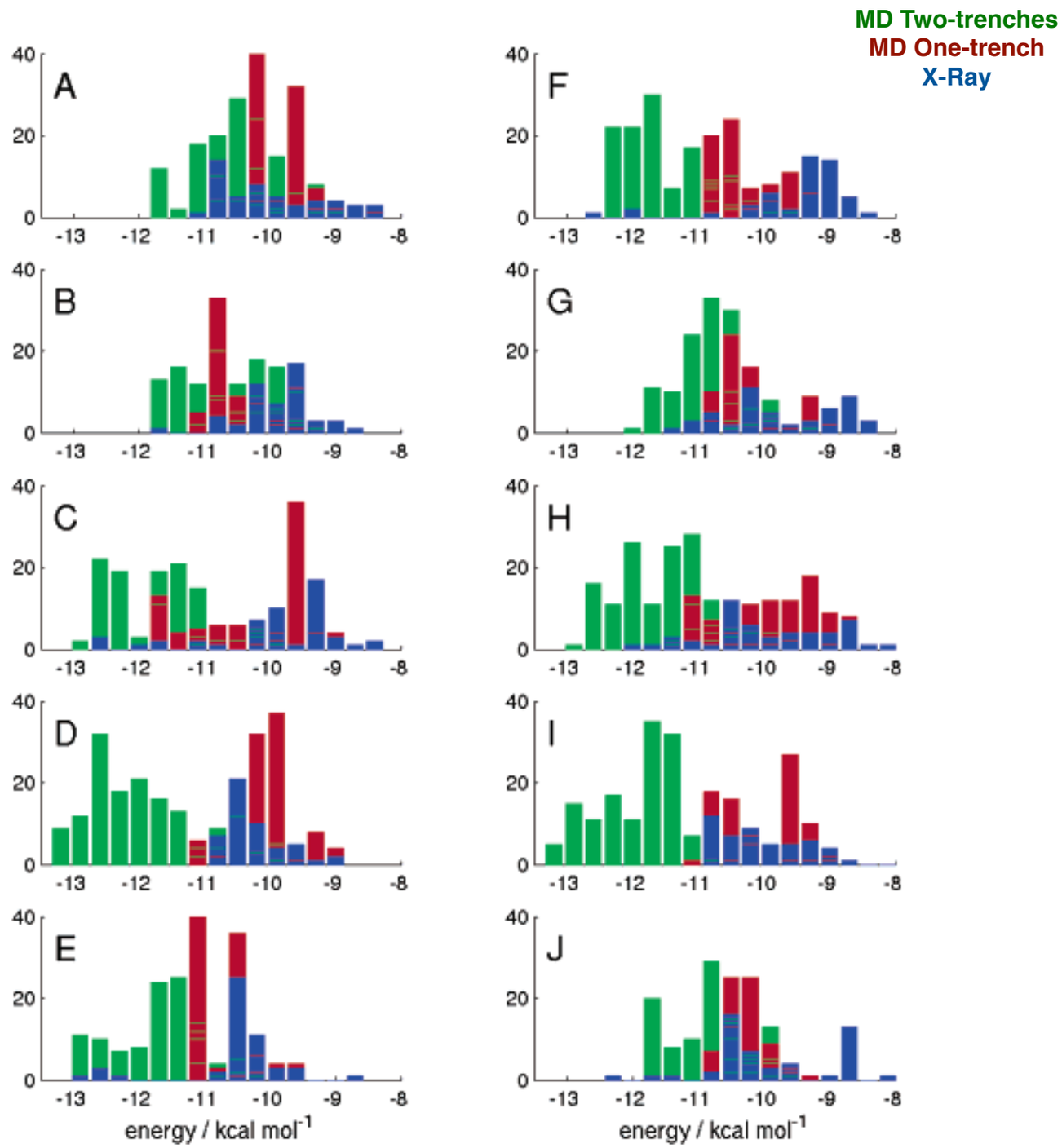

Schames, J.R., R.H. Henchman, J.S. Siegel, C.A. Sotriffer, H. Ni, and J.A. McCammon, Discovery of a novel binding trench in HIV integrase. J Med Chem, 2004. 47(8): 1879-81

ISENTRESS example

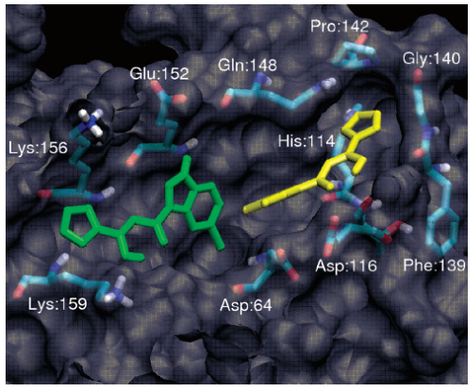

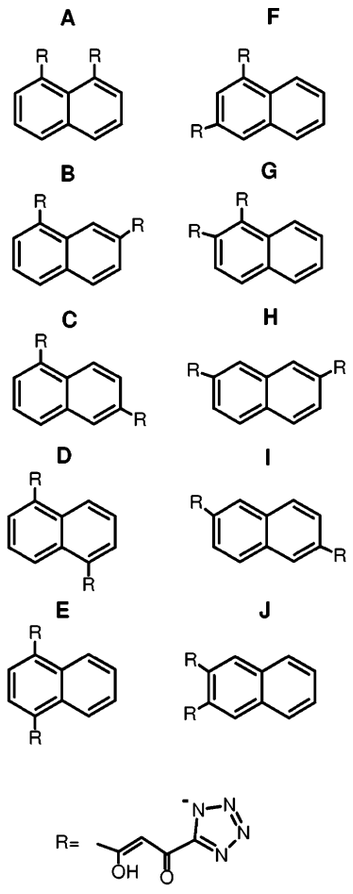

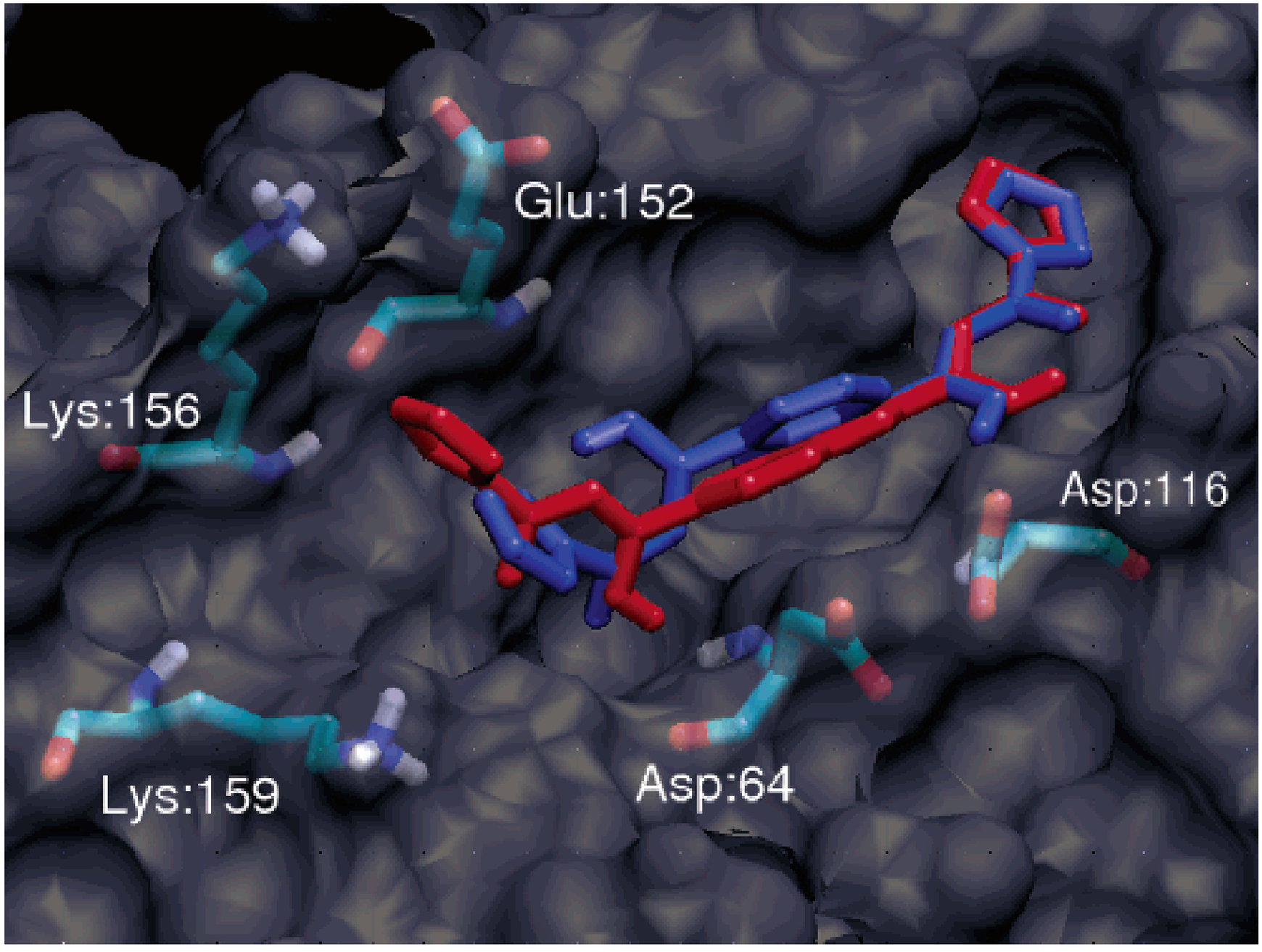

Schames, J.R., R.H. Henchman, J.S. Siegel, C.A. Sotriffer, H. Ni, and J.A. McCammon, Discovery of a novel binding trench in HIV integrase. J Med Chem, 2004. 47(8): 1879-81

ISENTRESS example

Where patients come first MERCK

Patients & Caregivers | Healthcare Professionals | Worldwide

Quick Find | Search

HOME | ABOUT MERCK | PRODUCTS | NEWSROOM | INVESTOR RELATIONS | CAREERS | RESEARCH | LICENSING | THE MERCK MANUALS

Newsroom

- Product News
- Research & Development News
- Corporate News
- Financial News
- Corporate Responsibility News
- Fact Sheet
- Executive Speeches
- Webcasts
- VIOXX® (rofecoxib) Information Center

Contact Newsroom

Podcast

RSS

Product News

FDA Approves ISENTRESS™ (raltegravir) Tablets, First-in-Class Oral HIV-1 Integrase Inhibitor

WHITEHOUSE STATION, N.J., Oct. 12, 2007 - Merck & Co., Inc., announced today that the U.S. Food and Drug Administration (FDA) granted ISENTRESS™ (raltegravir) tablets accelerated approval for use in combination with other antiretroviral agents for the treatment of HIV-1 infection in treatment-experienced adult patients who have evidence of viral replication and HIV-1 strains resistant to multiple antiretroviral agents.

This indication is based on analyses of plasma HIV-1 RNA levels up through 24 weeks in two controlled studies of ISENTRESS [pronounced i-sen-tris]. These studies were conducted in clinically advanced, three-class antiretroviral [nucleoside reverse transcriptase inhibitors (NRTIs), non-nucleoside reverse transcriptase inhibitors (NNRTIs) and protease inhibitors (PIs)] treatment-experienced adults. The use of other active agents with ISENTRESS is associated with a greater likelihood of treatment response. The safety and efficacy of ISENTRESS have not been established in treatment-naïve adult patients or pediatric patients. There are no study results demonstrating the effect of ISENTRESS on clinical progression of HIV-1 infection. Longer term data will be required before the FDA can consider traditional approval for ISENTRESS.

ABOUT ISENTRESS

- Full Prescribing Information
- Patient Product Information

Vina 1.1.1

Goodsell, D. S. and Olson, A. J. (1990), Automated Docking of Substrates to Proteins by Simulated Annealing Proteins:Structure, Function and Genetics., 8: 195-202.
Morris, G. M., et al. (1996), Distributed automated docking of flexible ligands to proteins: Parallel applications of AutoDock 2.4 J. Computer-Aided Molecular Design, 10: 293-304.
Morris, G. M., et al. (1998), Automated Docking Using a Lamarckian Genetic Algorithm and and Empirical Binding Free Energy Function J. Computational Chemistry, 19: 1639-1662.
Huey, R., et al. (2007), A Semiempirical Free Energy Force Field with Charge-Based Desolvation J. Computational Chemistry, 28: 1145-1152.

Vina 1.1.1

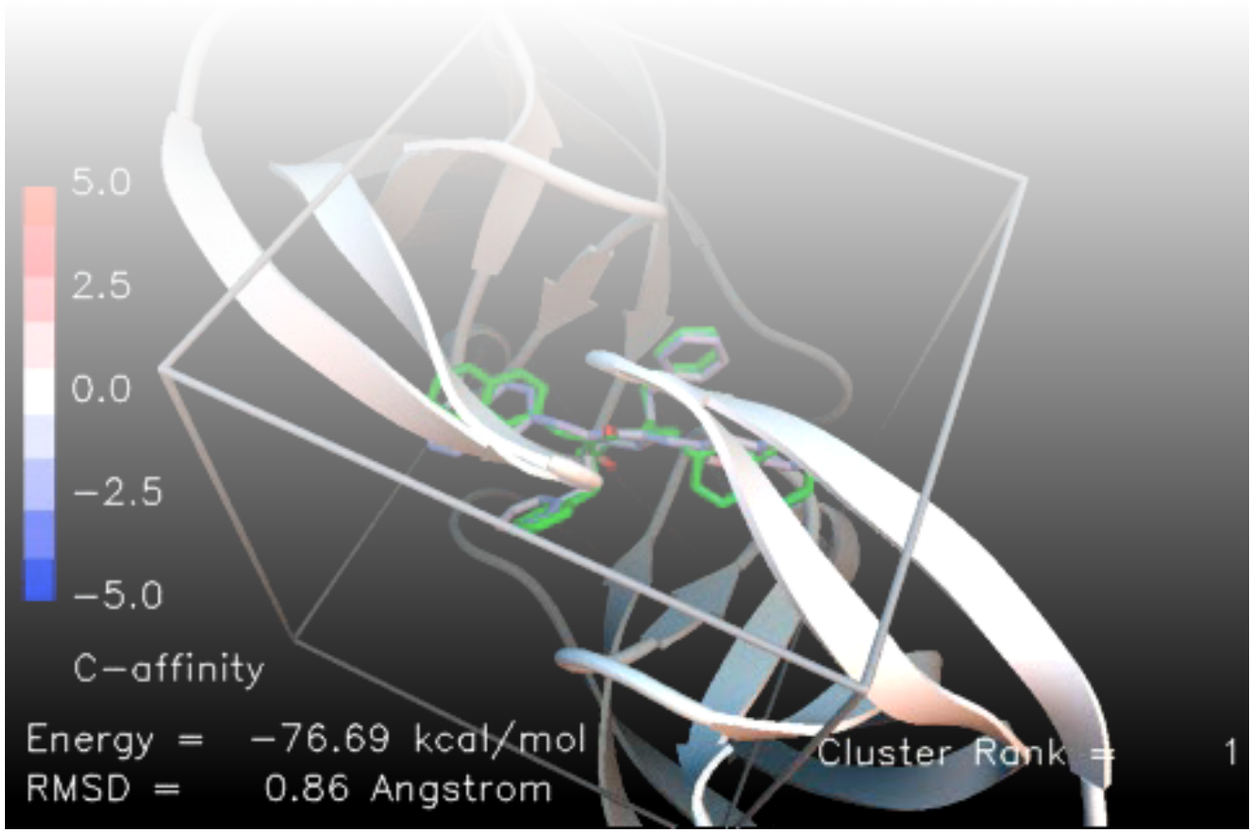

Goodsell, D. S. and Olson, A. J. (1990), Automated Docking of Substrates to Proteins by Simulated Annealing Proteins:Structure, Function and Genetics., 8: 195-202.
Morris, G. M., et al. (1996), Distributed automated docking of flexible ligands to proteins: Parallel applications of AutoDock 2.4 J. Computer-Aided Molecular Design, 10: 293-304.
Morris, G. M., et al. (1998), Automated Docking Using a Lamarckian Genetic Algorithm and and Empirical Binding Free Energy Function J. Computational Chemistry, 19: 1639-1662.
Huey, R., et al. (2007), A Semiempirical Free Energy Force Field with Charge-Based Desolvation J. Computational Chemistry, 28: 1145-1152.

Vina 1.1.1

Where to get help...

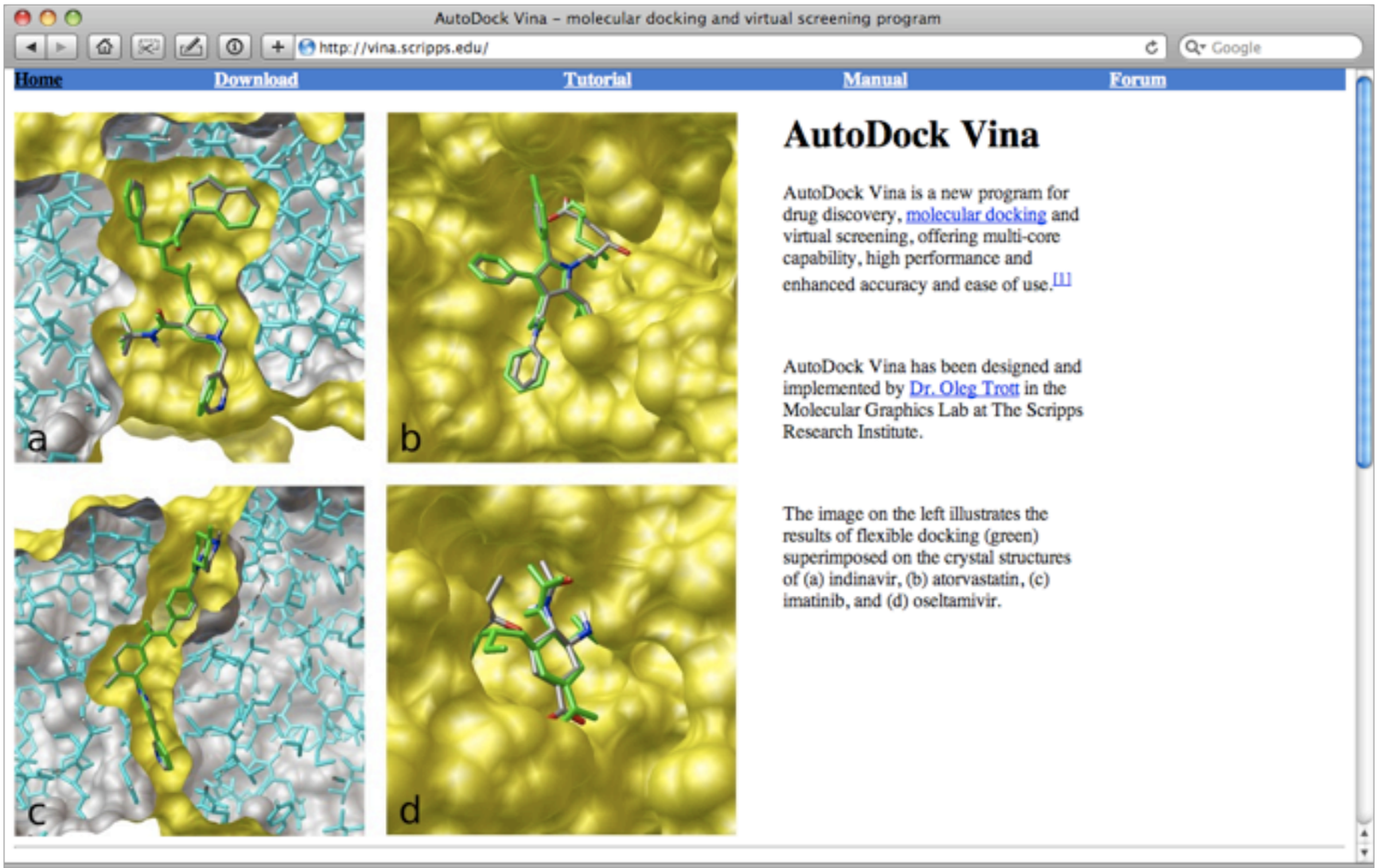

http://vina.scripps.edu

Vina 1.1.1

Alternatives

Progressive building

- FLEXX
- DOCK
- GROW
- GroupBUILD
- LUDI
- LEGEND
- SPROUT
- BUILDER
- GENSTAR

Conformational search

- MIMUMBA
- COBRA
- WIZRAD

Binding site description

- GRID

Genetic algorithms

- GOLD
- Others

Virtual screening

- AutoDOCK

Molecular dynamcis

- MCSS
- CONCEPTS

Databases

- CAVEAT
- FOUNDATION
- CLIX
- NEWLEAD
- LEAPFROG

AutoDock 4.0

Why AutoDock over others

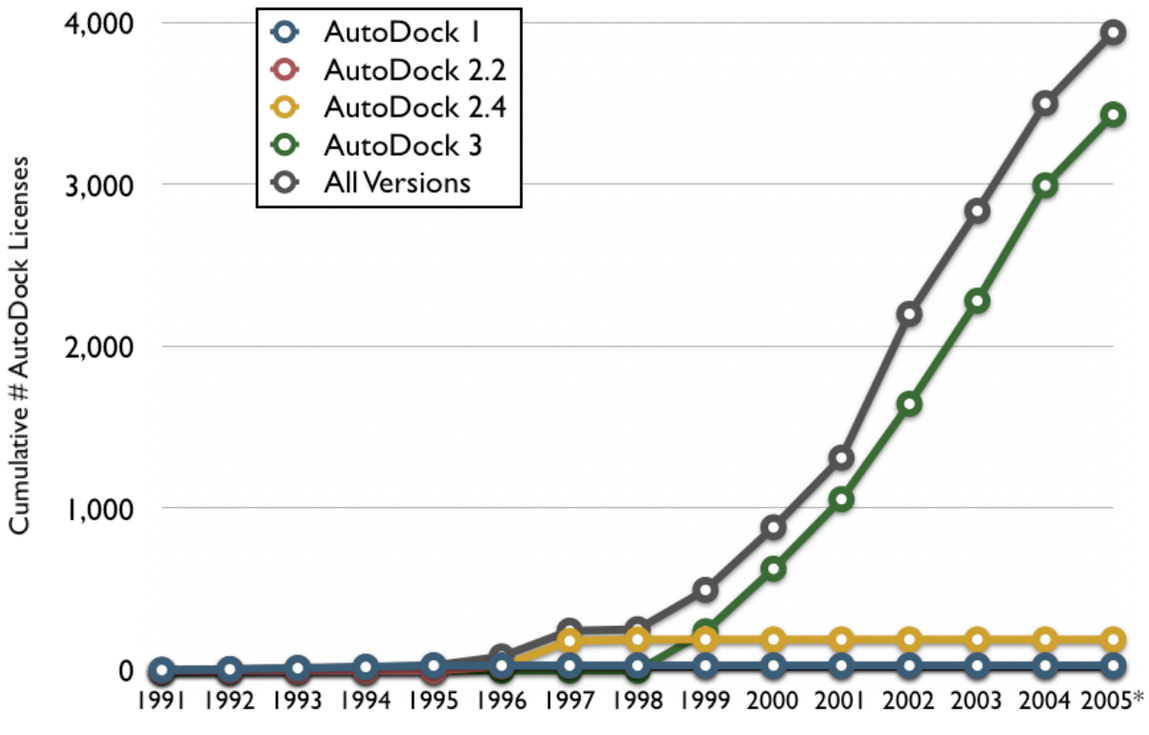

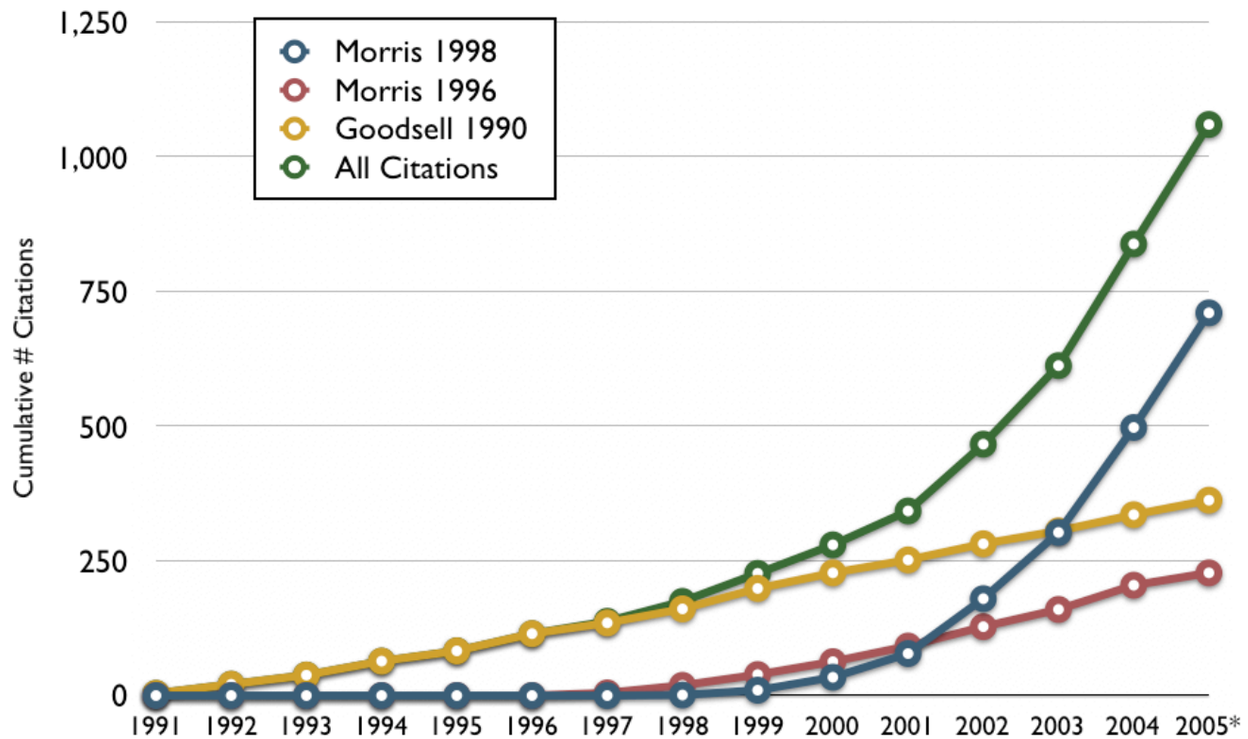

AutoDock 4.0

Why AutoDock over others

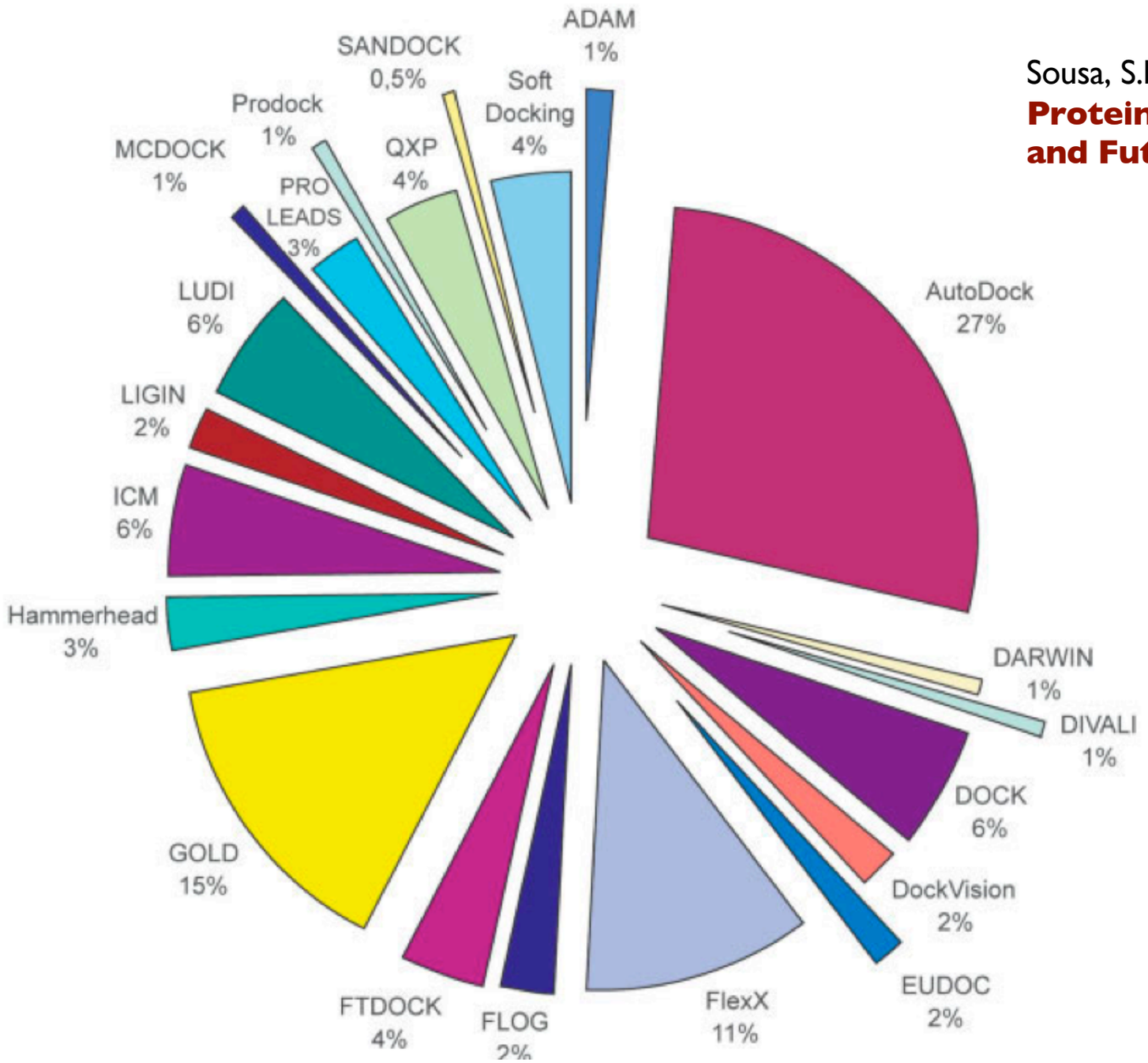

Sousa, S.F., Fernandes, P.A. & Ramos, M.J. (2006)
Protein-Ligand Docking: Current Status and Future Challenges *Proteins*, **65**:15-26

AutoDock 4.0

Why AutoDock over others

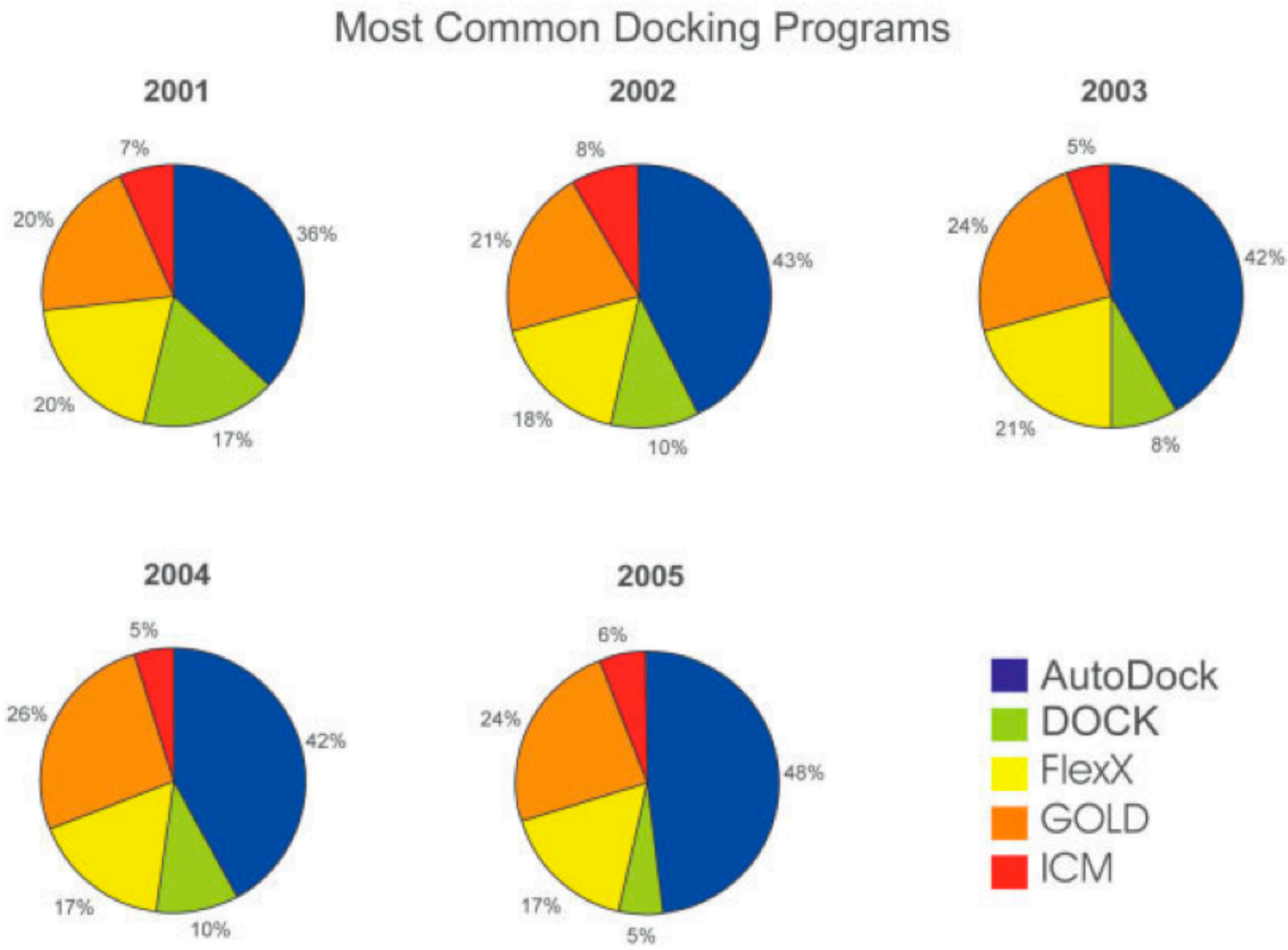

Vina 1.1.1

Vina and ADT

Vina

- 1990 (AutoDock)
- Number crunching (CPU expensive)
- Command-line!
- C & C++ compiled

AutoDock Tools

- 2000
- Visualizing set-up
- Graphical user interphase
- Python interpreter

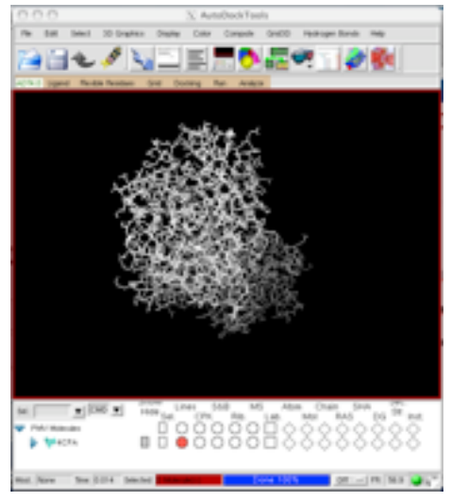

AutoDock / Vina

Practical considerations

- What problem does AutoDock solve?
  - *Flexible* ligands (4.0 *flexible* protein).
- What range of problems is feasible?
  - Depends on the search method:
    - LGA > GA >> SA >> LS
    - SA : can output trajectories, D < about 8 torsions.
    - LGA : D < about 8-32 torsions.
- When is AutoDock not suitable?
  - No 3D-structures are available;
  - Modelled structure of poor quality;
  - Too many (32 torsions, 2048 atoms, 22 atom types);
  - Target protein too flexible.

Vina 1.1.1

Things to know before using AutoDock

Ligand:

- Add all hydrogens, compute Gasteiger charges, and merge non-polar H; also assign AutoDock 4 atom types
- Ensure total charge corresponds to tautomeric state
- Choose torsion tree root & rotatable bonds

Macromolecule:

- Add all hydrogens, compute Gasteiger charges, and merge non-polar H; also assign AutoDock 4 atom types
- Assign Stouten atomic solvation parameters
- Optionally, create a flexible residues PDBQT in addition to the rigid PDBQT file
- Compute AutoGrid maps

Vina 1.1.1

Good that we have AutoDock Tools (ATD)

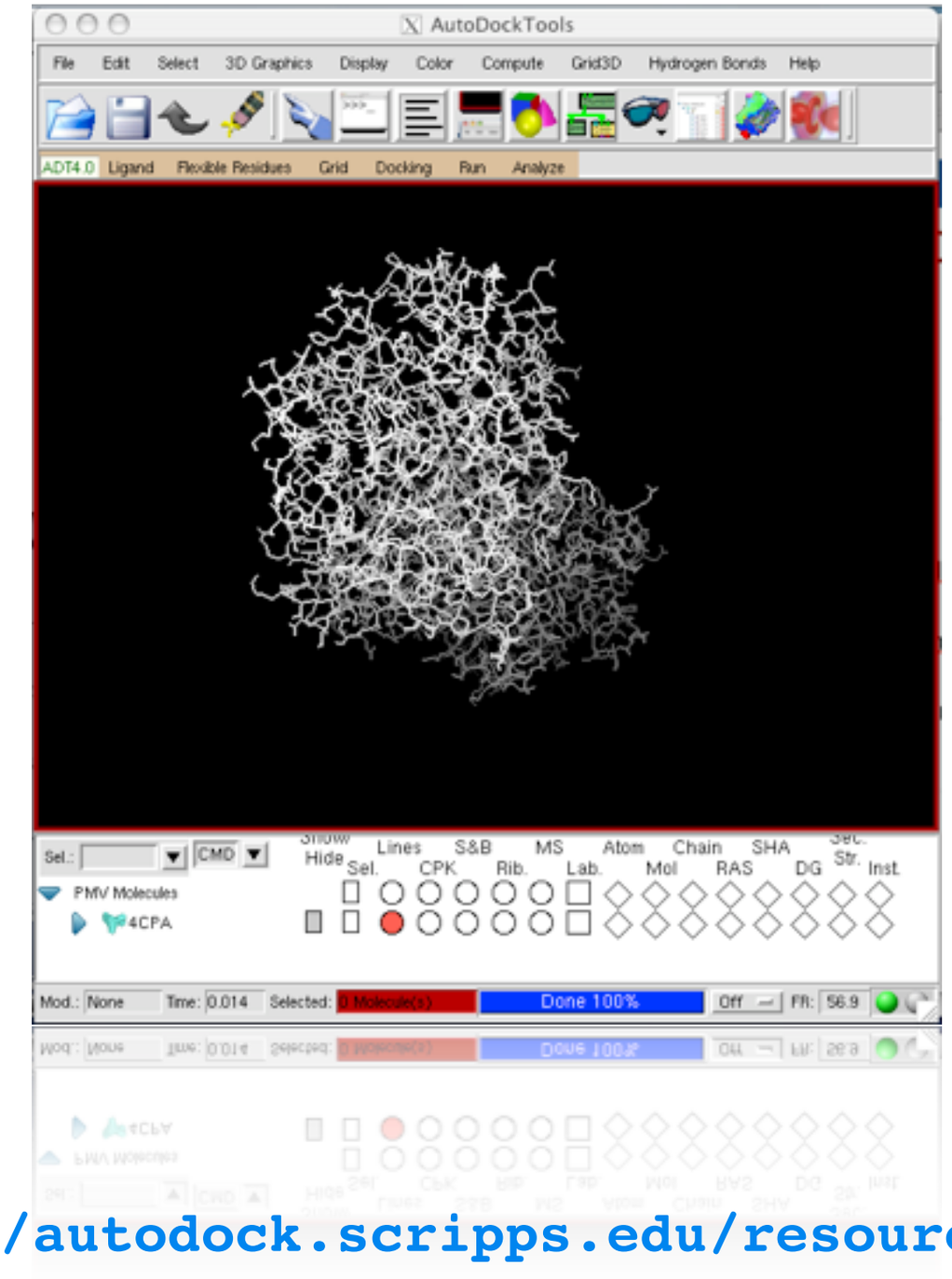

http://autodock.scripps.edu/resources/adt

Vina 1.1.1

Good we have a nice tutorial

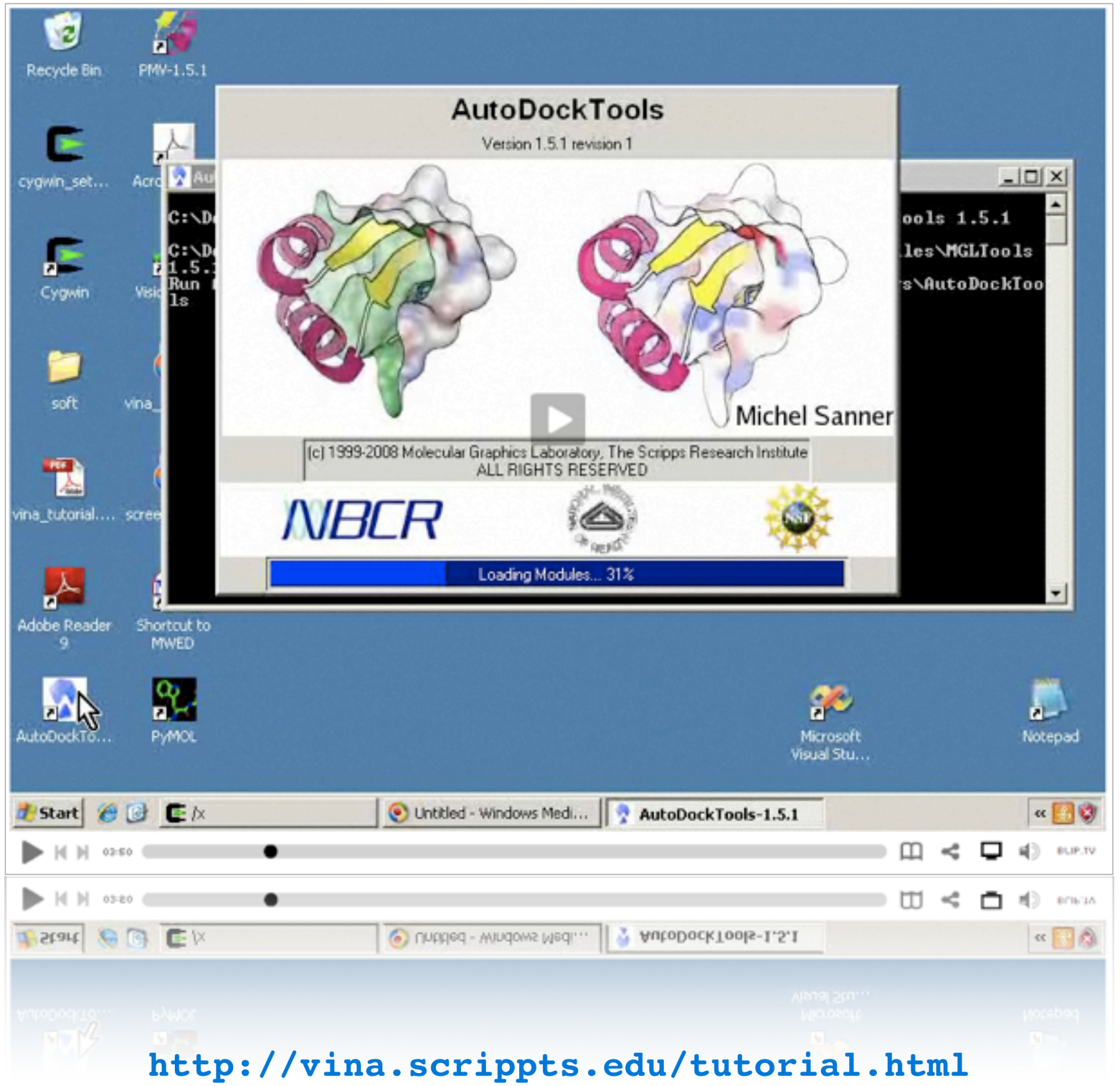

http://vina.scrippts.edu/tutorial.html

Acknowledgements

This presentation was based on:

“Using AutoDock 4 with ADT. A tutorial”
by Dr. Ruth Huey and Dr. Garret M. Morris

Vina Tutorial
by Dr. Oleg Trott